Chem Soc Rev

Fluorescence based explosives detection: from mechanisms to sensory materials

SCHOLARONE™
Manuscripts

Chem Soc Rev

Fluorescence based Explosives Detection: From Mechanisms to Sensory Materials

Xiangcheng Sun†*, Ying Wang† and Yu Lei*

Explosives detection is one of current pressing concerns in global security. In the past decades, a large number of emissive sensing materials have been developed for the detection of explosives in vapor, solution, and solid states through fluorescence methods. In recent years, great efforts have been devoted to develop new fluorescent materials with various sensing mechanisms for detecting explosives in order to achieve super-sensitivity, ultra-selectivity, as well as fast response time. This review article starts with a brief introduction on various sensing mechanisms for fluorescence based explosives detection, and then summarizes in an exhaustive and systematic way the state-of-the-art of fluorescent materials for explosives detection with a focus on the research in the recent 5 years. A broad range of fluorescent materials, such as conjugated polymers, small fluorophores, supramolecular systems, bio-inspired materials and aggregation induced emission - active materials, and their sensing performance and sensing mechanism are the centerpiece of this review. Finally, conclusions and future outlook are presented and discussed.

From the Contents

1. Introduction – background of explosives detection

† Equal Contribution

Department of Chemical and Biomolecular Engineering, University of Connecticut,
  191 Auditorium Road, Unit 3222, Storrs, CT 06269, USA

To whom correspondence should be addressed:
Email: ylei@engr.uconn.edu and xiangcheng.sun@uconn.edu;
Fax: +1-860-486-2959; Tel: +1-860-486-4554

One pressing concern in anti-terrorism and homeland security is explosives detection. Explosive bombs have been by far the most common form of terrorism, due to their ease to produce and deploy, and consequentially killed tens of thousands of people as well as caused enormous property damage. The recent rise in global terrorism has stimulated the necessity of standoff/remote, sensitive and low-cost detection of explosives. In addition, given the widespread use of explosive formulations, the analysis of explosives has been of importance in forensic research, landmine detection, and environmental problems associated with explosive residues.[1, 2] The extensive use of explosives for military purpose has also raised concerns about environmental contaminations where they are produced and stored.[3] Great public health threat, including anemia, carcinogenicity, abnormal liver function,

cataract development and skin irritation, etc., could also be posed to both animals and human beings through short-term or long-term exposure of nitroaromatic explosives. For example, TNT is classified as a EPA pollutant at concentrations above 2 μg L^{-1}.[4] Therefore, rapid, sensitive and selective explosive detection could provide rapid warning in case of terrorism attacks, help in tracking and locating explosive materials as well as reducing the continued fatalities of civilians from landmines, and offer appropriate feed-back during the characterization and remediation of contaminated sites.

Until November 2010, the Bureau of Alcohol, Tobacco, and Firearms (ATF) lists 229 explosive materials,[5] which could be loosely classified into six broad classes based on their structures, as listed in Table 1. Typically, nitroaromatics

Table 1. Six principal chemical categories of explosives, examples and vapor pressure data[7]

Class	Name	Acronym	Structure	P_{vap}, 25°C /Torr
Nitroalkane	2,3-Dimethyl-2,3-dinitrobutane	DMNB		1.88×10^{-3}
	Nitromethane	NM		36.5
Nitroaromatic	2-Nitrotoluene; 3-Nitrotoluene; 4-Nitrotoluene	NT		4.89×10^{-2}
	2,4-Dinitrotoluene; 2,6-Dinitrotoluene	DNT		2.63×10^{-4}
	2,4,6-Trinitrotoluene	TNT		5.50×10^{-6}
	2,4,6-Trinitrophenol (Picric acid)	TNP, PA		5.8×10^{-9}
	Nitrobenzene; o-, m-, p- dinitrobenzene; 1,3,5-trinitrobenzene	p-DNB		9.00×10^{-4}
Nitramines	1,3,5-Trinitro-1,3,5-triazacyclohexane	RDX		3.30×10^{-9}
	Octahydro-1,3,5,7-tetranitro-1,3,5,7-tetrazocine	HMX		3.01×10^{-15}
	2,4,6-Trinitrophenylmethylnitramine	Tetryl		6.51×10^{-9}
Nitrate ester	Nitroglycerin	NG		4.81×10^{-4}
	Pentaerythritol tetranitrate	PETN		1.16×10^{-8}
Acid salts	Ammonium nitrate	AN	NH_4NO_3	9.77×10^{-6}
	Ammonium phosphate	AP	$(NH_4)_3PO_4$	2.97×10^{-11}
Peroxides	Hydrogen peroxide	HP	H_2O_2	$^a\,2.05\times10^{-1}$
	Triacetone triperoxide	TATP		4.65×10^{-3}
	Hexamethylene triperoxide diamine	HMTD		^{b}

^{a} The HP vapor pressure is that for 32% HP; ^{b} No vapor pressure data for HMTD was reported, instead a number of decomposition products.

(NACs), such as 2,4,6-trinitrotoluene (TNT) and 2,4-dinitrotoluene (2,4-DNT), are the primary military explosives and also the principal components in the unexploded landmines worldwide.[6] Nitramines and nitrate esters (e.g., 3,5-trinitroperhydro-1,3,5-triazine (RDX) and pentaerythritol tetranitrate (PETN)), are main components of highly energetic plastic explosives, such as C-4 (91% RDX) and Semtex (40-76% PETN). Ammonium salts such as ammonium nitrate (AN) and ammonium phosphate (AP) are commonly used for the industrial applications, typically in solid rocket propellants. Peroxide-based explosives like triacetone triperoxide (TATP) and hexamethylene triperoxide diamine (HMTD) have grown rapidly as for homemade explosives because they can be easily synthesized from inexpensive materials. Most highly energetic explosives are nitro-substituted (nitrated) compounds, which have the top priority to be detected and are therefore the focus of the current review.

As nitrated explosives are extremely sensitive to shock, friction and impact, therefore, detection methods that permit contact-free analysis are desirable. Moreover, the demands of detecting hidden explosives in transportation hubs and buried explosives in warzones also have led to an intense interest in ultrasensitive detection of nitrated explosives in vapor phase. However, explosive vapors are notoriously difficult to be detected because of a number of issues. First, most explosives have substantially low volatility at ambient temperature (as shown in Table 1), especially for those with the highest priority to be detected (e.g., TNT, RDX and PETN). In addition, explosives are often concealed, and the package will further block the escape of explosive vapors for detection. As reported by Kolla, the vapor concentration of explosives is reduced by a factor of 1000 by wrapping in a plastic package.[8] Furthermore, the sticky nature of explosives renders them to adsorb onto surfaces, especially those surfaces with a high surface energy such as metals, resulting in the condensation of explosive molecules in the delivery lines of the sensor device and reducing the number of analytes in a sampling volume. Third, the physical properties of each class of nitrated explosives differ significantly from those of others, making the detection of broad-class explosives quite a challenge. For example, there is an increasing demand for the direct detection of RDX and PETN, both of which lack nitroaromatic rings, and have higher lowest unoccupied molecular orbital (LUMO) energies and even lower vapor pressures (RDX and PETN), rendering them hard to be detected by general optical approaches used for the NACs. Finally, many daily chemicals are likely to be interferences and lead to false alarms. In field test, the false positive alarms often come from environmental contaminants, and the false negative alarms are related to the lack of selectivity. For instance, bleach is a strong oxidant and is likely to generate a false positive alarm in TATP or HMTD sensing. All of these issues make it extremely difficult to achieve the sensitive and selective detection of a broad range of explosives by a single material.

In other occasions, the sensing applications are required to be performed in aqueous matrix.[9, 10] Sensing of explosives in aqueous solution is of paramount importance due to the extension of terrorism activities from land to marine environments, the location of underwater mine and the characterization of soil and groundwater contaminations. Although their solubility in aqueous solution is not as low as their ultralow volatility, saturated concentrations are hardly ever reached underwater as water movement will cause any degree of dilution and ppb (or below) levels would need to be detected for real applications. This makes the nitrated explosives detection in aqueous samples by 'tasting' them out very challenging.

Currently, the commercially available methods for detection of explosives are trained canines, metal detectors, and ion mobility spectrometry (IMS). While each method provides advantages, their use is not without problem. Trained canines are reliable for the detection of explosives due to the powerful olfactory system of dogs. Well-trained canines have been widely used in the field test and the transportation sites such as airports to identify and discriminate between different explosives. However, canine training is very expensive and dogs easily get tired for continuous sensing, thus it is not well-suited for widespread and long-time detection. Metal detectors are indirect technique and very efficient for landmine and weapons detection packaged in metals, however, this technique is not sensitive for explosives' chemical finger-print property thus cannot be applied for transportation sites screening. IMS is a commonly used explosive detection system in airports, and has sensitivity down to nanogram or picogram for common explosives, but this technique lacks enough sensitivity for broad range of explosives, such as PETN and RDX, which greatly limits its overall utility. Moreover, IMS requires sophisticated protocols with time-consuming calibration, along with its poor portability and high cost, making it not suitable for real-time field detection.[11] Similar limitations also apply to other laboratory explosive detection systems[12], such as gas chromatography coupled with mass spectrometry (GC-MS)[13], quartz crystal microbalance (QCM), surface plasmon resonance (SPR), electrochemical methods[14], immunoassay[15], etc. There thus remains an urgent need for innovative detection strategies that are not only low-cost and user-friendly, but also highly sensitive and selective.

One particularly attractive and promising approach would involve the use of optical methods, which offer many benefits over other common detection techniques, such as low-cost, good portability, high sensitivity and selectivity. Consequently absorbance (colorimetric) and fluorescence responses are the main focus of vast recently developed optical sensors for explosives detection.[1] Typically, fluorescence-based detection is one to three orders of magnitude more sensitive and has wider linear ranges compared to absorbance-based methods. Moreover, the source and detector of fluorescence method could be easily incorporated into a handheld device for field detection of explosives. Thus, fluorescence-based method has the great promise to be applied in the rapid, sensitive and selective detection of explosives, and thus becomes the focus of discussion in this review.

Recently several excellent reviews extensively described and discussed the fluorescence-based explosive sensors from different perspectives such as polymer sensors[16], optical chemosensors[1, 2, 17], and various fluorescent materials such as conjugated polymers[18-20], luminescent metal-organic frameworks[21], and nanomaterials[22]. The purpose of this review is to summarize the state-of-art of fluorescence based explosive sensors in a more exhaustive and systematic way and is especially to focus on the research progress up to date. Importantly, the innovative advances in this field are organized into a coherent overview aimed to rationally summarize the different strategies and improvements in the exploitation of fluorescent materials for explosive detection. Mechanisms of fluorescence explosives detection are reviewed, not only fluorescence quenching based mechanisms but also some novel mechanisms applied in explosives detection such as fluorescence turn-on, spectra shift, lifetime and anisotropy. Along with their sensing performance, various fluorescent materials are the centerpiece of this review. They cover a broad range of materials, including not only the popular conjugated polymers and small molecules, but also newly developed supramolecular systems, biologically-inspired materials and aggregation-induced emission (AIE) sensing materials. At the end of the review, the future directions and outlook are presented and discussed.

2. Methods and mechanisms for fluorescence based explosives detection

Due to the non-fluorescent properties of explosives, the fluorescence based explosive detection is an indirect method to utilize fluorophore species (fluorescent sensory materials) that undergo fluorescence changes upon interactions with explosives. Theoretically, any phenomenon that results in a change of fluorescence intensity (quenching or enhancement), wavelength, anisotropy, or lifetime related to the concentration and exposure time of explosives has the potential to be used to sense explosives.

2.1 Interactions caused fluorescence detection

During all the published work on fluorescence based explosives sensors, fluorescence quenching methods still dominate. There are several mechanisms responsible for fluorescence quenching such as photo-induced electron transfer, resonance energy transfer, electron exchange, intermolecular charge transfer, etc.[23]

2.1.1 Photo-induced electron transfer (PET)

Many explosives are highly nitrated organic compounds. This property renders them electro-deficient, which could bind to electron-rich fluorophore through donor-acceptor (D-A) interactions.[24] In the photo-induced electron transfer, the excited-state of fluorophore (D) is likely to donate an electron to the ground-state of explosive compounds (A) as shown in Fig. 1A.[25] In PET, a complex is formed between the electron donor and the electron acceptor. This charge transfer complex can return to the ground state without emission of a photon, but in some cases exciplex emission is observed. Finally, the
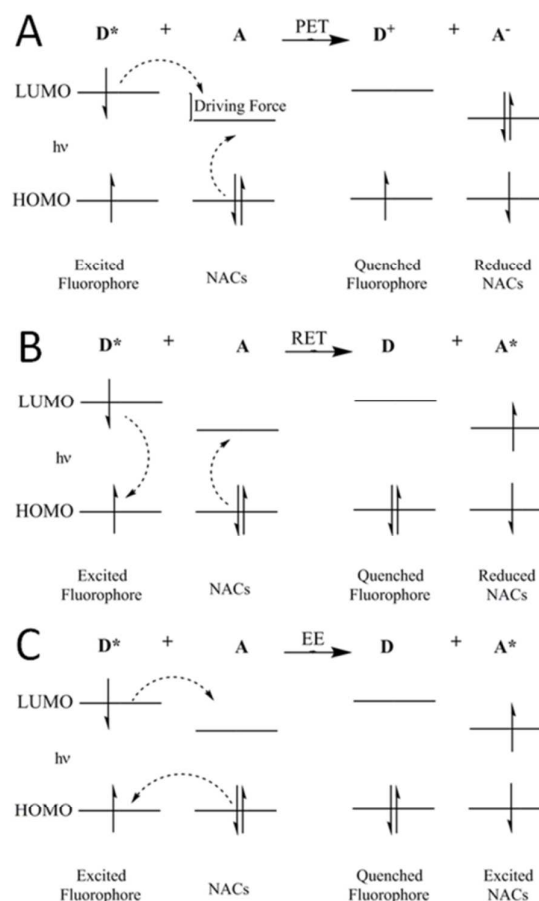

Fig. 1 Molecular orbital schematic illustration for different interactions. (A) photoinduced electron transfer (PET), (B) resonance energy transfer (RET), and (C) Energy exchange (EE).

extra electron on the acceptor is returned to the electron donor. The energy gap between the LUMO of donor fluorophore and that of the acceptor explosive is approximately the thermodynamic driving force for this oxidative electron transfer process. PET plays a major role in the fluorescence quenching process, and provides useful insights into the development of explosive fluorescence sensors.

Obviously, the quenching efficiency is directly proportional to the electron transfer. For conjugated polymers, electron transfer is based on π-π stacking in a D-A system. The semiclassical limit of Marcus theory has been developed to analyze the PET process, the electron transfer rate (K_{et}) is expressed as[26, 27]

$$K_{et} = A \exp\left(-\frac{\Delta G^*}{kT}\right) = \frac{2\pi^{\frac{3}{2}}}{h\sqrt{\lambda kT}}V^2 \exp\left[-\frac{(\Delta G^0+\lambda)^2}{4\lambda kT}\right] \qquad (1)$$

where h, k, T, are the physics parameters such as Planck constant, Boltzmann constant, and temperature in Kelvin. ΔG^0 means the standard Gibbs free energy difference of the

electron transfer reaction, V is the electron coupling between the initial state (D^*A) and final state (D^+A^-), and λ is the reorganization energy which is a relax energy of adjusting molecular structure for producing new stabilized state and includes two contributions: (i) the internal part λ_e related to the geometry changes of the D and the A and (ii) the external part λ_e related to the changes of the surroundings. Under the one-electron approximation, the ΔG^0 can be obtained by the energy gap between the LUMO of the A and that of the D, which can be readily calculated by using a quantum-chemical calculation method. Electron coupling (V) can be considered as direct LUMOs coupling between the D and the A, which is strongly dependent upon the distance between them and also on the relative orientation of them. Simply, ΔG^0 is considered as the thermodynamic driving force for the PET process.

Photo-induced electron transfer contributes to the fluorescence quenching by nitro-explosives, which accounts for the most of the fluorescence-based explosives detection. PET mechanism also leads to fluorescence enhancement and is used for explosives detection in recent years. It is believed that sensing by enhancement of fluorescence is superior to quenching due to several reasons.[28] Firstly, the appearance of a bright signal on a completely dark ground is qualitatively easier to detect than the dimming of an already bright signal and is little affected by the fluorescence background thus leading to higher sensitivity. Secondly, turn-on signals result from a stoichiometric binding event, rather than from a collisional encounter. For example, through introducing appropriate substituents onto the boron-dipyrromethene (BODIPY) framework, a specific fluorescence turn-on chemodosimeter for picric acid was achieved.[28] Without the addition of picric acid, the BODIPY is weakly fluorescent, due to the PET that occurs from the acetal oxygen to the BODIPY. The addition of picric acid breaks the PET process because of the interaction of the picric acid and acetal oxygen of the BODIPY core and formation of corresponding aldehyde.

In PET the excited fluorophore can be either electron donor or acceptor.[23] The direction of electron transfer is determined by the oxidation and reduction potentials and molecular orbitals of the ground and excited states. This unique theory has been utilized for differentiation between electron-

deficient explosives and electron rich compounds, leading to fluorescence-off and fluorescence-on phenomena, respectively.[29, 30] Since the LUMO levels of electron-rich arenes are higher than that of fluorophore, electron transfers from electron-rich compound to fluorophore, and resulting in fluorescence enhancement (Fig. 2). Due to the exciplex formation between arenes and fluorophores, emission spectra shift could also be observed. Therefore, combining the fluorescence intensity changes with spectra shift, the 2D map provides a new route to sensitive and selective detection of explosives and explosive-similar compounds.[31]

2.1.2 Resonance Energy Transfer (RET)

Energy transfer mechanism has also been used to develop a number of explosive sensors, and can dramatically enhance the fluorescence-quenching efficiency and improve sensitivity. In Förster resonance energy transfer (FRET), an initially excited molecule (donor) returns to the ground state orbital, while simultaneously the transferred energy provides an electron on the acceptor to the excited state as depicted in Fig. 1B.

RET is due to long-range dipolar interactions through D^* and A. RET is not sensitive to steric factors or electrostatic interactions. According to FRET theory[18, 32, 33], the rate of energy transfer depends on 1) the relative orientation of the donor and acceptor dipoles, 2) the extent of overlap of fluorescence emission spectrum of the donor (the fluorophore) and absorption spectrum of the acceptor (the analyte), and 3) the distance between the donor and the acceptor. The probability of resonance energy transfer depends upon the extent of overlap between these molecules. The efficiency (E) of energy transfer between the donor and the acceptor could be calculated by the following equation[23]:

$$E = 1 - \frac{F}{F_0} = \frac{R_0^6}{R_0^6 + r_0^6} \qquad (2)$$

Where, F and F_0 are the relative fluorescence intensities of the donor in the presence and absence of acceptor, respectively; r_0 represents the distance between the donor and the acceptor, and R_0 is the critical distance at which energy transfer efficiency equals to 50%. The value of R_0 is calculated using the equation:

$$R_0^6 = 8.79 \times 10^{-5} K^2 n^{-4} \emptyset J \qquad (3)$$

Where K^2 is the orientation factor related to the geometry of the donor-acceptor dipole, n is the refractive index of the medium, $\emptyset$ is the fluorescence quantum yield of the donor, and J expresses the degree of spectral overlap between the donor emission and the acceptor absorption, J is given by:

$$J = \frac{\int_0^\infty F(\lambda)\varepsilon(\lambda)\lambda^4 d\lambda}{\int_0^\infty F(\lambda)d\lambda} \qquad (4)$$

Where $F(\lambda)$ is the corrected fluorescence intensity of the donor in the wavelength λ to $\lambda+\Delta\lambda$, and $\varepsilon(\lambda)$ is the extinction coefficient of the acceptor at λ.

In recent years, FRET mechanism has been widely utilized for explosive detection to improve the sensitivity and selectivity by various research groups. Almost all the work applies this
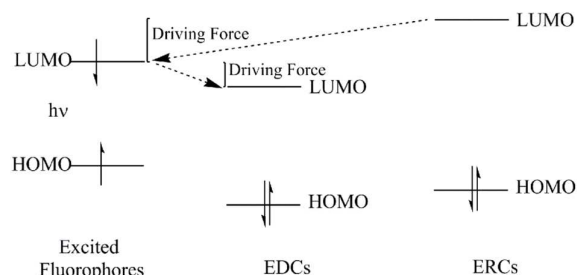

Fig. 2 Schematic drawings of the electronic structure of the fluorescence quenching process by electron deficient compounds (EDCs) and the fluorescence enhancement process by electron rich compounds (ERCs).

mechanism through fluorescence quenching phenomena to detect explosives, which could fall into two broad categories. One is the direct utilization of the unique spectrum of explosives. Through rationally designed fluorophore materials, the emission spectrum of the fluorophore efficiently overlaps with absorption of explosives.[34] For example, picric acid has a different absorption spectrum from other nitro explosives. Harnessing this difference, researchers developed highly sensitive and selective fluorescence sensors to detect picric acid.[34-36] The second method utilizes electron deficient properties of nitro-explosives and formation of Meisenheimer complex.[37, 38] For example, electron-rich primary amines have been exploited as promising binding sites to TNT, through a donor-acceptor interaction to form Meisenheimer complexes.[39, 40] Moreover, these amine-TNT complexes have strong absorption at ~ 525 nm and have been explored by Zhang and his group to couple with emission spectra overlapped fluorophores to induce a FRET quenching.[41-43] Several commercially available fluorophores, such as fluorescein 5(6)-isothiocyanate (λ_{em} ~ 518 nm), fluorescein 5(6)-carboxyfluorescein-N-hydroxysuccinimide ester (λ_{em} ~ 518 nm), and 7-nitrobenz-2-oxa-1,3-diazole (λ_{em} ~ 535 nm), were co-immobilized onto nanostructured silica surface functionalized with primary amines to achieve spatial proximity, providing a sensitive sensing platform to TNT detection. Compared to the corresponding pure dyes, these hybrid fluorophores showed 10-fold amplified quenching efficiencies with the limit of detection (LOD) of 1 nM for TNT in solution. Through this mechanism, the nitro-based electron-deficient explosives could be detected sensitively and selectively.

Besides the dominant use of explosive-induced fluorescence-quenching phenomena resulted from FRET mechanism, fluorescence-enhancement has also been reported for the detection of explosives.[44] Xia and co-workers found that addition of TNT molecules broke the pre-formed assembly between quantum dots (QDs) and gold nanorod (AuNR) and switched off the FRET from QDs to AuNR and then the fluorescent enhancement was achieved. This explosive sensor possessed a LOD of 0.1 nM which was one of the best results among fluorescent based explosive sensors. Such ultra-high sensitivity was attributed to the combination of a number of features including fluorescence turn-on effect, FRET switching-off and the unique design of fluorophore material.

For explosives detection, most of researchers have used PET and FRET mechanisms separately in individual sensing platform, our group recently demonstrated that the combination of FRET and PET mechanisms in dual wavelength nitro-explosive assay using a single material allowed an expansion of the dynamic detection range of 7 orders of magnitude (from 33 ppt to 225 ppm for TNT).[37] The pyrenyl-excimer emission was a suitable energy donor for the TNT-based Meisenheimer complex in a FRET-type interaction, while the nitro-explosives can also quench the pyrene monomer fluorescence along a PET pathway, which was inherently less efficient than FRET.

2.1.3 Electron exchange or Dexter interactions

Electron exchange (Dexter interactions) occurs between a donor and an acceptor, where the excited donor has an electron in LUMO (Fig. 1C).[23, 45] This electron is transferred to the acceptor, and the acceptor then transfers to an electron back to the donor. The electron comes from the HOMO of the acceptor, so the acceptor is left in an excited state. Dexter interaction is a short-range phenomenon that falls off exponentially with distance and depends on spatial overlap of donor and quencher molecular orbitals. RET association occurs over long distances, so if there is spectral overlap, the transfer occurs by RET is more important than the Dexter mechanism. Electron exchange can be observed and predominant over RET if the spectra overlap is small. Additionally, high concentrations are necessary for significant electron exchange, whereas RET occurs at much lower concentrations. With both RET and electron exchange processes, the shapes of the absorption and fluorescence spectra of the dyes are unchanged. Furthermore, the electron exchange process is a quantum mechanical effect that does not have an analogy in classical electrodynamics. Swager and co-workers reported on the selective detection of cyclic ketones via energy transfer, that was dominated by an electron-exchange mechanism to an upper excited state of the fluorophore followed by relaxation and emission to account for the efficient energy transfer in the absence of appreciable spectral overlap.[45] They proposed that the exquisite selectivity was due to a subtle balance of receptor specificity and the ability of analytes into the polymer matrix.

2.1.4 Intramolecular charge transfer (ICT)

ICT mechanism in sensing application is not new and researchers have already used ICT mechanism to develop conjugated polymer sensory materials for fluoride in the past.[46] However, application of ICT in explosive detection is relatively new. Recently in 2013, Xu's group employed this tactic and reported that DNSA-SQ could sense picric acid sensitively and selectively via an fluorescence turn-on signal in the near-infrared region.[47] DNSA-SQ behaved as a zwitterionic squaraine dye, where the stabilized negative charge on the nitrogen was connected to the conjugated backbone bearing a positive charge, and the dansylamide with a donor group was twisted away and perpendicular to the squaraine plane. The fluorescence change was attributed to the intramolecular charge transfer following the protonation of dimethylamine group by PA. Through judicious and rational design of ICT fluorescent molecules, a ratiometric approach for explosives sensing could be developed.

2.2 Fluorescence quenching theory

Fluorescence quenching requires molecular contact between the fluorophore and quencher. This contact can be resulted from diffusive encounters, which is dynamic quenching, or resulted from complex formation, which is static quenching.

The aforementioned two quenching processes possessing very different natures can be distinguished by time-resolved measurements of the fluorescence decays of the sensing materials. For static quenching, the fluorescence decay lifetime of a material will remain unchanged as the concentration of quencher is increased. Formation of a non-

6 | *Chem. Soc. Rev*., 2015, **00**, 1-3

This journal is © The Royal Society of Chemistry 20xx

fluorescent fluorophore-quencher complex is the origin of the quenching, and any molecules not bound to an analyte will decay with their native natural lifetime. For dynamic quenching (collisional quenching), collision of the quencher molecules to the excited fluorophores is a necessity, and thereby dynamic quenching is a diffusion-controlled process. The fluorophore and quencher are unbound and quenching occurs when a photoexcited material interacts briefly with a colliding analyte molecule. Thus it results in a decrease in the average fluorescence lifetime. The measurement of fluorescence lifetime change in the absence and presence of explosive quenchers represents the most prevalent way to examine whether the quenching is a static or dynamic process. Generally, the ratios of lifetime τ_0/τ are plotted versus the quencher concentration. For static quenching, $\tau_0/\tau=1$; in contrast, fluorescence intensity $F_0/F=\tau_0/\tau$ for dynamic quenching.

Collisional quenching of fluorescence is described by the Stern-Volmer equation and the correlation of lifetime with quencher concentration can be expressed as:

$$\frac{F_0}{F} = 1 + k_q\tau_0[Q] = 1 + K_D[Q] \qquad (5)$$

$$\frac{F_0}{F} = \frac{\tau_0}{\tau} \qquad (6)$$

where, F_0 and F are the fluorescence intensities in the absence and presence of quencher, respectively; τ_0 and τ are the lifetimes of the fluorophore in the absence and presence of quencher, respectively; k_q and K_D are the bimolecular quenching constant and Stern-Volmer quenching constant, respectively, and $[Q]$ is the quencher concentration.

For static quenching, the dependence of the fluorescence intensity upon quencher concentration is easily derived by consideration of the association constant for complex formation, and the equation is shown as follows:

$$\frac{F_0}{F} = 1 + K_S[Q] = 1 + K_D[Q] \qquad (7)$$

in which, K_S is the Stern-Volmer constant for static quenching process.

For combined dynamic and static quenching process, the change in fluorescence is to be given by

$$\frac{F_0}{F} = (1 + K_D[Q])(1 + K_S[Q]) = 1 + (K_D + K_S)[Q] + K_D K_S[Q]^2 \qquad (8)$$

when the analyte concentration is very low, the contribution of the $[Q]^2$ is less prominent and Equation (8) would yield to a linear plot. However, at higher concentrations, the plot deviates from linearity and bends upwardly. This equation greatly explains an upward bending curvature at high quencher concentrations or an exponential fitting of the Stern-Volmer plot under some circumstances.

While both pathways can be operative, static quenching prevails in explosives detection due to its larger K_{SV} for explosives binding to many polymeric indicators and a higher sensitivity in general. Although the fluorescent sensors of dynamic quenching have the potential to lead faster and more

reversible detection, they possess much smaller K_{SV} and demonstrate a lower sensitivity.[48]

Static and dynamic quenching can also be differentiated by their differing dependence on temperature and viscosity.[23] Higher temperatures result in faster diffusion and hence larger amounts of collisional quenching. While for static quenching, higher temperatures will typically promote the dissociation of weakly bound complexes, and hence result in lower amounts of non-fluorescent fluorophore-quencher complexes. One additional method to distinguish static and dynamic quenching is by careful examination of the absorption spectra of the fluorophore. Collisional quenching only affects the excited states of the fluorophores, and thus no changes in the absorption spectra are expected. In contrast, ground-state complex formation will frequently lead to perturbation of the absorption spectrum of the fluorophore. Furthermore, the bimodular quenching constant k_q is also used for discriminating between static and dynamic quenching, and k_q is calculated using the ratio of Stern-Volmer quenching constant (K_{SV}) to unquenched fluorescence lifetime (τ_0). For dynamic quenching, diffusion-controlled quenching typically results in values of k_q near 10^{10} M^{-1} sec^{-1}; while for static quenching, the k_q value is generally several orders larger than 10^{10} M^{-1} sec^{-1}.[49]

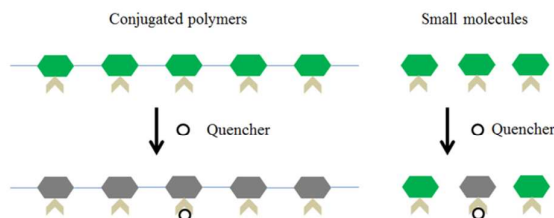## 3. Conjugated fluorescent polymers for explosives detection

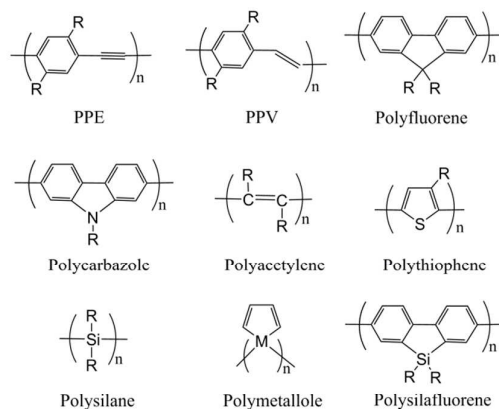Fig. 3 The schematic illustration of molecular wire theory.

Fig. 4 Basic backbone structures of the CPs in this review. PPE and PPV are the abbreviations for poly(phenylene ethynylene) and poly(phenylenevinylene), respectively.

Fluorescent conjugated polymers (CPs) have recently been used successfully in nitrated explosives detection.[20, 50, 51] Compared with small molecule fluorophores, they have extended exciton migration pathway and efficient electronic communication between quenchers along the polymer backbone. CPs are excellent electron donors, and their donor ability is enhanced by the delocalized π^* excited state, which facilitates exciton migration and hence increases the electrostatic interaction between the polymer and electron-deficient nitroaromatic analytes. For CP fluorescent sensors, Swager et al. proposed that binding one receptor site resulted in an efficient quenching of all emitting units in an entire conjugated polymeric molecule relative to single molecule systems. This amplification is known as the "molecular wire" effect, or "one point contact, multi-point response" effect, which is illustrated in Fig. 3. In general, fluorescent polymers can be divided into organic and inorganic categories considering their basic backbone structures as shown in Fig. 4.

3.1 Organic conjugated polymers
3.1.1 Poly(phenylene ethynylene)s
Poly(p-phenylene ethynylene) (PPE), a fully CP, exhibits high solution-state quantum yields and typically possesses wide band gaps, allowing for a bluer emission and broader range of explosives detection. PPE and its functionalized derivatives, or called PPEs, are the most prominent family of fluorescent CPs that used for the detection of NACs. The detection mechanism is the fluorescence quenching via electron transfer from electron-rich aryl groups on polymer chains to electron-deficient NAC molecules. However, condensed or solid-state PPEs suffered from self-quenching caused by inter-chain aggregation,[52] thus efficient sensing required the separation of PPE backbone with appropriate distance.

A pioneering work was achieved by Swager group to introduce pentiptycene units into the PPE backbone chains[51, 53], inspired by fluorescent sensing potentials for TNT detection of pentiptycene monomers, such as 1,4-diarylpentiptycenes[54]. The bulky rigid structure of pentiptycene could not only sterically isolate the PPE backbones in the solid state and therefore prevent self-quenching, but also create a porous structure and molecular scale channels which benefited the diffusion of explosive molecules into polymer films as shown in Fig. 5. Thin films of pentiptycene-derived PPE (parent PPE **1**) were highly emissive but underwent a dramatic reduction in emission intensity when exposed to NAC molecules. The fluorescence quenching of a 25 Å pentiptycene-derived PPE film was 50±5% by 30 s TNT vapor and increased to 70±5% at 60 s. The response of the same film to saturated DNT vapor was even faster (e.g., 91±2% fluorescence quenching at 60 s). The quenching rates by different NAC analytes depended on their vapor pressure, electron-deficiency, binding strength with the polymer diffusion rate through the polymer, and sensory polymer properties (such as electronic structures, film thickness and morphology). For a certain NAC, the response was strongly diminished with increasing the film thickness, which was due to binding of NACs near the film surface and thus blocking the pathways for the interior of thicker films.

These features of pentiptycene-derived PPE have been successfully utilized in a commercially available device, "Fido" (FLIR Inc.), for real-time monitoring buried explosives and landmines, roadside bombs, detection of suspected bomb makers, and some other homeland security-related fields.

Since then, great efforts were devoted by the same group for further optimization of pentiptycene-derived PPEs. In 2001, they reported one PPE based polymer **2** by introducing fused polycyclic aromatics, such as dibenzochrysene, and a longer excited-state lifetime and a more sensitive response to TNT were achieved.[55] In 2002, chiral aggregates of PPE **3** was demonstrated with a 4-fold increase in sensitivity toward TNT vapor compared with PPE **1**.[56] In 2005, electron-donating dialkoxyphenyl rings were fused onto the "wings" of the iptycene groups of PPE to synthesize a series of poly(iptycenebutadienylene)s **4**.[57] In 2011, they designed one kind of PPE polymer to selectively detect cyclohexanone via energy transfer. The good selectivity was possibly due to a subtle balance of receptor specificity and the ability of analytes to partition into the polymer matrix.[45] Compared with the parent PPE **1**, those polymers showed a manifestly higher quenching sensitivity toward DNT in chloroform, however, a slower quenching response to DNT than TNT vapor in the thin film, suggesting that the solid-state sensitivity might be
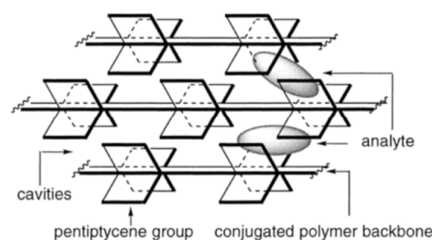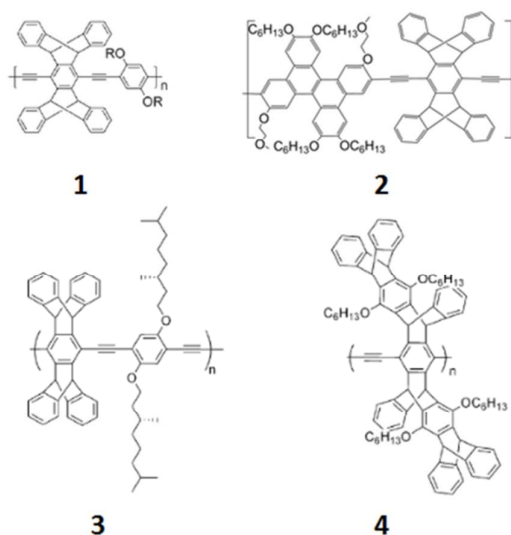
Fig. 5 Pentiptycene-derived PPE structure and cartoon of polymer porosity for analyte binding. Reprinted with permission from Ref. 53. Copyright 1998 the American Chemical Society.
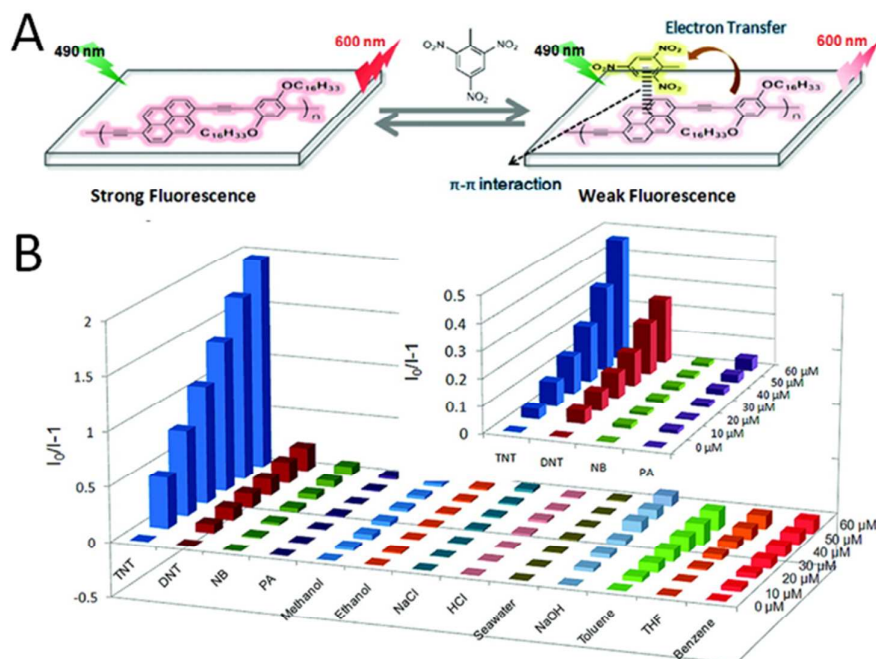
Fig. 6 (A) Schematic representation of the electron-transfer mechanism for the quenching of the fluorescent polymer film by TNT. (B) Stern–Volmer plots of NACs and common interferents to the fluorescence emission of the polymer film at different concentrations. The inset shows the Stern–Volmer plots of NACs to the fluorescence emission of film 3 at different concentrations. Reprinted with permission from Ref. 58. Copyright 2011 the American Chemical Society.

governed by different factors from those in solution-state.

Recently Fang's group also synthesized functional PPEs bearing pyrene units within their backbones.[58] Compared to the control polymer of PPE, the solution-casted thin films from these new polymers, poly(pyrene-co-phenyleneethynylene)s, showed dramatically enhanced quenching response to TNT in aqueous medium as shown in Fig. 6. The presence of pyrene units was ascribed to be responsible for the enhanced sensitivity and selectivity to TNT over other NACs (such as DNT, NB and PA), which gave much lower response with K_{SV} at least 1 order of magnitude lower than that for TNT. Such excellent sensing performance was originated from the specific interactions and the matching of the LUMO energies between TNT and pyrene units in the copolymers.

Recently, Wang et al. found that either by undercoating a layer of (3-aminopropyl)triethoxysilane or blending with a non-fluorescent polymer, poly(styrene-maleic anhydride), the detection sensitivity to DNT vapor was enhanced in the thin film of a pentiptycene containing PPE.[59] In another work, a series of PPE based CPs with commonly used conjugated units including thiophene, benzo[c][1,2,5]thiadiazole and benzo[c][1,2,5]selenadiazole were developed and applied for TNT detection in aqueous samples.[60] The researchers observed that bandgap of these polymers could be tuned effectively by co-polymerizing with different units, and the polymers demonstrated a better fluorescence quenching in response to TNT if electron-acceptor units had structures similar to diphenylquinoxaline in the PPE-derivatives chain.

By virtue of benefits of nanomaterials, Cheng et al. reported that the emission intensities of PPEs were increased by coating PPEs onto the surface of TiO_2 or ZnO nanoparticles.[61, 62] The resulted PPE nanocomposites, namely PPE/TiO_2 or PPE/ZnO, showed enhanced fluorescence responses to TNT vapor compared to pure PPE films. Similarly, Li et al. developed PPE-grafted silica nanoparticles that were applicable to detect TNT in solution.[63] The PPE-silica nanoparticles showed higher sensitivity than solutions of PPE alone, and the sensitivity increased with the decreasing of nanoparticles size.

3.1.2 Poly(phenylenevinylene)s

Poly(p-phenylene vinylene)s (PPVs, Fig. 4) family of conjugated polymers possess excellent photo- and electro-luminescence, and have been an extensive subject of fluorescent sensory materials. Similar to PPEs, PPVs also face the challenges of aggregation caused quenching in condensed state, and thus bulky substituted moieties have been incorporated into PPV backbones for their sensing applications in nitrated explosives. Hsieh et al. synthesized dialkoxy- and diphenyl- substituted PPVs **5** and **6**, both of which in spin-coated thin film were capable of fluorescence sensing towards TNT and 2,6-DNT vapors.[64] After that, a commercially available PPV derivative, poly[2-methoxy-5-(30,70-dimethyloctyloxy)-1,4-phenylenevinylene], showed not only quenched fluorescence when sprayed on a paper containing TNT fingerprints (~1-2 μg cm^{-2}), but also colour change from orange to dark brown.[65]

Since PPV is an anionic conjugated polymer, cationic compounds, such as methyl viologen (MV^{2+}) can also quench
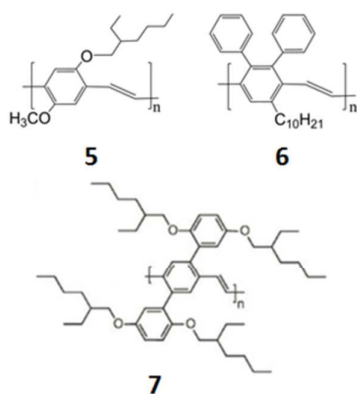
the fluorescence of PPV and thus become serious interferents during explosives detection. To address this issue, Chen et al. added a countercharged surfactant, odecyltrimethylammonium bromide (DTA), to neutralize the PPV matrix.[66] The interference response by MV^{2+} was reduced by 3 orders of magnitude and the quenching by TNT was amplified nearly 10-fold at a surfactant to polymer ratio of 1:3. A bilayered PPV-DTA film, which was prepared by dipping a PPV coated glass slide into an aqueous DTA solution, provided high sensitivity to quenching by NAC vapors and reasonable reversibility. Considering the effect of side-chains of CPs on fluorescence quenching performances, Smith's group designed a series of PPV and PPE derivatives and investigated their ability to detect TNT and DNT.[67] It was found that both electronic and steric influences of side-chains were important to the relative affinities for explosives detection in solution, while film porosity and the availability of free space around the π-system could affect the performance of sensing film.

Taking advantage of higher sensitivities of PPVs to NAC analytes by laser action, Swager and co-workers designed a ring-mode PPV with pendent phenyl groups with branched alkoxy substituent **7**, which endowed a lasing emission at 535 nm when excited with a nitrogen laser (λ=337 nm).[68] Upon exposure of the film to saturated DNT vapor for 1 s, the quenching at lasing emission was more than 30 times higher than observed from spontaneous emission peak at 500 nm. Similarly, Cheng et al. reported that exposed to saturated TNT vapor for 10 s, the attenuated lasing in a PPV-TiO$_2$ nanoparticle hybrid film displayed sensitivity over 20 times higher than that observed from spontaneous emission.[69]

RDX is a principal component of plastic explosives used in acts of terrorism and within improvised explosives devices. Detecting RDX vapor is an important and difficult task as it is 1000 times less volatile than TNT and is a weaker electron acceptor than nitroaromatic explosives. Through designing of conjugated PPV polymer network from olefin metathesis reactions, direct detection of RDX was achieved due to long exciton diffusion length, high surface area and improved control over film thickness by Dichtel and co-workers (Fig. 7).[70] The fluorescence of a cross-linked phenylene vinylene polymer network was quenched by trace amounts (even attogram) of RDX, and the films exhibited increased quenching responses as a function of polymer film growth time (Fig. 7B). The 72 h-

growth films showed 51±15% fluorescence quenching when exposed to 25 pg of RDX and saturated at about 71% at larger RDX doses. The polymer films had non-linear responses at pg RDX doses, while 72 h-growth films exhibited an approximately linear quenching response over the range of 1 ag to 30 ag (Fig. 7C), a promising level of sensitivity for detecting RDX from the vapor phase. The researchers hypothesized that the increased response of the 72 h-growth films, compared to those grown for shorter times, derived from longer exciton diffusion lengths that arose from the increased degree of polymerization of the network. The polymer film also demonstrated the ability to directly detect RDX vapors. This study indicates the great potential in the development of fluorescent materials for real-world explosive sensors. If the microscopic structures of amorphous, cross-linked polymer films could be controlled and improved, more promising sensing performance would be expected.
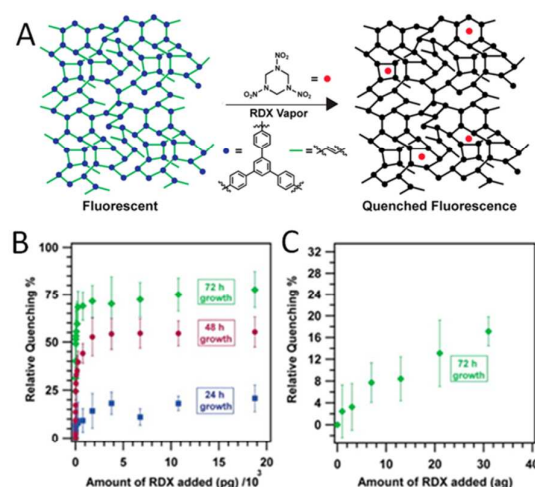

Fig. 7 (A) Schematic of RDX vapor detection by the tris(phenylene)vinylene (TPV) conjugated polymer network. (B) Quenching efficiency of TPV films on exposure to RDX in solution with varying time of reaction. (C) Quenching efficiency of 72 h TPV films in response to attogram quantities of RDX. Adapted with permission from Ref. 70. Copyright 2013 the American Chemical Society.

Considering larger surface area of materials favourable for sensing applications, the advances in the synthesis of nanomaterials have also been applied in this context. Due to the slow photon effect of photonic crystal and large surface areas of the inverse opal structure, optimized photonic crystal method was used to prepare fluorescent sensory materials through PPV **5**.[71] TNT sensors were prepared by spin-coating **5**-chloroform solutions with different concentrations onto inverse opal SiO$_2$ photonic crystal films and glass substrates. The fluorescence enhancement (up to 60.6-fold) for TNT detection was achieved when compared to the control sample. Such amplification of fluorescent signal provides a facile method for improving sensitivity and resolution of explosives detection.

10 | *Chem. Soc. Rev.*, 2015, **00**, 1-3

This journal is © The Royal Society of Chemistry 20xx

Besides the focus on the development of sensory materials, researchers also make use of the FRET mechanism in the construction of innovative explosives sensors. Amine-functionalized mesoporous silica nanoparticles containing poly(p-phenyvinylene) PPV@MSNs were designed for TNT detection due to formation of TNT-amine Meisenheimer complex.[38] The same group later designed water-soluble graphene-oxide (GO) functionalized amine-modified mesoporous silica nanoparticles containing PPV.[72] The sensing materials showed the high sensitivity and selectivity for TNT detection in the water system through FRET quenching. In this study, GO was introduced to the PPV-MSNs in order to increase the water-solubility and to improve the detection sensitivity of the hybrid systems, and a detection limit to TNT of 1.3×10^{-7} M was obtained. Although these systems showed great sensing performance through FRET mechanism, the preparation was rather complex and troublesome, which could potentially limit their wide applications.

3.1.3 Polyfluorenes

Polyfluorenes (PFs, see Fig. 4) are a very unique class of conjugated polymers that their highly emissive fluorescence can be tuned through the entire visible range. PFs are not naturally existed but designed and synthesized from their monomers, fluorene and fluorene derivatives. Pei et al. fabricated fluorescent nanofibers of a bulky dibenz (a, h)anthracene containing PF by electrospinning.[73] The applied electric field of electrospinning process accelerated the solvent evaporation to quickly freeze the polymer chains onto confined and dispersed locations before they reached self-aggregation states. Polystyrene was chosen as the supporting matrix because the phenyl groups in polystyrene side chains had π-π interactions with the rigid backbone of this new polymer and thus reduced the aggregation. Sodium dodecyl sulfate was added into the electrospinning precursor solution to introduce a secondary porous structure by subsequent solvent extraction. The fluorescence of electrospun membranes with secondary pores was quenched by around 40% after exposure to DNT vapor for 10 min and 75% for 1 h exposure, much higher than a spin-casting dense film in the same period of exposure (5% quenching). In another study, Wang's group coated an optic-fiber tip with a dibromide-dicholesteryl-terephthalate containing PF **8** for DNT detection.[74] Upon exposure to saturated DNT vapor, the fiber probe gave a 23% drop in fluorescence at 23 s and 60% within 1 min. The great sensitivity and rapid response to DNT suggested that the PF polymer on fiber-optic allowed remote detection of explosive compounds.

8   **9**
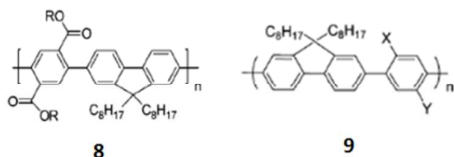
Furthermore, their biphenyl framework makes fluorene moieties out of ordinary by increasing the polymer band gap energy and producing a higher energy LUMO orbital and a

larger redox driving force for a wider range of explosives. For example, nitroalkanes, such as DMNB, have more negative reduction potentials than NACs and are lack of aromatic rings to form π-stacking with CPs, rendering them difficult to be detected by fluorescence quenching. To increase the efficiency of fluorescence quenching, a series of poly(fluorene-phenylene)s **9** were designed by Swager and co-workers for the detection of DMNB.[75] These polymers possessed a band gap of 0.3 eV larger than that of PPE **1** and allowed for a highly reversible and rapid quenching response of about 20% for DMNB vapor. However, interferents such as benzophenone, which had a similar reduction potential and vapor pressure to DMNB, gave a much stronger response with a slower recovery time.

Patil et al. also designed one novel fluoranthene based chemosensor with an asymmetric phenyl ring on the fluoranthene moiety, which weakened the π-π interactions and led to formation of layer-by-layer assembly of the molecules. The structural modifications of fluoranthene by increasing the electron-donating strength and extending conjugation by removal of bromine atoms would furnish highly selective fluorescent chemosensors for the explosives detection with higher sensitivity.[76] The incorporation of the two groups (phenylene spacers adamantine moieties) into polymer side chains could retain an effective conjugation length and prevent the π-stacking of polymer chains.[77] The pathways or cavities generated by the two spacers maintained the long conjugated length of the polymer chain, and were beneficial for the rapid diffusion of explosive vapor into the film interiors, thus increased the quenching efficiency.

The fluorescent polymer nanoparticles has also been introduced into the field of explosives detection and synthesized through re-precipitation methods from polyfluorenes.[78] The nanoparticles were formed from the hydrophobic collapse of fluorescent polymer chains and displayed quenching efficiencies. Non-covalent aggregation of the polymer chains was necessary for efficient energy transfer. This solvent-induced swelling caused the individual polymer chains in the nanoparticles to separate, which limited inter-chain aggregation and thus improved the nitroaromatic-induced quenching efficiencies. However, the overall quenching performance was relatively poor in the study and needs to be further improved.

Tong and co-workers found that the bulky spirobifluorene unit reduced the π–π packing of polymer backbones and the incorporated electron-donating carbazole units rendered the polymer gelator as a good sensory material for electron-deficient nitroaromatics.[79] The porous film generated from its toluene solution displayed high sensitivity to TNT and DNT vapors, with the fluorescence quenching efficiency reaching 85% within 60s for DNT vapor. The great sensing performance was attributed to its porous morphology, while the control dense film showed much lower sensitivity. The study here suggests that polymer film with facile morphology could be easily achieved by simple selection of suitable solvents.

Zhang et al. found that electro-polymerized (EP) PF polymer film showed the great sensing performance to TNT

explosives.[27] The alkyl-linked peripheral carbazole groups carried out the electrochemical coupling reactions under anodic oxidation and provided a cross-linking network structures during the process. The separation of the fluorescent units from the electro-active carbazole group ensured that the EP process had no impact on fluorescence. The same group also synthesized 9,10-bis(9,9-bis(6-(9H-carbazol-9-yl)hexyl)-9H-fluoren-2-yl)anthracene (TCAC) films through electrochemical polymerization. The as-synthesized film was then applied as sensitive and selective fluoremetric and electrochemical dual channel explosive sensors.[80]

Due to the hydrophobicity of most CPs, amphiphilic cellulose nano-micelles with a hydrophobic inner core and a hydrophilic outer shell were developed for explosives detection in aqueous phase.[10] The core was formed by alkyl segments, which acted as a reservoir for accommodating the hydrophobic fluorescent CPs. The hydrophilic outer shells formed by the polysaccharide main-chain favored the dispersion of the aggregates in water. The fluorescent poly(9,9-dioctylfluorene) - loaded micelle nano-aggregates possessed sensitivity to hydrophobic nitroaromatics in aqueous solution, which was 50-fold higher than that of the chromophores in organic solvent.

3.1.4 Polycarbazoles

Polycarbazoles (PCs) are relatively new and less-developed sensing materials in explosives detection. Yu and co-workers copolymerized 3-(N-methacryloyl) amino-9-ethylcarbazole (MAEC) with 2-hydroxypropyl methacrylate, and the membrane of this new polymer showed a linear fluorescence quenching response towards picric acid in the concentration range of 9.33×10^{-8} to 9.33×10^{-5} M.[81] The response was selective to picric acid and was little affected by co-existing organic and inorganic interferents. Recently, Zhang et al. reported a bulky side chain, 4-[tris-(4-octyloxyphenyl)methyl] phenyl, substituted carbazole **10** for explosives detection.[82] The rigid side chain moieties weakened self-quenching and generated pathways to improve TNT's diffusion. The spin-coating film of this fluorescent polymer generated about 57% quenching in 30 s and 73% in 60 s for TNT vapor. Interestingly, this polymer film showed lower response to DNT vapor, although the saturated vapor pressure of DNT was much higher than that of TNT, indicating that the analyte electron-deficiency was the dominant factor in this quenching process.

Carbazole based TCB-CMP **11** and CB-LP **12** were also developed and applied as fluorescence sensors for detection of arenes by Jiang et al.[29] Due to the better exciton migration over three-dimensional network, the TCB-CMP showed a
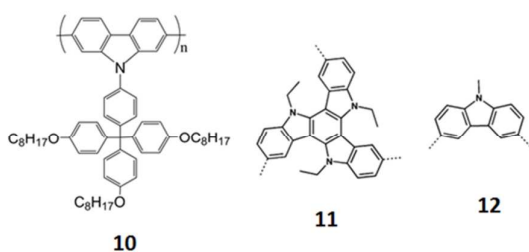
higher degree of quenching to DNT, NT, NB and BQ. These results indicated that the function of CMP architectures were multifold: the extended π-conjugation network allowed exciton migration, the high-surface-area skeleton provided a broad interface for electron transfer, and the micropores held the arene molecules in a confined space. The report here suggested that TCB-CMP materials may provide insights into discrimination between electron-rich and electron-deficient arenes due to opposite outputs with fluorescence-on and fluorescence-off characteristics through mechanisms as shown in Fig. 2.

Zhang and co-workers developed carbazole based polymers possessing 2-ethylhexyl and 4-[tris-(4-octyloxyphenyl)mehtyl] phenyl as side chains.[83] They observed that PC film with larger and more rigid side chain had much higher sensitivity to TNT vapors. Larger and more rigid side chain reduced the interactions between polymer chains in the solid state and enhanced the diffusion of explosives through more accessible space, thereby contributed to better sensing performance due to the higher electron donor abilities and unique microstructures. In addition, relative conformation of its backbone was almost unaffected by the choice of side chains and the relative conformation was the basis for the fluorescent conjugated polymers sensing materials.

3.1.5 Polyacetylenes

Polyacetylene and its bisubstituted derivatives (PAs) are another group of CPs and have been applied to explosives detection. Sabatani et al. applied polydiacetylene for TNT sensing directly without any polymer chain substitution.[84] A Langmuir-Blodgett film was coated on a porous silicon surface and exhibited a fluorescence quenching (although not completely) phenomenon to explosives after dipping in TNT aqueous solution (100 mg L^{-1}) overnight. The unsubstituted PA was unstable to oxidation and difficult to process, and thus much attention has been redirected to other substituted derivatives. A diphenyl-substituted PA, poly(1-(p-n-butylphenyl)-2-phenylacetylene) **13**, in spin-coated thin film (25 Å) by Chang et al. showed 10% quenching response by TNT vapor upon 10 s exposure. This response, however, was relatively weaker than substituted PPVs, which was ascribed to the highly twisted backbone structures of **13**.[64] Another diphenyl-substituted polyacetylene, poly (1-phenyl-2-(4-trimethylsilylphenyl)acetylenes (PTMSDPA, **14**) was spin-coated or freeze-dried into thin films.[85, 86] Schanze and co-workers demonstrated that thin films of this fluorescent polymer were selectively quenched by NAC vapors, and showed increased quenching rates with decreasing film thickness.[85] In the presence of saturated 2,4-DNT vapor, 50% quenching was reached in 20 s for a 3 nm thick film. Other aromatic compounds such as chloranil, 1,4-dimethoxybenzene (1,4-DMB), and 1,2-dimethoxybenzene (1,2-DMB) gave rise to very little quenching. Kwak et al. adopted a freeze drying method to prepare **14** as fine-structured nanofibrous membrane with a large free volume of about 0.26.[86] These fluorescent polymer fibers with a diameter of approximately 50 nm on average, obtained from 0.003 wt% cryogenic benzene solution, showed a 50% quenching in 35 s upon

10

11

12
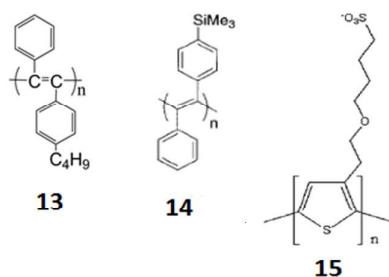
exposure to 2,4-DNT vapor and 95% within 25 min. In comparison, a 90 nm thick spin-coated condensed film had a much slower response time (240 s) to quench 50% of its initial fluorescence. Such enhanced sensitivity in freeze drying nanofibers compared with dense films was attributed to their higher porosity and larger surface area.

3.1.6 Polythiophenes

Polythiophenes (PTs) are π-conjugated polymers that demonstrate interesting optical properties, such as visible absorption and strong fluorescence emission, which render them suitable for nitrated explosives detection. However, there were only a few reports of PTs based optical sensors in this area. Rubio-Retama et al. reported a poly(thiophene-ethyl buthyl sulfonate) (PTEBS, **15**) entrapped microgel for the detection of picric acid.[87] This fluorescent colloidal microgel was formed through the polymerization of N-isopropyl acrylamide in the presence of commercially available PTEBS, and showed in swollen or collapsed state when the temperature was lower or higher than the low critical solution temperature at 32 °C. The fluorescence quenching sensitivity for picric acid was better in swollen state than in collapsed state, due to the stretched microgel chains increased the quencher accessibility to the fluorophore PTEBS. The microgels could be reused by increasing the temperature above the low critical solution temperature, when the collapsed microgels squeezed out the quencher molecules and recovered the fluorescence signal (Fig. 8). Recently, Venkataraman et al. investigated the effect of PT side chains on the NACs sensitivity.[88] They found that 1,2,3-triazole side chains had interactions with NACs and therefore enhanced the
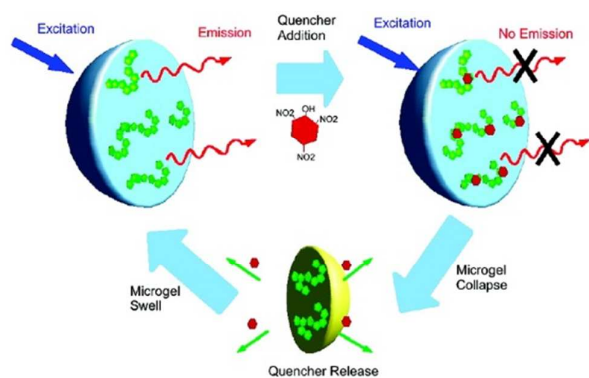

Fig. 8 Mechanism of PL quenching and recovering of the initial fluorescence of interpenetrated microgels. Reprinted with permission from Ref. 87. Copyright 2009 the American Chemical Society.

fluorescence quenching in the presence of DNT and TNT vapors. In addition, bulky side chains decreased the chain packing in thin films and resulted in higher sensitivity towards DNT vapor. A 30 nm thin film of PT containing 1,2,3-triazole with appropriate alkyl side chains showed 89% and 47% quenching efficiency towards DNT and TNT vapors for 5 min, respectively.

Liu et al. also fabricated nanofibrous film through electrospinning by doping sulfur-containing fused ring benzothiophene based conjugated polymer (fluorene) containing heteroatom polycyclic units with a polystyrene supporting matrix.[89] The produced explosive sensor showed stable fluorescence property, as well as satisfactory selectivity and reproducibility. The sensing performance of fluorescence nanofibrous film was attributed to unique porous structures and the limited aggregation and self-quenching of polymer. Saeki et al. proposed detection and distinction between DNT and TNT using one polythiophene cyclopentadithiophene-bithiazole-based polymer as sensory materials through combination of fluorescence and conductivity techniques.[90] The conventional fluorescence quenching experiments showed turn-off of polymer fluorescence by both DNT and TNT, while the photoconductivity of the polymer was still turn-off in presence of TNT, and turn-on in presence of DNT. Through the combinations, the TNT and DNT can be detected and differentiated, thus enhancing the selectivity.

3.1.7 Other organic fluorescent polymers

In addition to those typical polymers discussed above, many other organic fluorescent polymers have also been reported to demonstrate sensitivity to the detection of nitrated nitro-explosives. Zhang et al. synthesized two organic conjugated polymers that composed of benzene and quinoxaline moieties and alternatively linked by C=C double bonds and C≡C triple bonds (**16** and **17**).[91] Both of the polymers in solutions and thin films showed fluorescence quenching sensitivity towards TNT. 5 ppm TNT in chloroform solution resulted in **16**'s and **17**'s fluorescence quenching of 11% and 26%, while exposing to saturated TNT vapor for 1000 s brought 79% and 85% quenching to **16** and **17** films, respectively. Very recently, a 2D cross-linked polymer was designed and synthesized via a light-induced tetrazole-alkene cycloaddition reaction in mild and green condition, and then applied as fluorescent materials for explosives detection.[92] Buruiana and co-workers reported two side-chain dansyl-labled acrylic copolymers.[91] Fluorescence emission of both dansyl-copolymers was quenched in the presence of NACs (e.g., picric acid, NT, nitrophenol, dinitro-m-xylene, NB) in solution. For nitrobenzene vapor, the fluorescence quenching of DnsSA-co-DA **18** film reached 36% after 130 min exposure, and that of DnsSA-co-MMA **19** reached 12.5% after 75 min without further quenching. However, metal ions, such as Cu^{2+}, Fe^{2+}, Ni^{2+}, also quenched the polymer fluorescence, which may interfere with explosive detection. Sun's group fabricated poly(ethylenimine) and poly-(propionylethylenimine-co-ethylenimine) wrapped single-walled carbon nanotubes that were strongly fluorescent in both solution and solid state.[93] The fluorescence emission was sensitive to NACs such as NB, 4-NT, and 2,4-DNT. Interestingly,

this quenching phenomenon was more efficient at a shorter excitation wavelength or in a more polar solvent. Lin et al. used a fluorescent curcumin moiety as a 2,6-DNP binding site to substitute poly(vinyl chloride) (PVC) **20**.[94] This curcumin-PVC conjugate showed better sensitivity and selectivity in explosive detection compared to PVC membrane with physically entrapped curcumin. 5 µm plasticized curcumin-PVC membrane exhibited an optimal sensing performance for 2,6-DNP at pH 3.5 with a LOD of 1.0×10^{-6} M. The selectivity for 2,6-DNP was originated from the space geometry matching between the quencher and the polymer to form a cyclic complex. Later Liu et al. reported on a highly cross-linked and organic-inorganic hybrid polymer microspheres PCPC-MS, which was facilely prepared by a one-step precipitation copolymerization of HCCP and curcumin.[95] The experimental results demonstrated that the high-efficiency and highly selective quenching of the fluorescence emission by PA was due to the acid-base interactions, enriching PA on the surface effectively, and thus facilitating the formation of a ground-state energy transfer process.


16 **17** **18** **19** **20**
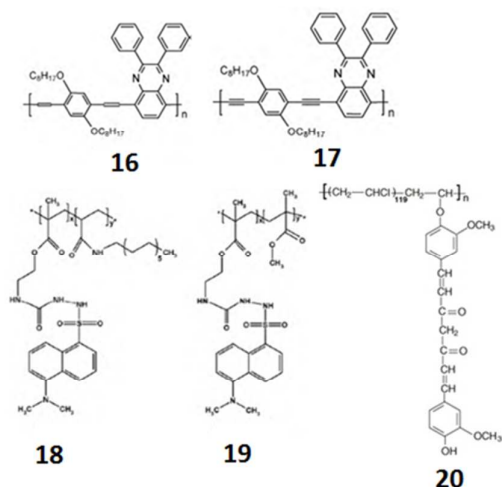
Changing the charge of the polymer is another solution to improve the sensing performance of CPs to explosives detection. For example, one new cationic CP PMI was developed using post-functionalization method through appending imidazolium groups as side chains.[96] PA detection at ppt levels with remarkable selectivity was achieved in aqueous media and on a solid platform using paper strips and chitosan films. Both theoretical and experimental studies suggested that charge transfer was a predominant process. The formation of a ground state charge transfer complex, RET as well as favourable electrostatic interaction between PMI and PA were the key aspects for unprecedented selectivity and remarkable sensitivity of PMI towards PA.

3.2 Inorganic conjugated polymers

3.2.1 Polysilane

Polysilanes are air-stable highly fluorescent polymers with high mobility and unique electronic properties. These properties arise from their σ-conjugated Si-Si backbone, along which electrons are delocalized to provide an effective exciton migration pathway, similar to that of conjugated polymers.

Early research in applying polysilane for the detection of NACs has been explored by Fujiki and co-workers.[97] They synthesized a NAC chemosensory material based on fluoroalkylated polysilanes **21**, and revealed that this material was very sensitive to NACs in THF solution and in the solid film for aqueous detection. The fluorescence quenching mechanism was the photo-induced electron transfer (PET) from Si atoms of σ-conjugated to the NAC nitro groups. Electron-withdrawing CF_3 groups were further introduced to the Si atoms in the backbone for an enhanced sensitivity, which was nearly 200 times better than that of non-fluoroalkyl polysilane. The fluorescence was reversible by rinsing with water or methanol and had no response to interferents such as organic solvents, aqueous inorganic acids and oxygenated air.

21
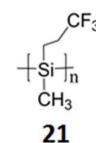
3.2.2 Polymetalloles

Polymetalloles (Fig. 4) are inorganic derivatives of polypyrrole in which the N atoms are replaced by metallic atoms, such as Si, Ge, etc. Among them, polysiloles **22** and polygermoles **23** are of much research interests as chemical sensors, because of their unusual electronic and optical properties. Similar to polysilanes, polysiloles also possess σ-σ* delocalized Si-Si backbones for efficient exciton migration. In addition, the unsaturated five-membered rings of the silole in the backbone provide σ*-π* interaction between the σ* orbital of the silicon chain and the π* orbital of the butadiene moiety, resulting in a lower reduction potential and LUMO energy. The Trogler group reported on a series of polysiloles for explosives detection.[98, 99] Their early research demonstrated the application of polysilole-coated films for NACs solid residues and in seawater.[98] The response of polysiloles was 38% higher than that of 15-repeat unit oligomeric silole, which was ascribed to the longer diffusion length of excitation in polysiloles. Thin film of polysilole was sensitive to NACs in seawater with the detection limits of 50 ppb and 6 ppb for TNT and picric acid, respectively, and was also capable of visual sensing of TNT solid residues on surface. A later research compared the fluorescence quenching response to NACs from a series of poly(tetraphenyl)metalloles containing Si-Ge polymetalloles **23**, silole – silane **24**, and germole - silane **25** copolymers.[99] Each polymer had a unique ratio of quenching efficiency to the corresponding analyte and each analyte had a variety of different responses to different polymers, which could be utilized in a sensor array for discrimination of specific explosives. The bulk phenyl substituents on the cyclopentadiene rings served as the spacers to protect polymers from self-quenching in solid state and featured a helical arrangement through the close packing of side chains. Compared with PPE **1**, those poly(tetraphenyl)siloles had higher quenching efficiencies to detect NACs in toluene solution, but lower efficiencies for vapor detection in polymer

solid states (thin films). The same group also found that the aggregation-induced emission (AIE) phenomenon in oligo(tetraphenyl)silole nanoparticles was favorable for TNT detection in aqueous solution.[100] Oligosilole nanoparticles were prepared by precipitation from its THF solution by the addition of water, and showed an over 4 times higher of fluorescence quenching efficiency than that of the dissolved oligosilole and a LOD of 100 ppb for TNT in pH 7 buffered solution was realized.
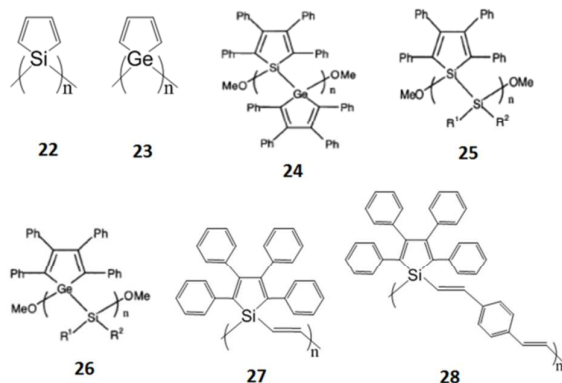
Vinylene repeating units were later introduced into the backbones of poly(tetraphenyl)siloles **27** through a hydrosilylation reaction to provide regioregular trans-products.[101] These vinylene bridges between backbone siloles extended the conjugation and diminished the band gap in the polymeric materials by replacing Si-Si backbone with a strong Si-C stronger backbone, and the trans-stereotype maximized $\sigma^*(Si-C)-\pi/\pi^*(vinylene)$ delocalization through the polymer backbone. As a result, higher K_{SV} were obtained for NACs such as DNT, TNT and picric acid in solution. Similarly, another research incorporated phenylene divinylene with silole units **28**, and achieved 100 pg cm^{-2} detection limit for TNT.[102] Tang's group later reported the synthesis of one 3-silolene derivative bearing four dimethylsilyl groups.[103] The aggregates in aqueous mixture can be quenched efficiently by picric acid with large K_{SV} values. The sensing performance could be explained by AIE mechanism.

3.2.3   Polysilafluorene

Silafluorenes are 9-Si substituted derivatives of fluorene possessing similar core electronic features but they are more stable to environment. Trogler's group synthesized poly(tetraphenylsilole-silafluorene-vinylene) **29** and poly(silafluorene-vinylene) **30** for a wider range sensing applications not limited to NACs.[101] Compared with
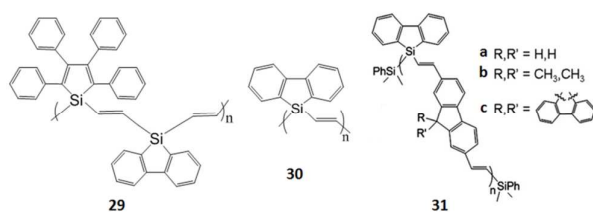
poly(tetraphenylsilole-vinylene) **27**, the incorporation of silafluorene units in the polymer backbone widened the band gap and allowed for the detection of a broader range of explosive materials. In the solid state, polymer **27** was quenched only by NACs, while polymer **29** was able to detect both RDX and NACs, and polymer **30** was capable of detection the entire range of nitrated explosives, including RDX, HMX, TNG, PETN and NACs. For example, although RDX was unable to be detected by polymer **30** in solution, RDX particulates efficiently quenched the polymer **30** film fluorescence with a detection limit of 2 ng cm^{-2}. However, the fluorescence of polymer **30** was mainly in UV range (λ_{em}=362 nm in solution, and λ_{em}=376 nm in thin film state) and was difficult for visual assessment. In this case, they synthesized polysilafluorenes through introduction of phenylene units into polymer backbone for an enhanced visible blue emission and easier visualization.[102] Further studies by the same group concentrated on improving the detection sensitivities and polymer quantum efficiencies.[104] A series of poly(silafluorene fluorene)s **31a-c** were synthesized and they had fluorescence quantum efficiencies in the range of 20-100%, much higher than their previous reported polymers such as **29** and **30**. The steric bulky fluorene units in the polymer backbones afforded large intramolecular spacing and allowed better binding of analytes to the Lewis acidic silicon. The entire range of nitrated explosives particulates were able to be quenched by the polymer thin film. Typically, Tetryl had the lowest detection limit down to 1 pg cm^{-2} in the solid state. In addition, they found that **31a** showed an initial fluorescence quenching by PETN with UV-light, followed by a subsequent green fluorescence "turn-on". This "turn-on" fluorescence originated from a selective photo-oxidation of fluorene units by PETN, as described in the Fig. 9.
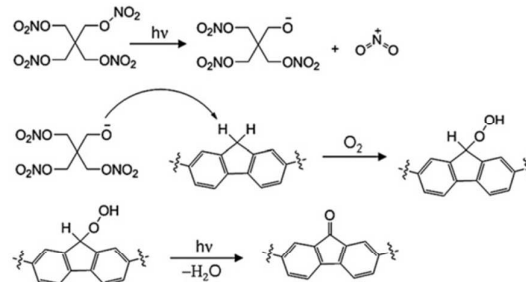
Fig. 9 Proposed mechanism for the selective oxidation of polymer 31a by PETN. Adapted with permission from Ref. 104. Copyright 2008 the Royal Society of Chemistry.

Trogler's group further reported on the covalent surface attachment of polysilafluorene polymers on a silica gel thin layer chromatography support, and more efficient quenching by the explosives analytes was achieved due to the presence of small amounts of fluorophores.[105] The attachment of the sensing polymer onto the support also allowed for simultaneous separation of an explosive mixture. Later Wan and co-workers synthesized a series of linear 2,5-tetra-phenlysilole-vinylene type polymers.[106] The tetraphenylsilole moieties were linked at their 2,5-positions through vinylene

bridges to obtain 2,5-tetraphenylsilole-vinylene polymers (PSVB and PSVC) and through an ethyne bridge to obtain 2,5-tetraphenylsilole-ethyne polymer (PSEB). The PSEB exhibited AIE effect, but the 2,5-tetraphenylsilole-vinylene-type polymers were AIE-inactive. Both the AIE-active and -inactive polymers have been used as chemosensors for the detection of explosive compounds.

Besides the experimental explosives sensing studies, Monari et al. investigated the optoelectronic properties of the polysilafluorene and polysilole polymers and their constituents units by modeling the properties of their excited states.[107] They found that the improved optoelectronic properties of the polymers arose from the increased delocalization of the conjugated bridge through the silicon centers in the silafluorene and silole moieties. The complexation of polymers with the analytes produced a tail in the absorption spectra of the complexes, which was attributed to the charge transfer from the polymer to the analyte and static quenching mechanism.

4. Small molecule fluorophores for explosives detection

Small fluorophores are the main focus in the early development of fluorescence-based explosive sensors, because they provide a variety of benefits such as simple synthesis, varied pathways of fluorescence quenching and ability to detect a wide range of explosives. The main difference between conjugated polymeric systems above and small molecule-based detection lies in the mechanism of fluorophore quenching and the absence of excitonic migration in the small molecules. Polymer-based sensors frequently detect explosives through static quenching; in contrast, well-resolved small molecules typically work through collisional quenching. A further difference is that conducting polymers exhibit increased quenching efficiency as several excitons within a polymer can be quenched by one molecule of bound analyte; small molecule fluorophores are quenched in stoichiometric fashion of one analyte per fluorophore (as shown in Fig. 3). Generally, small molecules have been divided into organic ones and inorganic ones. Besides simple small molecules, functional small molecule fluorophores have been appearing and attracting great attention in recent years, and presumably show greater potential in explosive sensing by the form of oligofluorophores, self-assembling small fluorophores or doping of these molecules into a matrix, because they can enhance binding and/or introduce exciton migration.

4.1 Organic small molecules

4.1.1. Polycyclic aromatic hydrocarbons (PAHs) and PAH-derivatives

Polycyclic aromatic hydrocarbons (PAHs) are structurally similar organic molecules characterized by the presence of fused aromatic rings, such as pyrene, anthracene, perylene, naphthalene, etc. Most PAHs have high fluorescence quantum yields with remarkable electron donor nature, which allows for the formation of non-fluorescent charge transfer complexes

with electron deficient molecules. Considering the fact that they also facilitate π-π interactions with aromatic compounds, PAHs constitute an important class of small fluorophores for nitrated explosives, NACs in particular.

Among PAHs, pyrene and its derivatives have been widely explored. Their fluorescence spectra show monomer emission characteristics in the UV range (below 400 nm) at dilute concentrations (e.g., < 0.001 M in solution). With increasing dye concentration in solution or fabricated in the solid state, the fluorescence peak shifts bathochromically to the visible range, which is assigned to the formation of excimer, or "excited dimmer". Both pyrene monomer and excimer emission can be quenched by electron-deficient nitrated explosives, and the planar shape of pyrene forms strong π-π stacking with NACs. McGuffin and coworkers reported that nitrated explosives could effectively quench pyrene monomer fluorescence at 375 nm in solution.[108] The K_{SV} of pyrene with seventeen common explosives were calculated and the result showed that NACs were more effective quenchers than aliphatic or nitramine explosives. This quenching mechanism was further studied by the same group via ab initio calculations using the quencher NM.[109] A theoretical model was developed and the most likely mechanism was concluded to be the formation of excited fluorophore-quencher ion pairs followed by the electron transfer from pyrene to nitrated explosives. Focsaneanu and Scaiano compared the quenching profiles of pyrene monomer and excimer, and proposed that the ratio of monomer-to-excimer emission intensities allowed discrimination towards different explosives.[110] Lee et al. reported the dipyrene-appended calix[4]arene with the two pyrene substitutes oriented to the same side of the ensemble.[111] Both the monomer (λ_{em} = 375 nm) and excimer (λ_{em} = 470 nm) emission were quenched upon the addition of TNT in acetonitrile with a detection limit down to 1.1 nM. A further single-crystal X-ray diffraction analysis revealed that TNT formed a charge-transfer complex with the two pyrene subunits at a distance of 3.2-3.6 Å through an intermolecular π-π interaction. Later, Cho et al. reported a dipyrenyl pocket chemosensor which was able to detect < 2 ppb of TNT in a semi-aqueous solution.[112] Upon addition of TNT, the excimer band decreased, whereas the monomeric bands increased upon addition of TNT. These fluorescence changes were unique compared with other fluorescence quenching sensors, which was possibly due to interference of excimer formation. TNT and the receptor formed a charge-transfer complex between two pyranyl group (dipyrenyl chemosensor); this was supported by an AM1 calculation, a Job plot analysis, and the binding constants obtained for TNT. Very recently, researchers reported on the utilization of pyrene excimer emission (intensity and lifetime measurements) of a pyrene derivative that allowed sensing and distinction of electron deficient explosive compounds.[113]

Besides dissolved in solution, pyrene has also been incorporated onto solid state materials to detect nitrated explosives. Balkus et al. developed 2,7-diazapyrene grafted periodic mesoporous organosilicas, which showed 81% quenching upon exposure to 120 μM of NB, but no appreciable

16 | *Chem. Soc. Rev.*, 2015, **00**, 1-3

This journal is © The Royal Society of Chemistry 20xx

response for NM.[114] Shen et al. reported an optical sensor fabricated by covalently immobilization of 1-aminopyrene on the outmost surface of quartz glass slides.[115] Au nanoparticles were used as bridges and carriers for anchoring indicator dyes. The linear response to picric acid covered the range of 9.55×10^{-7} to 1.91×10^{-4} mol L^{-1} with the detection limit of 7.8×10^{-7} mol L^{-1}. Chen et al. carried out a study to examine the application of pyrene-functionalized Ruthenium (Ru) nanoparticles for the detection of NACs.[116] The metallic Ru core served as a conducting medium for an extended intraparticle charge delocalization, leading to a quenching efficiency more than 1 order of enhanced magnitude than the equivalent concentration of 1-bromopyrene in DMF solution. Nagamura and co-workers found a pyrene ammonium derivative (PyAm) formed nano-sized aggregates in poly(vinylalcohol) (PVA) matrix.[117] PyAm was simply mixed with PVA in solution and then the mixture was spin-coated or drop-casted onto quartz plates, where the PyAm aggregated to nanoparticles by phase separation. The quenching efficiencies of these nano-aggregates to NACs were related to the amount of pyrene excimer species and increased with enhancing initial PyAm concentrations. Paz et al. also used novel pyrene motifs as chemosensors for explosives and found that phosphonated pyrene derivatives showed high selectivity to TNT.[118] The phosphonate groups attached to the pyrene and decreased the LUMO energy, with the pyrene tetraphosphonic acid (PO) exhibiting simultaneous π-π stacking and strong hydrogen bonding interactions between the phosphonic acid and the nitro groups of TNT, thus enhancing sensitivity and selectivity. In addition, the phosphonate groups attached to pyrene favored the formation of a porous or fibril-type layer of thin films, and promoted the easy diffusion of analytes to the film. In addition, in our opinion, there might be some other reasons that contribute to the higher quenching efficiency of PO than that of PE, possibly similar to the enhancement by supramolecular polymers which might be formed in PO due to hydrogen bonding. The details will be discussed in the Section of supramolecular polymers.

Naphthalene is another frequently studied PAH. For example, binaphthyl functionalized stilbenes was synthesized by Takeuchi and co-workers for the detection of DNT and TNT vapors.[119] The sensing ability was studied in the film state by drop-casting 1:3 (v/v) chloroform-toluene solution of the derivative, where the film showed self-assembled entangled networks of nanofibers and a bright yellowish-green fluorescence. Upon exposure to saturated DNT and TNT vapors for 10 min, the self-assembled film showed 91% and 72% quenching, respectively. Fang and co-workers reported a series of 5-dimethylamino-1-naphthalene-sulfonyl (dansyl)-immobilized glass surfaces for the detection of NACs in aqueous solution.[120-122] Dansyl was covalently attached onto oxidized glass slides and the resulted films avoided the leaching of the fluorophore in solution. Das et al. designed and synthesized a tripodal naphthalene ether ligand amine (L1) as a supramolecular fluorescent host to form inclusion complexes with electron deficient aromatic molecules.[123] The fluorescence quenching efficiency depended on the electron

deficiencies of the aromatic guests coupled with their acidic nature, and as a result, the addition of picric acid gave the highest quenching degree. A self-assembled packing of L1 with picric acid through intermolecular π-π stacking interactions and hydrogen bonding was proposed to illustrate this supramolecular host-guest fluorescence signal systems (Fig. 10). Following that, researchers developed similar tripodal chemosensors using fluorophore such as anthracene, pyrene, corannulene and biphenyl for the detection of explosives.[124-126]

Another example is iptycene. Iptycenes are a family of molecules containing multiple arene units joining together to form bridged ring systems. The interests in iptycenes have been sparked by the fact that they can bind NAC molecules. Anzenbacher et al. synthesized a series of 1,4-
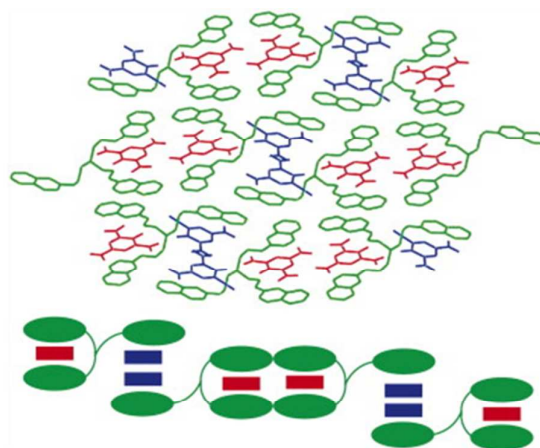

Fig. 10 Packing of $[(L_1H^+) (Pic^-)] \subset PicH$ along a-axis showing the π-stacking interaction scheme. Reproduced with permission from Ref. 123. Copyright 2008 Elsevier.

diarylpentiptycenes **32a-e**, and studied their ability to detect nitrated explosives.[54] The fluorescence quenching efficiency could be modulated by the 1,4-aryl residues. In dichloromethane solution, **32d** and **32e** showed the highest quenching degree with K_{SV} in the range of 1000-3000 M^{-1} for TNT. Solution-cast films of **32d** and **32e** exhibited different quenching sensitivities to TNT vapor, which was explained by the difference in the LUMO-levels of these pentiptycenes. The same group further developed iptycene based fluorophores and suggested that iptycene provided a cavity suitable for binding nitroaromatic compounds in an edge-to-surface mode.[127] Following this, three-dimensional nanographene based on triptycene was also reported to sense explosives by others.[128]

Different from previous discussed work, Ji and co-workers reported on the facile synthesis of a series of PAH nanowires such as decacyclene,[129] triphenylene[130] and ellagic acid[131] through simple heating due to the π-π stacking direction parallel to the longitudinal axis of the nanowires. The fluorescence and conductivity of the nanowires changed selectively in the presence of nitrobenzene, indicating their potentials for the detection of explosive chemicals. Although the research provides a facile method to prepare fluorescent nanowires, the sensitivities of these materials to TNT or DNT

vapors have not been reported. In addition, the size of nanowires was still relatively large and difficult to be tuned. Further improvement of this preparation method is necessary.

32
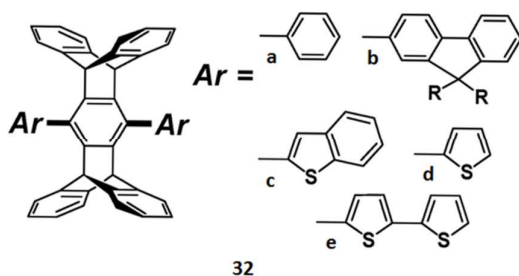
Through comparing the sensing capabilities of a series of PAHs, an array-based sensing device consisting of multiple fluorophores provided one powerful method to detect and differentiate between nitrated explosives from their chemically related compounds. Anslyn et al. developed a sensor array consisting of micelle-solubilized PAHs, including pyrene, pyrene-perylene pair, and diphenylanthracene, for differential sensing of TNT, Tetryl, RDX and HMX.[132] Micellar (Tween 80) solutions were used to pre-concentrate analytes and to protect pyrene from being quenched by atmospheric oxygen. The application of statistical discriminant analysis (linear discriminant analysis, LDA) generated quenching patterns for nitrated explosives with 96% accuracy and a detection limit of 19 μM. In order to prevent self-quenching of the initial intensity through π-π interactions and to maintain the spectroscopic stability in solution, Shanmugaraju et al. synthesized a series of trimethylsilylethynyl (TMS) substituted cyclic organic compounds (benzene, biphenyl, carbazole, anthracene, and pyrene) as selective and sensitive fluorescent materials for the detection of NACs.[133] All these derived compounds showed high selectivity towards NACs over other electron deficient non-nitroaromatic interferences. Typically, the 9,10-bis(trimethylsilylethynyl) anthracene provided a detection limit of ppb level for picric acid, and a thin film made by spin-coating 1,3,6,8-tetrakis(trimethylsilylethynyl)pyrene in chloroform or dichloromethane solution (1.0×10^{-3} M) over a quartz plate showed a 50% reduction in the initial emission intensity upon 120 s exposure to saturated NB vapor.

Although PAHs and their derivatives offer excellent sensitivity and selectivity for the detection of nitrated explosives, the associated safety hazards may limit their routine use and encourage the development of alternative fluorophores with reduced toxicity. Meaney and McGuffin tried to find one low-toxic fluorophore.[24] They screened 11 PAHs and PAH derivatives, including pyrene, 4-hydroxycoumarin, 4-bromomethyl-7-methoxycoumarin, 7-diethylamino-4-methylcoumarin, purpurin, acridine orange, methylene blue, malachite green, phenol red, rhodamine 6G, and fluorescein. The sensitivities were compared by their K_{SV} to NB and 4-NT, and the selectivity was examined over a range of interfering compounds, including aniline, benzoic acid, and phenol. It turned out that among all the fluorophores examined, purpurin, malachite green, and phenol red had

comparable sensitivity and selectivity for nitrated explosives detection compared to that of pyrene.

4.1.2. Porphyrins

Porphyrin-based compounds are a type of heterocyclic macrocyclic organic molecules composed of four modified pyrrole subunits interconnected via methane (=CH-) bridges. Porphyrins are typically intensely fluorescent with emission bands between 600 and 750 nm, and have been used in a wide range of optical applications. Moreover, their rich π-electrons delocalized over the macrocycles facilitate the π-π stacking with electron-deficient NACs, making porphyrins of great interests in detecting NACs. Harmon et al. reported that TNT could form a 1:1 (molar ratio) complex with meso-tetrakis(4-sulfonatophenyl)porphyrin (TPPS) and quench TPPS emission at 645 and 702 nm in aqueous solution.[134] On the basis of a linear Stern-Volmer plot, TNT interacted with TPPS in the ground state and the static quenching constant was found to be 1786 M^{-1}. The interaction between porphyrins and TNT was further explored by UV–vis and fluorescence spectroscopy, which suggested binding of TNT to the pyrrole nitrogens in porphyrins via hydrogen bonds.[135]

A series of porphyrins doped porous silica films were developed by Li et al. with high fluorescence quenching efficiencies towards NAC vapors.[136-138] Porphyrins were directly incorporated onto silica surface through co-condensation of porphyrin-functionalized silanes with tetraethoxylsilane (TEOS). It was revealed that the pore structure played a key role in the sensing response. A bimodal porous structured (combination of macropores and mesopores) meso-tetra(4-siloxyphenyl) porphyrin doped silica film, which was generated by the removal of template polystyrene and surfactant cetyltrimethylammonium bromide (CTAB), provided a 55% quenching of initial fluorescence intensity upon 10 s exposure to TNT vapor and 97% after 2 min, a much higher sensitivity than the tightly-linked amorphous films and single modal porous (macroporous or mesoporous) films.[136] DNT and NB also quenched those porphyrin doped bimodal porous films, but to a much less extent. The use of metalloporphyrins further improved the sensing performance, as the metalloporphyrins had larger binding constants for NACs relative to free-base porphyrins.[139] Typically, the Cd-porphyrin doped silica film with continuous worm-like mesostructure increased the quenching efficiency from 33% of free base porphyrin doped silica film to 60% by 10 s TNT vapor exposure.

Electrospinning, a simple and versatile technique, has also been adopted to fabricate porphyrin-doped nanofibrous membrane for NACs detection.[140, 141] Li et al. reported that the porphyrin-doped silica gel could be directly electrospun into smooth and uniform nanofibers without addition of assistant polymers.[140] Surfactant CTAB was added into the electrospinning precursory solution and was later removed from the fibers by solvent extraction using HCl-ethanol, generating a bimodal porous structure (macropores made out of electrospun nanofibers, and microspores created by CTAB). This hierarchical nanofibrous membrane exhibited a fluorescence quenching of 20% after 60 s exposure of TNT

vapor and of more than 80% after 1 hr. The quenched films can be recovered for future use by soaking in ethanol for 6 hrs followed by puffing with nitrogen gas or washing with toluene. Another study reported the detection of TNT and RDX by the porphyrin-embedded periodic mesoporous orgaosilicas (PMO), which was imprinted with a target analog (decylamine trinitrobenzene) during the condensation to produce a more favorable binding site on the pore wall.[142] The selective binding of nitrated explosives resulted in unique changes in the visual color and fluorescence spectra. Panda et al. synthesized a series of porphyrins and their Zn(II)-derivatives which possessed both electron donating and withdrawing substituents at their periphery.[143] The effect of substituents at the porphyrin periphery could be clearly observed with regard to their interactions with nitrated explosive molecules along with the effect of the metal ion at its core, where β-octamethoxyporphyrin displayed the maximum response towards TNT with a K_{SV} of 324 M^{-1}. Although porphyrin based fluorophores have shown great potentials to detect explosives, the sensitivity was generally lower than that of previously discussed conjugated polymers and fluorescent polyaromatic hydrocarbons. The sensing performance could be further improved through optimization of electronic structures and functionalization of binding properties.

For example, the structural modification of porphyrins can be achieved either by acting on the central core through complexation with a variety of metals or by chemical functionalization at the periphery. The quenching behavior was found to be strongly dependent on the nature of the substituents at the periphery and central porphyrin core. Harnessing this, several porphyrin based materials for explosives detection with improved sensing performance appeared in 2015. Phosphonate groups was appended on prophyrins, decreased the LUMO energy level of porphyrins, and consequently facilitated the electron inoculation to TNT through a PET process.[144] The hydroxyl groups of phosphonates and pyrrole's –NH protons were further engaged in donor-acceptor interactions with TNT by strong intermolecular hydrogen bonding interactions showing fluorescence quenching behavior. The designed phosphonate porphyrins were highly selective toward detection of TNT with a LOD of about 5 nM in solution and 10 ppb in the vapor phase. An electron-deficient porphyrin-based polyfunctional Lewis acid was shown to be useful for the selective detection and discrimination of nitroaromatic explosives, because suitable Lewis acid side groups could modulate the electron density of porphyrin systems.[145] The modified π cloud of the conjugated molecules may show selectivity towards TNT or PA. The presence of Lewis acids on the organic π system facilitated intermolecular hydrogen-bonding interactions with the hydroxyl group of PA and thereby was discriminated from TNT, which had no hydroxyl group.

4.1.3 Other small organic fluorophores

Besides the discussed small organic fluorophores above, some other new small fluorophores have also been reported in explosives detection such as quinoline[146, 147], fluorescein[148], Rhodamine[149], squaraine dye[47], dipyrromethene[28] based

fluorophores. Different kinds of fluorophores have different properties, and they may possess different reaction mechanisms or fluorescence phenomena upon exposure to explosives.

For example, Xu's group employed ICT mechanism and found that DNSA-SQ could sense picric acid sensitively and selectively via a fluorescence turn-on signal in the near-infrared region (Fig. 11A).[47] DNSA-SQ behaved as a zwitterionic squaraine dye, where the stabilized negative charge on the nitrogen was connected to the conjugated backbone bearing a positive charge, and the dansylamide with a donor group was twisted away and perpendicular to the squaraine plane. The fluorescence change was attributed to the intramolecular charge transfer following the protonation of dimethylamine group by PA. PA was linked to DNSA side group through acid-base interactions. The ICT interaction, however, was limited to PA and DNSA segment, as the sulfone linkage in DNSA-SQ prevented the spread of the ICT interaction to squaraine backbone, thereby minimizing its fluorescence quenching effect. Furthermore, the twisted dimethylamine phenyl unit prevented the squaraine plane from its π-π interaction with PA, reducing the efficiency of electron and energy transfer. The limited influence of PA on the squaraine backbone slightly shifted the fluorescence signal without quenching, thereby enabling the ratiometric detection of PA (Fig. 11B). Judicious and rational design of ICT fluorescent molecules has the great potentials in developing a ratiometric approach. Inspired by
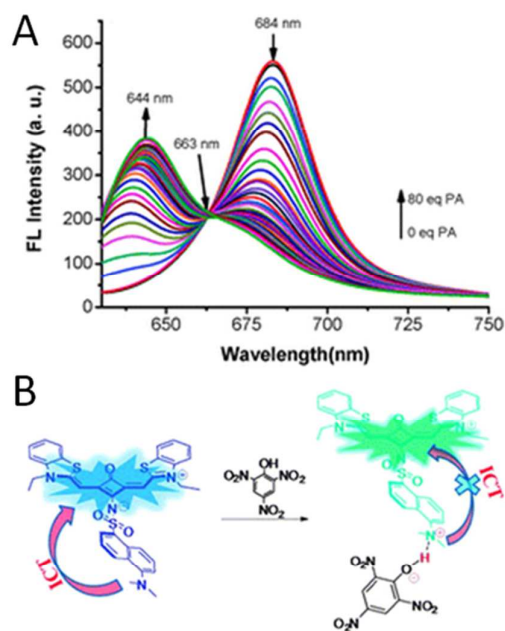

Fig. 11 (A) Fluorescence spectra of probe SNSA-SQ upon addition of various concentrations of PA in CH$_3$CN. (B) Schematic illustration of the proposed intermolecular interaction mode, where the protonation of dimethylamine by PA inhibits the ICT of DNSA-SQ. Adapted with permission from Ref. 47. Copyright 2013 the Royal Society of Chemistry.

this, Sivaraman et al. designed a rhodamine based derivative as highly sensitive and selective turn-on chemosensor towards picric acid.[149] In the study, other NACs showed little interference and picric acid even at picomolar concentration could be easily detected.

Ravikanth et al. reported another specific fluorescence turn-on chemodosimeter for the detection of picric acid through introducing appropriate substituents onto the boron-dipyrromethene (BODIPY) framework.[28] Without the addition of picric acid, the BODIPY was weakly fluorescent due to the PET that occurs from the acetal oxygen to the BODIPY. The addition of picric acid broke the PET process because of the interaction of the picric acid and acetal oxygen of the BODIPY core and formation of the corresponding aldehyde. Due to the unique conversion of the acetal to an aldehyde by picric acid, the sensor showed remarkable selectivity towards PA over other explosive nitroaromatics.

Taking advantage of the special properties of fluorophore, Wang and co-workers reported a highly sensitive and selective sensor to PA detection and proposed a unique sensing mechanism.[146] Via a facile strategy, a fluorescent composite nanosphere was formed by functionalization of the hydrophobic 8-hydroxyquinoline aluminum (Alq3) and coating a hydrophilic polymer shell. Alq3, emitting strong bluish green fluorescence with an excitation peak at 365 nm, was a highly favourable fluorescent donor for PA detection. The dramatic decrease of the excitation intensity by obvious absorption at 365 nm of PA resulted in the charge transfer between the two and consequently highly selective detection of PA compared with other NACs.

4.2 Inorganic small molecules
4.2.1 Quantum dots

Quantum dots (QDs) are colloidal semiconductor nanocrystals that have high quantum yields, broad absorption spectra, narrow size-tunable emissions, and are resistant to photobleaching. They are commonly comprised of heavy metals and chalcogens (e.g., ZnSe, CdS, PdTe and CdSe/Te CdHgTe alloys) and have dimensions smaller than the exciton Bohr radius of the corresponding bulk material (e.g., 10 nm for CdS spheres). The smaller the QDs, the more blue-shifted their fluorescence, and thus a range of colors can be obtained by controlling the size of QDs. Due to their special properties, QDs have been investigated for the fluorescence detection of explosives. Wang and co-workers reported the NACs could efficiently quench the fluorescence of CdSe QDs in chloroform, while toluene and benzene gave no significant response.[150] The detection limits for TNT, 2,4-DNT, p-NT, NB, and 2,4-dinitrochlorobenzene were 1.5×10^{-6}, 1.2×10^{-7}, 1.1×10^{-6}, 6.5×10^{-8}, and 4.5×10^{-6} M, respectively.

Since then, other research groups have introduced recognition sites onto the surface of QDs to enhance their quenching selectivity. Luo et al. investigated water-soluble L-cysteine-capped CdTe QDs to detect TNT.[151] The surface immobilized L-cysteines played an important role as their electron-rich primary amines can bind electron-deficient TNT molecules via the formation of Meisenheimer complex, through which the fluorescence of the synthesized QDs was quenched. The synthesized QDs showed selective quenching to TNT but not to other NACs, such as DNP, TNP, and NT. As low as 1.1 nM of TNT could be detected, promising as a laboratory detection method. However, this system required strict operation pH range (6.8-7.2) and long incubation time (150 min), which may limit the utility of this material in field test and real applications.

Because the surface of quantum dots affected fluorescence quenching efficiency, surface-modified QDs have received much attention and were applied for explosives detection in order to improve the sensitivity of sensors. The Willner group have reported a selective RDX detection based on 1,4-dihydronicotinamide adenine dinucleotide (NADH)-modified CdSe/ZnS core/shell QDs, with a very low detection limit of 0.1 nM.[152] RDX can be reduced nonenzymatically by NADH with the assisted activation of NO_2 groups by Lewis acidic Zn^{2+} ions in the QDs shell, accompanied by the transformation of luminescent NADH-capped QDs to the quenched NAD^+-QDs. Similar to the limitations of L-cysteine-capped QDs, the NADH-modified QDs required incubation time of 21 min. Following this, Willner's group also reported on the use of chemically modified CdSe/ZnS QDs as fluorescent probes for the analysis of TNT or RDX.[153] The QDs were functionalized with electron donating ligands that bound nitro-containing explosives, via supramolecular donor-acceptor interactions. The researchers employed a series of electron-donating amine capping layers for the modification of the QDs, and demonstrated that the donating properties of the surface modifier influenced the sensitivity of QDs sensor. With increasing of the electron donating functions of the capping layers, higher surface densities were associated with the QDs, leading to enhanced quenching of the QDs. However, the sensitivity and response time of this explosive sensor still needs to be improved. Silva and co-workers reported the application of CdSe quantum dots capped with PAMAM-G4 dendrimer for explosives detection.[154] Both the dendrimer and α-CD in hybrid QD materials helped to enhance the sensing performance for explosives detection. Furthermore, creatinine-capped[155], methionine capped[156], APTES-TEOS functionalized[157] quantum dots have been designed for sensitive and selective detection of TNT due to the formation of Meisenheimer complex between TNT and NH_2 on the surface of fluorescent materials.

Wang and co-workers reported the ratiometric fluorescence probe that employed both functional dual-emission quantum dots hybrid as the recognition element specific for TNT and ratiometric fluorescence as visual signal output for the indication of TNT presence.[158] Ratiometric fluorescence technique possessed advantages in terms of sensitive visual-detection for trace TNT due to its independence of the probe concentration and the ability of quantitative analysis. The ratiometric probe comprised two differently sized QDs and emitted green and red fluorescence, respectively, due to single-excitation/multiple-emissions for signal transduction of quantum dots (Fig. 12A). Although unchanged, the red fluorescence with polyamine selectively bound TNT by the formation of Meisenheimer complex, leading to the green fluorescence quenching due to resonance energy transfer. The

variations of the two fluorescence intensity ratios displayed continuous color changes upon exposure to various amounts of TNT (Fig. 12B). The advantages of the ratiometric fluorescence for visual detection (more sensitivity and reliability) was confirmed by comparison to quenching performance using single fluorescence method, which was difficult to distinguish the images by the naked eye. The design principle was further developed by the same group using a dual-emission nanohybrid which comprised blue-colored fluorescent graphene oxide being conjugated with red-emitting Mn doped ZnS nanocrystals.[159] The blue fluorescence was insensitive to TNT, while the red fluorescence can be quenched by TNT through electron transfer.
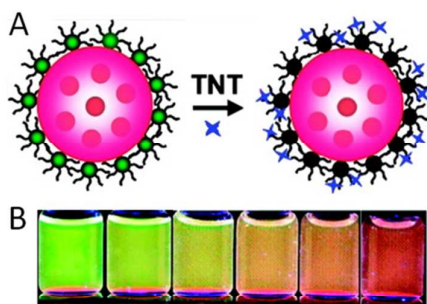

Fig. 12 (A) Schematic illustration of the structure of the ratiometric fluorescent probe and the working principle for the visual detection of TNT, and the red QDs were inert to TNT, while the green QDs were quenched to TNT by forming the Meisenheimer complex. (B) Photographs taken under UV lamp of the fluorescence colors of the ratiometric probe solutions after exposure to TNT (0-10 ×10^{-5} M) increased from left to right. Adapted with permission from Ref. 158. Copyright 2013 the American Chemical Society.

However, most of quantum dots consist of toxic elements such as Cd, Pb, As, etc., and the leaking of these elements from quantum dots would be toxic to biological systems and eventually cause serious environmental problems. Therefore, various methods have been proposed to address this issue. Firstly, QDs are commonly involved in the overgrowth of an additional passivating inorganic shell of a semiconductor material with a larger bandgap (e.g., CdSe/ZnS or InAs/ZnSe core–shell nanocomposites), which at the same time, prevents the leaking of toxic metals. In addition, researchers have been trying to develop environmental-friendly quantum dots, and graphene quantum dots have been synthesized and applied for explosives detection through FRET mechanism.[160] Su and co-workers used non-Cadmium $CuInS_2$ as fluorescent probes for the detection of nitro-explosives.[161] Involvement of tedious and time-consuming steps for particle surface modification is another potential issue limiting current QD sensors for explosives detection, simpler and more facile methods are required to be developed before any large scale application.

Due to its low toxicity, easy preparation and excellent aqueous solubility, fluorescent carbon dots have also been used for sensitive and selective explosives detection of picric acid by Wu's group.[162] Furthermore, a similar carbon based g-

C_3N_4 nanosheet was successfully prepared by exfoliating bulk materials and was found to be sensitive to nitro aromatic explosives, especially selective towards to PA.[163] Most of reported carbon based quantum dots for explosives detection emit blue fluorescence, therefore, it is necessary to develop carbon dots with dual fluorescence emission color or other emission color besides the blue emission, which could be achieved by doping of other elements into carbon nanomaterials. In addition, the newly developed carbon based quantum dots demonstrate very different fluorescent properties with traditional semiconductor quantum dots, thus, we expect to see their vast investigation and applications in explosives detection in the near future.

4.2.2 Quantum clusters

Metal clusters typically consist of clusters only a few to several hundred metal atoms and have diameters < 2 nm, which is comparable to the electron Fermi wavelength of metals such as Au or Ag.[164] The spatial confinement of free electrons in metal nanoclusters endows the clusters luminescence or unique charging properties. A variety of fluorescent Au nanoclusters (NCs) have been synthesized using various methods. Very recently, Xie and co-works prepared a high red fluorescent gold nanoclusters through a simple, and facile green method using a common commercially available protein, bovine serum albumin (BSA).[164] Following Xie's work, Chai and co-workers found that red fluorescent Au NCs could be quenched by TNT and 4-NP, with a detection limit of 10 nM and 1 nM, respectively.[165] Senthamizhan et al. incorporated gold nanoclusters in a single nanofiber and realized ultrafast on-site selective visual detection of TNT.[166] The ligand BSA possessed rich primary amine groups, which led to formation of Meisenheimer complex between amino groups and TNT, thus fluorescence quenching of Au NCs could be achieved through this charge transfer interaction. Along this line, we expect that EDC functionalization on protein can be applied to tune the amine density or surface charge of the BSA-AuNC complex and to further improve the sensing performance. In addition, through rationally engineering fluorescent nanoclusters such as tuning emission spectra, a broad range of nanoclusters could be synthesized. For example, green fluorescent nanoclusters may demonstrate greater potentials in explosives detection. Since their emission spectra overlap efficiently with the absorption of Meisenheimer complex formed between amine groups on protein surface and electron-deficient explosives, higher sensitivity and selectivity are expected to be achieved through contribution of FRET mechanism.

Pradeep's group designed Au core/silica shell structures for enhanced fluorescence and Raman scattering selective visual detection of TNT at the sub-zeptomolar level.[167] The quenching of cluster luminescence was ascribed to formation of Meisenheimer complex by the chemical interactions between TNT and the free amine groups on BSA. The specificity of the Meisenheimer complexation endowed the cluster selectivity for TNT; and for ease of visual detection, a change in the luminescence color in the presence of an analyte was a more desirable indicator than the

disappearance/quenching of luminescence. By combining the high sensitivity and selectivity offered by surface enhanced Raman scattering with the fluorescence sensing method, the accuracy and reliability of the detection technique was greatly enhanced. The materials possessed advantages such as ease of functionalization, better stability of the QCs on the silica layer, along with a reduction in luminescence quenching of the QCs on the mesoflower surface.

4.3 Functional small molecule materials

4.3.1 Oligo-fluorophores

It is well known that the fluorescence quenching increases with the molecular weight for conjugated polymers, which is attributed to the increased diffusion length of the exciton through molecular wire theory (as shown in Fig. 3). In order to enhance the exciton diffusion in the case of simple small molecules, oligo-fluorophores have been synthesized and investigated. Generally the oligo fluorophores are defined as 3-10 repeating units of small molecule fluorophores or the previous basic bones (Fig. 4). Due to their molecular structures, they possess some unique properties.

As an important and thoroughly investigated small molecule fluorophore, pyrene is pretty attractive in the construction of novel fluorescent materials. Oligopyrenes on the other hand, have higher molecular weights and more rigid plane of repeated units, and exhibit many advantages compared to monomer pyrene, such as stronger fluorescence, higher electrical conductivity and thermal stability, and lower toxicity. Shi and co-workers reported a 2.5 nm thin film of oligopyrene for sensitive detection of both NACs and nitroaliphatic explosives.[168] The obtained oligopyrene had a dark green color with 3-6 repeating units. The spin-coated oligopyrene thin film showed fast fluorescence quenching response upon exposure to TNT, DNT, NB, NM, and p-benzoquinone vapors. For TNT vapor, 50±5% quenching at 10 s was observed and this quenching level increased to 75±5% at 30 s exposure. The same group also synthesized a cationic oligopyrene salt, oligo(2-(4-(1-pyrenyl) butanoyloxy) ethyltimethylammonium bromide) (OPBEAB), through a combination of chemical and electrochemical routes.[169] OPBEAB had an average of 4 repeating units with a high quantum yield of 0.7 in aqueous solution. To prevent aggregation induced self-quenching, anionic surfactant SDS was introduced into the solution to form a hydrophobic protective layer around OPBEAB chains. The fluorescence of OPBEAB was quenched by TNT in aqueous solution with a K_{SV} of 5.3 × 10^5 M^{-1} and a detection limit of 70 ppb.

Li and co-workers synthesized fluorescent oligotriphenylene and oligofluoranthene materials for explosives detection.[170, 171] The fluorescence intensity of oligofluorophore was much stronger than the corresponding monomer, due to the reduced self-quenching. And the strong fluorescence was effectively quenched by specific electron-deficient species, enabling the fabrication of low-cost, high performance chemosensors for explosives detection. For the reported oligofluoranthene, the strong fluorescence was linearly and selectively quenched by electron deficient substances, such as picric acid, even at an ultra-trace level down to picomole.[171]

The morphology of the oligotriphenylene could be tuned from 3D aggregates to 2D nanosheets or 1D nanofibers by controlling the reaction parameters such as monomer concentrations, the acid, and the temperature.[170] The self-assembly along the π-π stacking direction was believed to be the dominant driving force for the growth of nanofibers. The nitroaromatic explosives acted as electron acceptors for photo-excited electrons from the oligotriphenylene, leading to a rapid and amplified fluorescence quenching (Fig. 13). This amplification effect led to electron donors and acceptors forming π-electron or charge transfer complexes between the oligotriphenylenes and their quenchers. The oligotriphenylene formed a spiral-like architecture, which could easily capture electron-deficient analytes, forming stable static complexes.
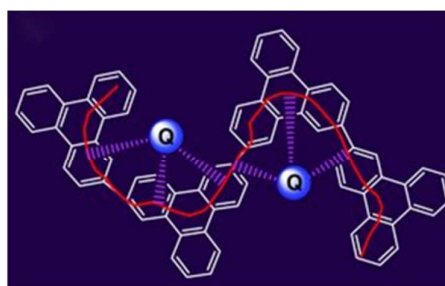

Fig. 13 A model of the π-electron transfer complex formed between the oligotriphenylene and quenchers (Q, blue balls), where the red solid line and magenta dotted line represent the "molecular wire" pathway for transfer of the π-electrons. Reprinted with permission from Ref. 170. Copyright 2012 Wiley-VCH.

Ajayaghosh et al. reported that a perfluoroarene-oligo (p-phenylenevinylene) (OPVPF) based gelator film demonstrated about 20% quenching within 5 s of TNT exposure, indicating a fast response and detection limit of between ppb and ppt concentration levels, although the solution based experiments showed a low quenching efficiency to TNT.[172] The detection level reached as low as attogram level in contact mode (as shown in Fig. 14A). XRD studies revealed that the presence of absorbed nitro-aromatics in the interstitial space of OPVPF had a limited effect on packing. The high fluorescence quenching was attributed to excited-state phenomena and fast exciton migration within the self-assembled structures (Fig. 14B). Following that, morphologically different self-assemblies of a carbazole bridged fluorine derivative was described for quantitative sensing of nitroaromatics through a combined fluorescence and quartz-crystal microbalance approach by the same group.[173] Picomolar level detection of TNT in water and nanogram level TNT sensing in the vapor phase was achieved.

Besides previous oligo-organic fluorophors, inorganic oligosiliane has been demonstrated by Fang et al. in sensing NAC vapors.[174] A monolayer of oligo(diphenylsilane) was assembled onto a glass plate and presented a very sensitive and static quenching to NAC vapors. By 10 s exposure of TNT, DNT or NB vapor, the film showed 55%, 80%, or 44% reduction in its initial fluorescence emission, respectively. Further 30 s exposure to those vapors made the film fluorescence almost completely quenched. Common organic solvents, daily
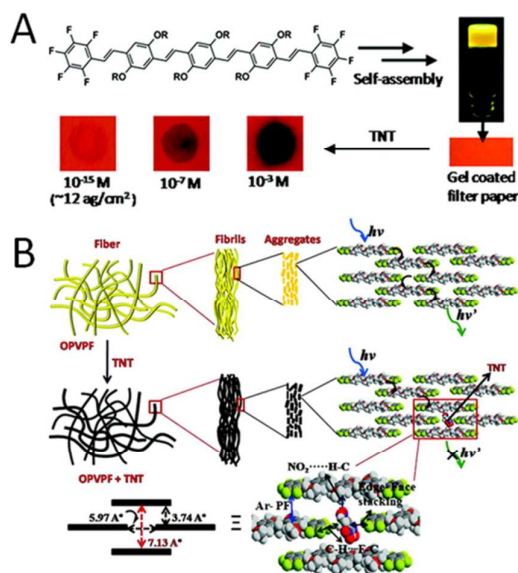
Fig. 14 (A) Molecular structure of OPVPF and its self-assembly to gel coated filter film and the ability for attogram TNT detection in contact mode. (B) Schematic illustration of the fluorescence quenching mechanism of OPVPF xerogel fibers in the presence of attogram levels of TNT. The bottom right picture shows various noncovalent interactions, and the bottom left picture illustrates the approximate distance between neighboring OPVPF in a brickwall-type arrangement. Reproduced with permission from Ref. 172. Copyright 2012 the American Chemical Society.

chemicals, fruit juice, smoke and ozone did not result in any interference; however, chlorine, HCl, and SO_2 gas quenched the film fluorescence to some degree although in a weaker and slower mode compared to NACs.

4.3.2 Self-assembled small fluorophores

Spin-coating, dip-coating, casting and other physical methods have been applied in most of the film preparation due to the simplicity and effectiveness, but leaking of fluorophore in solution sensing and self-quenching of CPs are unavoidable problems. Even more, the thickness of the CPs deposited onto the substrate is very difficult to control, and this affects not only the consistency of the film's performances but also the smartness of the film's responses. Considering the above issues, assembled monolayer of small molecule fluorophore film (Fig. 15) was proposed for explosives detection.[175]

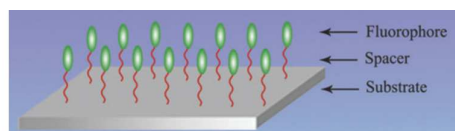A number of PAHs sensing applications which involved their

Fig. 15 Schematic illustration of the structure of surface-supported monolayer assembly of fluorophores. Adapted with permission from Ref. 175. Copyright 2010 the Royal Society of Chemistry.

immobilization onto solid material surface with the linkers were systematically investigated by Fang and co-workers.[120-122, 176-178] The effects of linker length were investigated through a series of dansyl-functionalized glass surfaces with different length of hydrophobic spacers.[120-122] For shorter linkers, such as 1,3-diamino-propane, the sensing ability was dominated by the nature of the target molecules and their electron-transfer interactions, so the film exhibited higher sensitivity to TNT than NB in aqueous solution. Whereas, a longer chain linker, 1,6-hexanediamine would bury dansyl moieties in a compact layer (termed "spacer layer") in polar solvents and prevent bulky targets from accessing the fluorophore entrapped "spacer layer", and therefore, the quenching efficiency by TNT was less than that of smaller targets such as NB. A recently study pointed out the introduction of benzene structure in the linker between pyrene moieties and glass plate surface favoured the π-π stacking with NACs in aqueous solution.[177] They also introduced a naphthalene unit into its conjugated backbone, 5-(1-naphthyl)-2,2':5',2''-terthiophene in order to increase the photostability.[179] The compound was further employed as a sensing element for the fabrication of a monolayer-chemistry based fluorescent sensing film. The film was highly sensitive and selective to picric acid, with LOD of 0.32 μM. The good sensing performance was due to the specific binding of the film to the analyte because of proton transfer from PA to the amino group in the spacer.

Considering the importance of the spacer of the monolayer function layer, Fang's group further investigated the effect of spacer on sensing performance. They found that length and structure of the spacer connecting the sensing element and the substrate played an important role in mediating the sensing performance of such film sensors in detecting analytes in aqueous solution. Benzene structures in the spacer favoured π-π stacking between pyrene moieties on the end of each other and promoted direct exposure of the fluorophore residues to aqueous phase.[177] Further understanding in the microenvironments of immobilized PAHs was studied by the same group. They reported on a self-assembled monolayer film sensor with discriminatory power which was accomplished by using pyrene as fluorophore and oligo(oxyethylene) unit as hydrophilic spacer.[180] The hydrophilic spacer plus the hydrophobic pyrene may generate a multidimensional microenvironment for sensitive and selective detection of nitro explosives. The present film exhibited cross-reactive responses to different NACs including PA, TNT, DNT and NB through four specific wavelengths (peaks for pyrene's monomer and excimer emission). The results from principle component analysis revealed that the present film had discriminatory power to identify structurally similar NACs and may open a novel route to design film sensors towards particular targets.

ARTICLE

Fluorophores functionalized on nanoparticles and nanofibers have also been investigated. [116, 181] For example, the chemical linkers that bound the pyrene moieties onto the Ru nanoparticle surface was examined by Chen et al. using Ru-1-vinylpyrene (Ru=VPy) and Ru-1-allypyrene (Ru=APy) immobilized glass substrates.[116] The lower sensitivity of Ru=APy than the Ru=VPy counterparts was ascribed to the insertion of a sp^3 carbon into the chemical linker which turned off the extended conjugation. The high surface-to-volume ratio of nanoparticles was used to obtain a high local concentration of pyrene units on their periphery, making the formation of both pyrene emissive species possible by using amazingly low pyrene concentrations. The encapsulation capacity of the nanoparticle may result in an increased sensitivity to the analyte. Substituted pyrene compounds were also coated on the conjugated polymer nanofibers. 14-fold of sensitivity enhancement in detection of H_2O_2 was achieved due to high area-to-volume ratio, excellent gas permeability, and more importantly, the evanescent-wave effect.[182]

4.3.3 Small molecule fluorophore doped into the matrix

Recently, Liu et al. developed an electrospun nanofibrous film based on tetrakis(4-methoxylphenyl) porphyrin (TMOPP) as the fluorophore and polystyrene as the substrate.[141] Secondary porous structures were similarly introduced by adding Triton X-100 as the water-soluble porogen into electrospinning solution followed by washing in water for 24 h. Our group later reported on the pyrene doped in the polymer system for naked-eye based ultra-sensitive detection of nitro-explosives.[183, 184] A wide spectra of nitro explosives, in particular, TNT, Tetryl, RDX, PETN and HMX could be "visually" detected at their sub-equilibrium vapors (less than 10 ppb, 74 ppt, 5 ppt, 7 ppt and 0.1 ppt) (Fig. 16A). Besides the large surface area of nanofibrous films (Fig. 16B), the outstanding sensing performance could also be attributed to the proposed "sandwich-like" conformation between pyrene and phenyl pendants of the polymer (Fig. 16C) which may allow efficient long-range energy migration.[185] In addition, the work presented the first report that the detection of buried explosives without the use of any advanced analytical instrumentation. We also found that the fluorophore and the polymer matrix concentrations affected the electronic structures of fluorescent materials and thus the fluorescence quenching processes by explosives in vapors and aqueous solution.[49, 186] The system has been further developed through
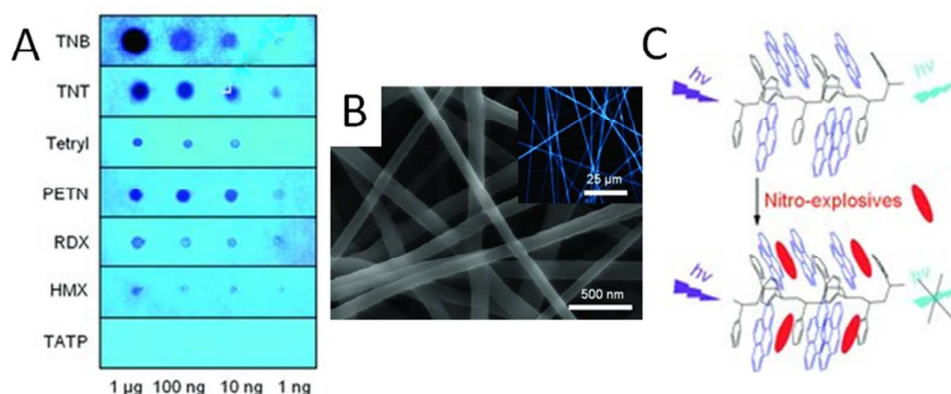

Fig. 16 (A) UV excited images of 3 μm thick films after exposure to sub-equilibrium various vapors generated from 1 μg, 100 ng, 10 ng, and 1 ng solid analytes. (B) SEM image of electrospun nanofibrous films, Inset shows the fluorescence microscopy image of the film. (C) Proposed "sandwich-like" conformation of pyrene/polystyrene in electrospun nanofibrous film (top) and the potential intercalative bindings of nitro explosives (bottom). Adapted with permission from Ref. 183. Copyright 2012 Wiley-VCH.

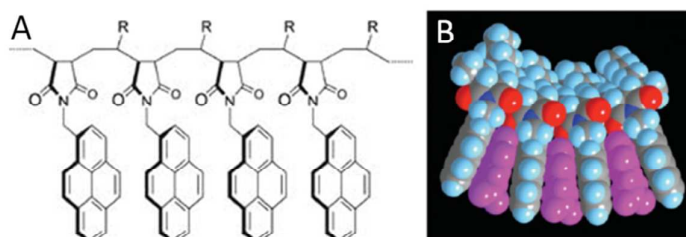Fig. 17 (A) Comb-type structure of a generic poly(1-pyrenylmethylmaleimide-alt-1alkene) (B) A prediction from computational modeling of the potential π-π stacking interactions between poly(1-pyrenylmethylmaleimide-alt-1-hexene) and TNT. Reprinted with permission from Ref. 194. Copyright 2009 Wiley-VCH.

24 | *Chem. Soc. Rev.*, 2015, **00**, 1-3

This journal is © The Royal Society of Chemistry 20xx

doping of additional graphene oxide[187], using modified silica ormosil network[188] and silica nanoparticles[189] by other researchers. Besides, to improve the sensitivity through doping of small molecules into the matrix, Anzenbacher et al. doped a series of iptycene-based small molecules into the polymer in order to increase the film-forming properties of small molecules.[127]

Stein and co-workers reported a phenyl-substituted pyrene fluorophore doped in various surfactant-templated, mesoporous silica thin films.[190] Films with wormlike mesopore architecture exhibited a better quenching performance than those with 2D-hexagonal or 3D-hexagonal structure. The poorer performance of 2D-hexagonal films was attributed to the long channels that lay parallel to the substrate, slowing down the diffusion of DNT through the film. The improvements in quenching performance may be attributed to the decrease in initial intensity (due to oxygen quenching), which meant fewer fluorophore molecules needed to be quenched, while the number of DNT molecules in the vapor phase was the same for the two experiments. Fang et al. recently reported on the cationic bispyrene fluorophore doped into surfactant micelles for the detection of explosives such as picric acid and PYX explosives.[191] Besides, substituted-pyrene fluorophores, dansyl chloride, fluorescein isothiocyanate,[192] and naphthalene[193] have also been doped into the mesoporous silica particles and applied for explosives detection.

Another interesting method for explosives detection is to introduce pyrene moieties into polymer side chains as the active sites. Colquhoun et al. developed a pyrene-functionalized copolymer through a side-chain functionalization of a commercially available polymer containing an alternating maleic anhydride.[194] The functionalization was accomplished in a simple one-step imidization reaction and afforded the pyrene units bound to the polymer with a tweezer/comb-like conformation as shown in Fig. 17A. The new polymer formed complexes with NACs through an intercalative π-π interaction in solution, and the separation between pyrenyl side-group and TNT molecules was very close to van der Waals contact distance (ca. 3.42 Å). The solution-casted thin films of this polymer had a fast fluorescence quenching upon exposure to the vapor of 2,5-dinitrobenzonitrile, an analogue for TNT. The prediction of computational modelling (Fig. 17B) also demonstrated the feasibility of electron deficient TNT binding to the polymer chain by interaction between the electron rich pyrenyl side groups. Another successful example was reported by Samuelson et al. through a covalent attachment of pyrene methanol into poly(acrylic acid).[195] This new polymer, namely PAA-PM, was mixed with thermally cross-linkable polyurethane latex and then co-electrospun into nanofibers. The electrospun film was cured at 255 ºC for 60-90 s to cross-link polyurethane, within which the PAA-PM was immobilized and formed a water-insoluble porous network structure. Our group also developed a polyethylenimine polymer derivatized with pyrene moieties suitable for the fluorescence-based detection of nitroaromatic explosives in aqueous phase.[37] The

synthesized materials exhibited an exceptionally wide dynamic range of 7 orders and ultra-sensitivity to nitro-explosives with a limit of detection of 145 pM for TNT. The pyrenyl-excimer emission was a suitable energy donor for the TNT-based Meisenheimer complex in a FRET-type interaction, while the nitro-explosives also quenched the pyrene monomer fluorescence along a PET pathway.

5. Supramolecular systems for explosives detection

5.1 Macrocycles

5.1.1 Cyclodextrins (CDs)

Cyclodextrins (CDs) are a group of cyclic oligosaccharides consisting of 6, 7, or 8 glucose units. Due to the chair conformation of the sugar units, CDs are shaped like a truncated cone rather than perfect cylinders. The hydroxyl groups of the glucose residues are orientated to the cone exterior and the central cavity is lined by the skeletal carbons and ethereal oxygens, which give it a hydrophobic central cavity with a hydrophilic outer surface. When in polar solvents (e.g., water), the inside cavities of CDs are hydrophobic and they are capable of binding hydrophobic fluorophores, such as pyrene and anthracene within them. Thus, CDs cavities (hosts) are well known to encapsulate hydrophobic molecules (guests), such as PAHs, and form host-guest inclusion complexes if there is a good match between the sizes of both PAH and the CD cavity. The cavity diameters of α-, β-, and γ-CD are 5.3, 6.5 and 8.3 Å, which have been chosen to selectively accommodate a PAH molecule or a specific nitrated explosive molecule for an enhanced sensing response.

An early research was carried out on a pyrene-β-cyclodextrin (β-CD) co-immobilized chitosan film.[175, 176] The hydrophobic pyrene moieties tended to be incorporated in the hydrophobic β-CD cavity when the film was immersed in polar solvents, making it difficult for those polar quenchers to access pyrene moieties but selectively favoured neutral quenchers such as NM (as shown in Fig. 18). As a result, the pyrene and β-CD co-functionalized chitosan film showed high selectivity towards NM over ion quenchers such as Cu^{2+}, Co^{2+}, and I⁻. Anslyn et al. studied the CD-based fluorescence sensor in THF/H_2O (1/19) solution for the classification of aromatics, such as TNT and
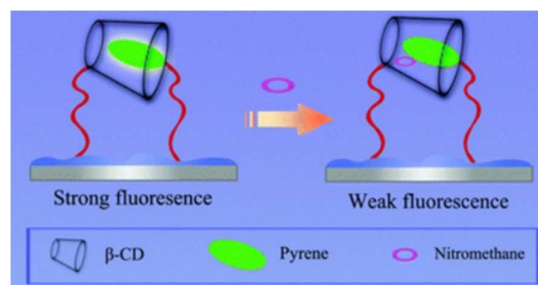

Fig. 18 Schematic cartoon for pyrene-and-β-CD co-functionalized film sensing nitromethane. Reproduced with permission from Ref. 175. Copyright 2010 the Royal Society of Chemistry.

Tetryl, and non-aromatics, such as RDX, HMX, PETN, and nitrated explosives.[196] Fluorophore 9,10-bis(phenylethynyl)anthracene (BPEA) was used to show a selective fluorescence quenching response towards NACs (e.g., TNT and Tetryl), and no response to non-aromatic nitrated explosives. By adding CDs into the solution, the supramolecular inclusion complex of CD-BPEA was formed in the presence of γ-CD but not with α- or β- CDs due to size match between the BPEA (7.3 Å) and CD cavity. Compared with the BPEA in the absence of γ-CD, the K_{SV} was enhanced through the γ-CD-BPEA by 1.6 times for TNT and 1.3 times for Tetryl. The higher improved TNT sensing performance over Tetryl was concluded to be the better accommodated TNT molecule than Tetryl in the γ-CD cavities.

Very recently, Lü and co-workers fabricated a FITC-NH$_2$-CD fluorescent sensor for TNT detection in aqueous solution.[197] This sensor demonstrated sensitivity and selectivity to TNT sensing through FRET mechanism due to energy matching between TNT-amine complexes and FITC on cyclodextrin. By taking a single cyclodextrin molecule as fluorescence carrier, the distance between the donor and the acceptor could be greatly reduced, and the efficiency of energy transfer was enhanced, thus improving the detection sensitivity to analyte. The limit of detection for TNT was 20 nM, while other metal ions had no significant interference with TNT sensing in aqueous solution. α-CD was also used to promote the formation of inclusion complexes with nitroaromatic compounds by Silva et al., in order to increase their water solubility and further improve sensing sensitivity and selectivity to nitroaromatic compounds.[154]

5.1.2 Calix[n] arenes

Owing to the presence of a specific binding core and supramolecular architecture, calix[4] arene can act as a good receptor to impart selectivity to guest species when they are functionalized appropriately using suitable chemical moieties. Calix[4] arene-based derivatives were reported by Prata and co-workers to detect nitro-explosives in aqueous solution as well as vapor phase through fluorescence spectroscopy in recent years.[198-201]

The calixarene-carbazole conjugates such as a dipyrenyl-1,3-alternate-calix[4]arene,[202] a p-phenylene ethynylene trimer integrating calix[4]-arene[198] moieties showed great potentials in detection of nitroaromatic and nitroaliphatic explosives as well as explosive taggants. The calixarene substituents of polymers could prevent π-stacking in the solid state, and thus preserve the optical properties of the material. In addition, the bulky, bowl-shaped building block helped form porous materials, and allowed to create films that were highly sensitive to explosives vapors. Prata's group further observed superior performance of calix-carbazole films relative to their calixarene-free analogous films as chemosensors.[199] Although lack of long range exciton migration mechanisms, the calix-carbazole films had the potential to extend cofacial electronic coupling intermolecularly as the differentiating features responsible for an amplified fluorescence detection response, which was capable of offering high sensitivity towards various explosive analytes. The exceptional sensing performance was

attributed to the importance of the calixarene units in the overall solid-state and the establishment of a tridimensional network of strong π-π and CH–π interactions with electron deficient guests developed near the transduction centers, as well as the improved photophysical and morphological properties imparted to thin films due to their tridimensionality. The same group later corroborated the working hypotheses that the calixarene hosts were the unique differentiating element responsible for overall enhanced sensing in the solid state in another report.[200]

Furthermore, the researchers also tried to explain the sensing mechanism of the calix[4] arene system through molecular dynamics simulation.[201] The chemical interactions of the newly synthesized upper rim benzimidazole functionalized calix[4] arene receptor with different nitro explosive analytes were studied by fluorescence spectroscopy and through a molecular dynamics approach. The simulation results indicated possible π-π interactions between TNT and the benzimidazole target moieties that formed an aromatic binding core at the upper rim. The crevice of receptor suggested effective interactions with three TNT molecules, while RDX had only one and PETN did not form a complex at all, which well reflected and supported the selectivity of the receptor toward TNT.

Through functionalization and modification of calix[4] receptor, various materials could be obtained for sensitive and selective interaction with the guest explosive species and may pave the way to the development of analogous molecular structures with improved capabilities for probing recognition events.

5.1.3 Cucurbits[n] urils

Cucurbit[n] urils (CB[n], n = 5–8 glycoluril units) are one class of barrel-shaped macrocyclic hosts possessing a hydrophobic cavity accessible through both identical carbonyl-fringed portals for guest molecules. These unique structural features make them very useful as versatile synthetic receptors and building blocks for construction of supramolecular architectures and functional chemical systems. In particular, in comparison with CB[6] and CB[7] that typically bind to one equivalent guest molecule, the larger homologue CB[8] is able to simultaneously accommodate two guests. Taking advantage of the unique binding ability of CB[8] to form heteroternary complexes, Li's group reported on a novel strategy for selective detection and discrimination of explosives based on naphthalene-core-threaded CB[8] rotaxane structure on solid surface (Fig. 19A).[203, 204] Dependent on the electronic structures and the sizes of explosive compounds, the fluorescence of the naphthalene core would be quenched or enhanced to different extents, leading to direct detection and discrimination of different explosives in the vapor phase (Fig. 19B). The nitro aromatics resulted in fluorescence quenching phenomena which was attributed to the host stabilized charge transfer complexes, whereas the challenging aliphatic nitro-organics (RDX, HMX and PETN) led to the fluorescence enhancement possibly due to the "rigidifying effect" where the encapsulated bulky guest molecule limited the motion of the naphthalene core and reduced its final non-radiative decay processes (Fig. 19C). Further experiments showed that the

26 | *Chem. Soc. Rev.*, 2015, **00**, 1-3

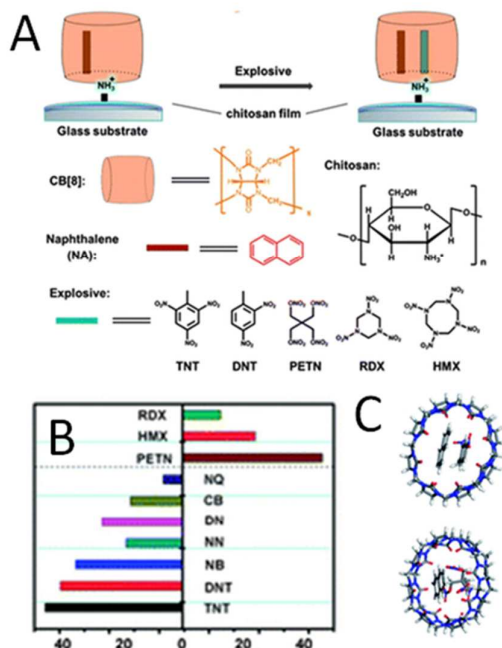This journal is © The Royal Society of Chemistry 20xx

Fig. 19 (A) Schematic illustration of the construction of the NA-CB[8] complex attached to a chitosan-coated glass substrate. (B) Comparison of fluorescence response of the fabricated sensors to different explosives (Fluorescence-off to nitroaromatics; Fluorescence-on to aliphatic nitro-organics). (C) Optimized structures of NA-CB[8]-DNT complex (up), NA-CB[8]-PETN complex (bottom). Reprinted with permission from Ref. 204. Copyright 2013 the Royal Society of Chemistry.

trapped molecules in the rotaxane structure were facilely removable by simply washing, demonstrating the excellent regeneration of the current sensing materials. Detection and discrimination of a broad range of explosives especially in the vapor phase through fluorescence method is very difficult and remains a challenge, and the studies here possibly open a new avenue to develop novel fluorescence-based explosives materials.

5.1.4 Carbazole based cycles

Carbazole-based materials are good electron-donors and could be a promising sensor material to detect nitroaromatic explosives with high fluorescence quenching sensitivity. Zang and Moore developed a porous nanofibrous film by self-assembling of carbazole-ethynylene tetracycles (namely ACTC, Fig. 20A, B).[205, 206] ACTC possessed a planar and shape-persistent geometry that facilitated intermolecular 1-dimensional π-π stacking and extended exciton migration. The film enabled fluorescence quenching by gaseous NAC explosives, such as TNT (83%, 1 min), DNT (90%, 1 min), and nitroalkane DMNB (73%, 2 min). This efficient sensing response was attributed to the extended exciton migration along the long-axis of nanofibers and the nanoporous morphology, which favored adsorption and diffusion of explosive analytes within the film. In addition, the quenching showed little dependence on film thickness and the regeneration could be accomplished by immersing the film in a saturated vapor of hydrazine. The same group later reported a linear carbazole trimer for sensing of NACs and nitroaliphatic explosives.[207] 1D self-assembly of 2,7-linked carbazole trimers formed nanofibers through a bi-solvent phase transfer process, with diameter around 30 nm and length to several microns. The nanofibrous film exhibited strong blue fluorescence at 438 nm, and was quickly quenched by both NAC vapors, such as saturated vapors of TNT (50% and 70% after 30 and 60 s, respectively) and DNT (50% after 10 s), and volatile nitroaliphatic vapors, such as 1800 ppm NM vapor (11% quenching after 0.63 s).

Following this research direction, the same group reported the selective detection of TNT vapor using the self-assembly of carbazole-based macrocyclic molecules, which allowed for slow diffusion and strong encapsulation of TNT molecules within the nanopores, resulting in post-exposure fluorescence quenching behavior (Fig. 20C).[208] In contrast, the porosity caused by entangled piling of nanofibers enabled no post-exposure fluorescence quenching for other analytes. The as-synthesized nanoporous materials demonstrates excellent sensing performance to explosive vapors, and the study may provide a simple and novel way to accomplish detection selectivity for nitro-explosives through creating nanoporosity and tuning molecular electronic structure.

5.1.5 Metallocages

Coordination polyhedra are synthesized using organic ligands
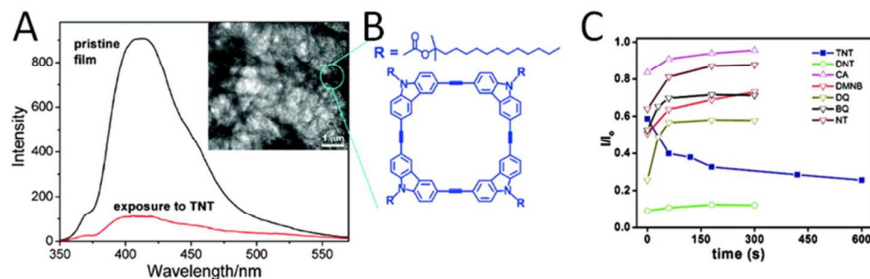
Fig. 20 (A) Fluorescence spectra of a 90 nm thick ACTC film before and after 60s exposure to saturated vapor of TNT. The inset shows a TEM image of a thin ACTC film. (B) Molecular structure of ACTC. (C) Post-exposure fluorescence intensities change (I/I$_0$) measured over the nanofibers as function of time after reopening to clean air. The values at time zero represent the fluorescence intensity measured after 10 s of exposure to the saturated vapor of different oxidizing reagents including TNT. Reprinted with permission from Ref. 205 and 208. Copyright 2007 and 2012 the American Chemical Society.

and metal ions and have been extensively studied due to their applications in gas adsorption, catalysis, separation, chemosensing and so on. The binding unit and fluorophore receptor are structurally integrated so as to maximize the communication between the units. Since the luminescence is very sensitive to subtle changes in geometry upon binding to a guest, fluorescent chemosensors are attractive for sensing of various analytes. Recently electron rich and fluorescent heterometallic self-assembled metallocages were shown to exhibit high quenching selectivity and sensitivity toward nitro-explosives by Mukherjee's group.[209-212] They synthesized trigonal cages from pre-organized metalloligands via coordination-driven self-assembly, and the ethynyl functionalities integrating into the prisms imparted them electron-rich and fluorescent nature, which was quenched by electron-deficient nitroaromatics.[209] The efficient electron transfer from the prisms to the nitroaromatics was responsible for the quenched fluorescence emission, demonstrating that the concept of host cages enabled the development of selective and discriminatory fluorescent sensors for nitroaromatics. Following this idea, a dinuclear organometallic acceptor 4,4'-bis[trans-Pt(PEt$_3$)$_2$(O$_3$SCF$_3$)(ethynyl)]biphenyl containing Pt-ethynyl was synthesized (Fig. 21A).[210] The obtained metallomacrocycle showed a marked quenching of initial emission upon titrating with picric acid, and a K$_{SV}$ constant as high as 5.0×10^6 M^{-1} was obtained (Fig. 21B). The improved fluorescence quenching performance was attributed to the enhanced electron donating ability of the macrocycles, originated from the linking of anthracene and ethynyl moieties.

An organometallic Pt planar tritopic acceptor and its [2+3] assembly of trigonal prismatic architectures (3a-3c) were further obtained (Fig. 21C).[211] The extended π-conjugation including the presence of Pt-ethynyl functionality made them electron rich as well as luminescent. The nanocages had electron rich flat roof and floor to accommodate electron deficient planar nitroaromatics between the roof and the floor. The Pt macrocycles exhibited fluorescence quenching by picric acid both in solution state and vapor phase, and the fluorescence quenching by picric acid was attributed to strong π-π stacking interaction between the electron deficient PA and electron rich macrocycle as well as deprotonation of highly acidic phenolic –OH group followed by anion exchange with the assemblies. By the same group, a fluorescent [3+2] self-assembled nanoscopic organic cage was later developed.[212] The use of fluorescent macrocycles (especially, calix[n] arene, cucurbits[n] urils, metallocages) in explosives detection is relatively new compared with previously discussed materials, and the macrocycles materials are expected to have greater potentials for explosives detection in terms of the sensitivity, selectivity, and response time due to their unique porosity and fluorescent properties.

5.2 Dendrimers

Dendrimers are well-defined, highly branched macromolecules containing three regions: core, branch, and surface.[213] They commonly have a mono-dispersed spherical morphology with three-dimensional architectures. From a topological viewpoint, luminescent units can be covalently incorporated in each
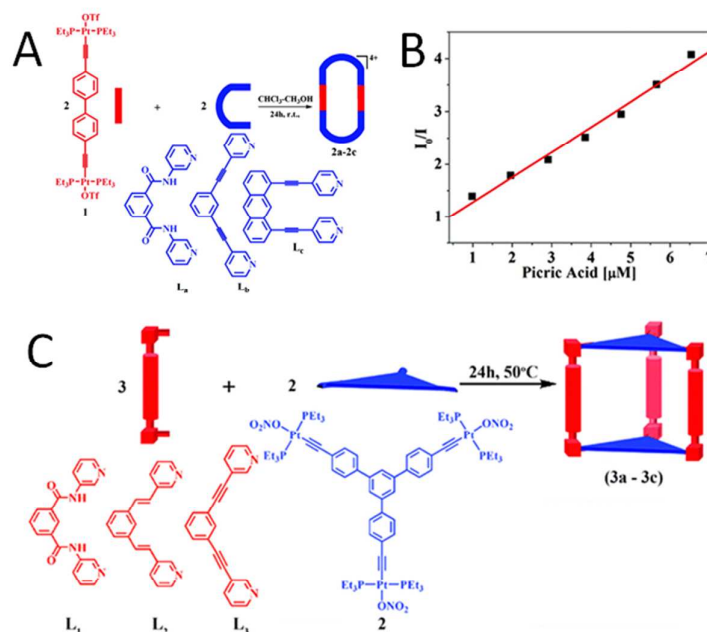
Fig. 21 (A) Schematic illustration of [2+2] self-assembly of metallamacrocycles using organometallic acceptor 1 in combination with three different ditopic donors (L$_a$-L$_c$); (B) The obtained Stern-Volmer plot from fluorescence quenching of 2c with picric acid. (C) Schematic illustration of three different donors (L$_1$ - L$_3$) and a new planar tritopic acceptor (2) and their [3+2] self-assembly into trigonal prismatic architecture (3a-3c). Adapted with permission from Ref. 210 and 211. Copyright 2011 the American Chemical Society and 2013 the Royal Society of Chemistry.

region of a dendritic structure and also non-covalently host in the cavities of a dendrimer or associated at the dendrimer surface. Therefore, dendrimers containing fluorophores are particularly interesting and have great potentials to be applied in explosives detection.

Abruna et al. has reported the synthesis of five generations (G0-G4) of tris(bipyridyl)ruthenium(II) pendant poly(amidoamine) (PAMAM) dendrimers (dend-n-[Ru (bpy)$_3$]), n=4, 8, 16, 32 and 64 for generations G0-G4).[214] Stern-Volmer analysis implied a combined dynamic and static quenching mechanism in the presence of TNT. The accessibility of TNT quencher molecules to starburst dendrimers depended on the generation (size) and played a dominant role in the quenching efficiency. The least crowded dendrimer structure was at generation 3, so the quenching efficiency for TNT was found to be maximum for dend-16-Ru (bpy)$_3$. Goodson and co-workers reported that the fluorescence of organic dendrimers was sensitive to TNT, and the fluorescence quenching response was effectively activated by the near-infrared light with the use of two-photon excitation.[215, 216] The enhanced sensitivity was attributed to the extended exciton migration over the dendrimer surface.

In 2011, Shaw and co-workers reported on a new series of zeroth- and first-generation fluorescent chromophore dendrimers which interacted with nitro-explosives primarily via a collisional process.[48] They also developed two carbazole-containing dendrimers capable of detecting the explosive analytes (e.g., DMNB and NM) in solution.[217] Later, three generations (G1, G2, G3) of fluorescent carbazole dendrimers with spirobifluorene cores (Fig. 22) were developed.[218] In solution, experiments showed that the quenching efficiency increased between the first and second generations, while only a minor increase was observed in moving to the third. With the exception of DNB there was no significant difference in quenching between the three generations in the solid state. In order to explain the quenching differences between different generations of carbazole dendrimers, the research group studied the absorption and release of 4-NT from thin films of the dendrimers using combination of time-correlated neutron reflectometry and PL spectroscopy.[219] In another report, they proposed that the more three-dimensional shape of the sBF(Gx)$_4$ dendrimers created a cleft for the analyte, the more interactions between a single bound analyte and fluorophores, thus reducing the average distance between the analyte and an excited state for the equivalent generation.[220] They proposed that there was a trade-off between steric
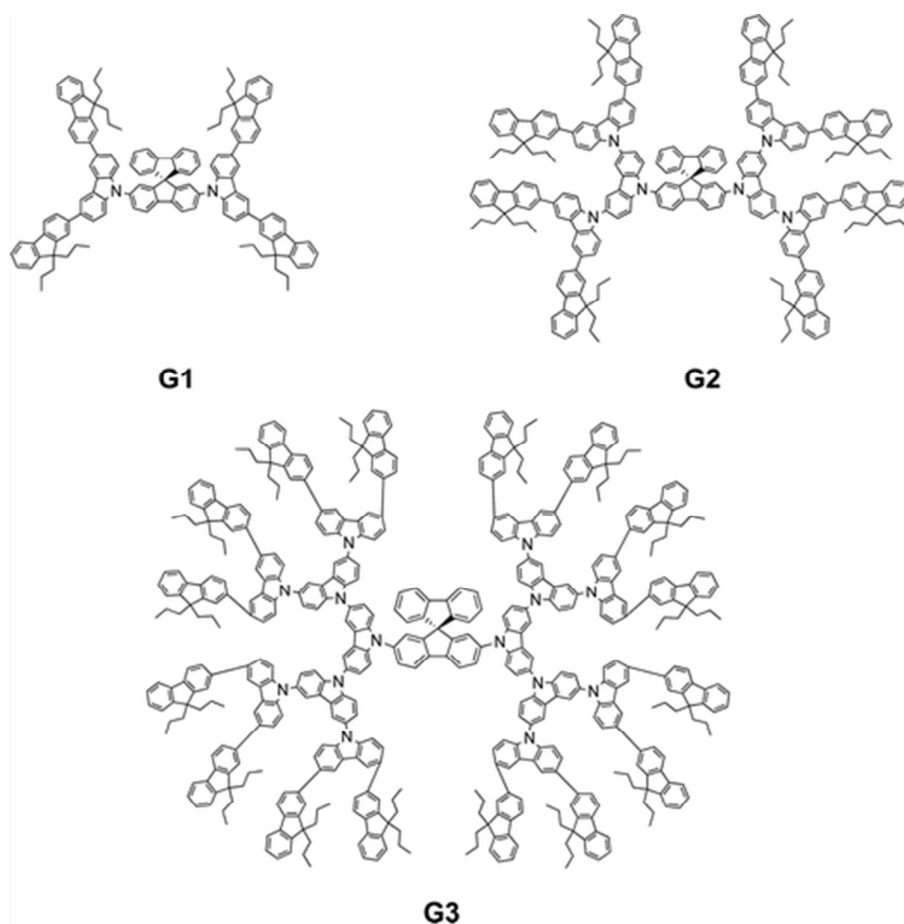

Fig. 22 Structures of dendrimers for three generations, defined as G1, G2 and G3. Adapted with permission from Ref. 218. Copyright 2013 the Royal Society of Chemistry.

hindrance of the analyte interacting with the chromophores within the dendrons and the number of chromophores in the second- and third-generations. The first generation dendrimers behaved as single chromophores with the excited state localized on a chromophore that included the core. Increasing the generation enhanced the number of chromophores per dendrimer, and intramolecular interactions between dendrons resulted in the formation of excimer-like excited states. The more planar fluorine-coated dendrimers showed a gradual decrease in sensing performance, while an increase was observed for the more three-dimensional dendrimers. However, generally quenching by explosives was collisional quenching for the dendrimer fluorescent materials, and Stern-Volmer constant was rather small, thus resulting in a poor detection sensitivity.

Taking advantage of gelation behavior of the carbazole-based conjugated dendrimer H2-BCz with tert-butyl groups, Han et al. observed the formation of one dimensional fibers, the driving force of which was the π-π interactions between the aryl units.[221] Due to the electron-donating property of the H2-BCz molecule and the porosity of the fibrous film, the xerogel film demonstrated efficient fluorescence quenching for the detection of nitroaromatic explosives.

5.3 Supramolecular polymers

Conjugated polymers have been successfully utilized in a commercially available device, "Fido" (FLIR Inc.), for real-time monitoring of explosives in homeland security-related fields, but their synthesis involves multi-step routes, ends with a low yield, and is usually time consuming. In addition, the control of molecular organization or structure determination is not easy for polymers with non-crystalline nature and poor solubility. Therefore, it is necessary and attractive to develop a new sensory material that can address those issues and still enable long-range exciton migrations. Mukherjee's group developed a series of π-electron rich supramolecular polymers for the detection of nitro-explosives.[222, 223] For supramolecular polymers, two or more molecular entities self-associated spontaneously to adopt an infinite network like a structure possessing well-defined molecular organization and large internal porosity through non-covalent interactions such as hydrogen bonding, van der Waals interactions, etc. In addition, the polymers were easy to construct from judiciously pre-designed molecular building units. They identified the role of hydrogen-bonding in dramatic amplification on sensitivity and fluorescence quenching efficiency for nitro-explosives detection. The researchers also synthesized a series of pyrene-based polycarboxylic acids along with their corresponding discrete esters.[224] The fluorescence quenching results by PA and TNT suggested that the supramolecular sensors demonstrated the potential to detect nitro-explosives at ppt levels in solution. The ultra-high sensitivity of the carboxylic acids was attributed to supramolecular polymer formation through hydrogen bonding in the case of the acids, and the enhancement mechanism was based on an exciton energy migration upon excitation along the hydrogen-bond backbone as shown in Fig. 23. It was proposed that collective bulk polymeric materials contributed to the exciton migration
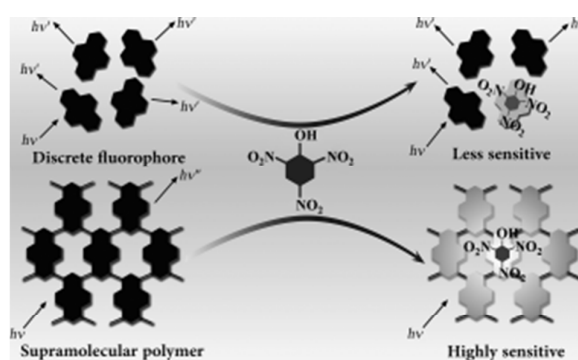

Fig. 23 Schematic representation of the fluorescence quenching mechanism by using discrete fluorophores and the corresponding supramolecular polymers. The supramolecular polymers had a higher sensitivity compared to the discrete analogues due to the exciton migration through hydrogen bonding upon excitation. Reprinted with permission from Ref. 224. Copyright 2014 Wiley-VCH.

rather than the discrete units. When the fluorophores were present as single sensory receptor molecule, upon excitation (hv) each molecule had a particular emission (hv'). In the presence of the quencher (here the NACs), the emission of the particular sensor molecule would be quenched, and the rest of the sensor molecules would still emit. However, for a polymeric system, the whole molecule had an emission (hv") upon excitation (hv), and in the presence of quencher the fluorescence of the whole molecule was quenched.

5.4 Metal-organic frameworks

Metal-organic frameworks (MOFs) are constructed via self-assembly of single metal cations (primary building unit or PBU) or metal clusters (secondary building unit or SBU) with organic ligands having multiple binding sites, thus forming one, two, or three dimensionally extended coordination networks. MOFs have emerged as a new class of molecularly tunable porous crystalline solids. The organic ligands often contain aromatic or conjugated π moieties that are subject to excitation, leading to optical emission or photoluminescence upon irradiation. In addition, the metal components can also contribute to photoluminescence. Detectable changes in luminescence by tuning the host-guest chemistry along with tailorable pore size, shape, surface area, surface environment and chemical composition makes MOFs excellent candidates in sensing applications. Regarding to the number of published work, MOFs are possibly the most popular and fastest growing fluorescent materials for explosives detection in recent years.

The pioneering work of Li et al. has demonstrated the potential of luminescent MOFs in explosives detection (as shown in Fig. 24A).[225] They reported that the highly luminescent microporous MOF [Zn_2(bpdc)$_2$(bpee)] (bpdc = 4,4'-biphenyldicarboxylate; bpee = 1,2-bipyridylethene) was capable of very fast and fully reversible detection of both DNT and DMNB with unprecedented sensitivity. The film had a microporous 3D network with a high Langmuir surface area, providing a fast response time and less film thickness
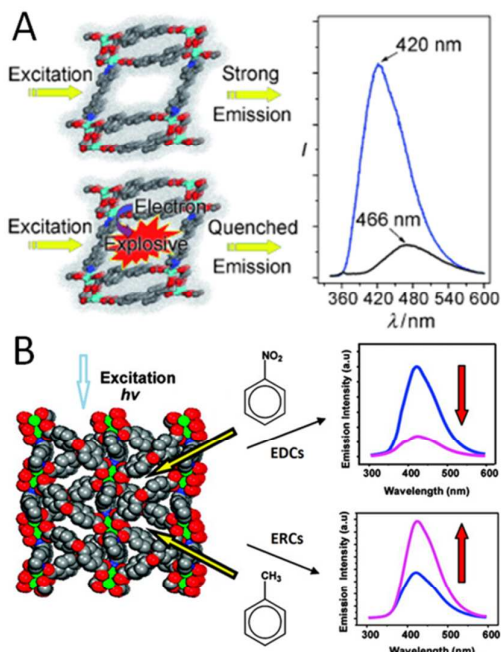
Fig. 24 (A) A highly luminescent microporous metal–organic framework, [$Zn_2(bpdc)_2(bpee)$] (bpdc=4,4'-biphenyldicarboxylate; bpee=1,2-bipyridylethene), capable of very fast detection of the vapors of nitro explosives and the fluorescence spectra before and after exposure to DNMB vapor for 10 s. (B) A highly luminescent 3D microporous MOF, [$Zn_2(oba)_2(bpy)$]·DMA, demonstrates unique selectivity for the detection of electron-deficient explosives (EDCs) and electron-rich aromatics (ERCs) via a fluorescence quenching and enhancement mechanism. Adapted with permission from Ref. 225 and 30. Copyright 2009 Wiley-VCH and 2011 the American Chemical Society.

dependence. A fluorescence quenching efficiency of 84% was achieved upon 10 s exposure to DMNB vapor. The same group later demonstrated the unique selectivity of nitro explosives and other arenes through fluorescence quenching, enhancement and spectra shift (Fig. 24B).[30, 31, 226, 227] The phenomenon was explained through electron transfer between conduction band of MOFs and LUMO of analytes (as shown in Fig. 2) and the formation of exciplex complexes. In 2013, Li's group also discovered that MOF materials possessed fluorescence quenching or enhancement behavior to different types of aromatic molecules.[228] The combination of fluorescence intensity change and frequency shift provides 2D maps, which can be of great assistance to accurate and effective recognition and identification of a large number of analytes with extremely similar physicochemical properties.

For the development of MOF materials in explosives detection, there are several powerful approaches in general. One is to enhance the electron density of the MOFs and to facilitate the exciton migration through using conjugated ligands or backbones with metal ions which possess a non-detrimental nature of fluorescence, or using fluorescence tag in the backbone of the ligands which possess benzene,

naphthalene, pyrene, etc.[229] Secondly, the introduction of secondary functional groups which endows preferred binding of the chosen analyte resulting in better selectivity to the specific analyte.[230] Furthermore, decreasing MOF size particles favours the increase of surface area and porosity and promotes the diffusion of analytes into the MOFs.

Optimization of organic ligands or metals in MOF preparation is the key to achieving superb performance. For example, Ghosh's group developed one kind of picric acid sensor using [$Cd(ndc)_{0.5}(pca)$]·xG (G = guest molecules, pca = 4-pyridinecaboxylic acid) through incorporation of Lewis basic sites to tune the emission spectrum of MOFs (Fig. 25A).[34] The combination of both effective electron and energy transfer led to a sensory profile with ultra-selectivity and sensitivity to the detection of picric acid (Fig. 25B). The MOF was preferentially quenched by PA in MeCN, while exposure to other nitro compounds resulted in insignificant change on its fluorescence intensity. The high PA sensitivity and selectivity were attributed to three factors. Firstly, PA had the lowest LUMO
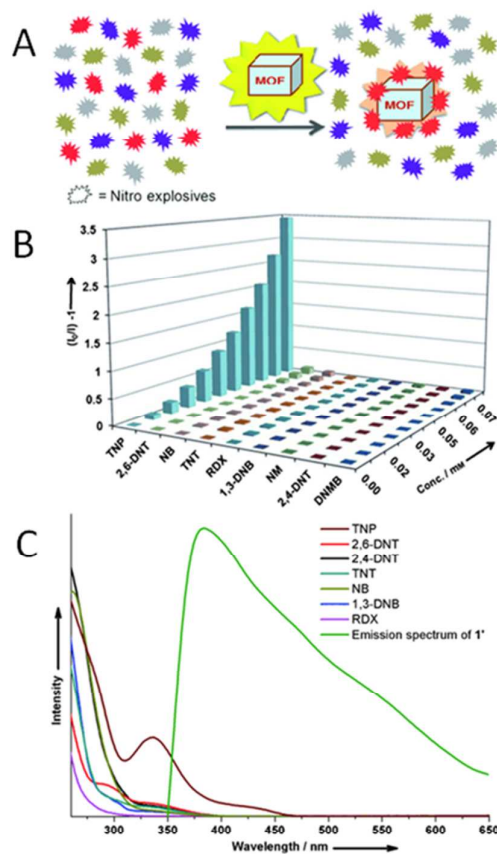

Fig. 25 (A) MOF-based sensor for selective detection of target nitro explosives in the presence of other nitro compounds. (B) Stern-Volmer plots of MOF sensor with different nitro-based explosives. (C) Spectral overlap between the absorption spectra of analytes and the emission spectrum of MOF 1'. Reproduced with permission from Ref. 34. Copyright 2013 Wiley-VCH.

energy during all the investigated analytes, which provided the largest thermodynamic driving force for PET process. Secondly, the Lewis basic sites (pyridine nitrogen) from pca could interact with PA through electrostatic interactions. More importantly, FRET mechanism played a pivotal role in quenching process due to the large spectra overlap between the emission spectrum of the MOF and the absorption spectrum of PA (Fig. 25C). Although the detection was performed in organic solvent and the sensitivity was rather poor, this study provides a new insight into the design of MOF-based explosive sensors. Based on these findings, Ghosh and co-workers later designed MOF sensors with improved sensing performance to PA.[230]

Selective detection of NACs in ethanol solution has also been accomplished by Mukherjee et al. through a micro-particle Zn(II) MOF, $[Zn_4O(L)_2 \cdot (H_2O)_3] \cdot 3DMA \cdot 3EtOH \cdot 6H_2O$.[231] In this case, MOF pores were filled with guest solvent molecules so this material could be viewed as non-porous micro-particles in ethanol. The quenching mechanism was ascribed to PET from the excited MOF to the close NACs adsorbed on the surface of the MOF particles. The detection limit for TNT was reached at ppb level, and the signal was recovered by centrifuging and washing with ethanol. However, some strong oxidants (such as benzoquinone and 4-methoxybenzoic acid) also generated considerable quenching response to MOF. Later, a dynamic MOF has been constructed using triphenylene-2,6,10-tricarboxylate and Tb^{3+} as building blocks, which exhibited guest-responsive structural dynamism towards different sizes of guest molecules and selective detection of nitroaromatic explosives.[232] In Venkatesan's work, triptycene receptor was self-assembled into macroporous metal-organic materials, which facilitated long-range exciton migrations for explosives detection.[233] Similar research such as tripodal ligand H_3L (2,4,6-tris[1-(3-carboxylphenoxy)ylmethyl]mesitylene) and d_{10} configuration metal ion Cd^{2+} based building units were also used to prepare MOF under solvothermal conditions.[234, 235] Lan et al. reported the hydrothermal synthesis of a magnesium metal-organic framework compound with benzenetetracaboxylic acid (BETC) ligands.[236] The material, pentanuclear magnesium clusters as the secondary building units gave rise to the 1D channels along the a axis and demonstrated high fluorescence sensing capability for nitroaromatic compounds. Huang and co-workers designed a highly fluorescent MOF constructed by a rare dendritic multicarboxyl acid with a pyrene chromophore ligand and then applied in explosives detection very recently.[237] Ghosh's group designed and synthesized a novel 2D MOF with a starfish array and a super π-electron-rich surface, showing supramolecular wire effect (Fig. 26).[238] The interaction occurred mostly on the super π-electron rich surfaces of the framework, which endowed highly quenching efficiencies for both nitroaromatic and nitro-aliphatic explosives. Size-dependent sorption studies clearly suggested that the interaction occurred mostly on the super π-electron rich surfaces of the framework. This facile strategy to generate super π-electron rich surfaces by the supramolecular wire effect may also be extended to prepare

other novel MOF-based compounds like nanomaterials, coordination polymer gels, etc.

Recently Mukherjee et al. also synthesized multicomponent MOFs by employing ligands embedded with fluorescent tags modification from phenyl to naphthalene to pyrene to enhance the electron density.[229] The as-prepared electron-rich fluorescent MOFs have been utilized for the selective and sensitive detection of the electron-deficient explosives. The single-crystal structures of MOFs demonstrated the formation of porous networks with the aromatic tags projecting inwardly into the pores, which may affect the porosity inside the channels and consequently the ability to encapsulate the analytes. Jaworski et al. prepared nanocomposite MOF material, assembled from azobenzoic acid-functionalized graphene oxide/trans-4-4'-stilbene dicarboxylic acid - Zn^{2+} complex.[239] The unique GO functionalization of MOF structure
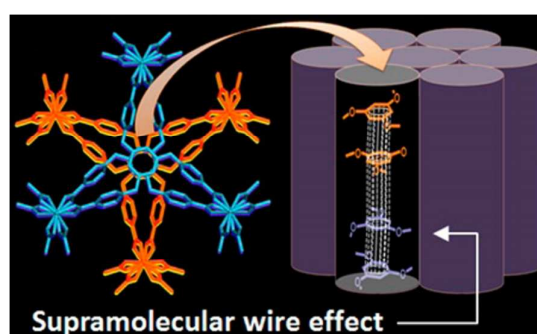

Fig. 26 The perspective view of the starfish array of the MOF and the corresponding schematic visualization of cylindrical units of the π-stacked L moiety in a framework along the c axis (orange and blue color indicate two different 2D sheets) Reprinted with permission from Ref. 238. Copyright 2013 the American Chemical Society.

showed fluorescence enhancement with a long lifetime and fluorescence quenching behaviour to DNT molecules.

Compared with other fluorescent materials, MOF shows greater potential to achieve selective detection and differentiation between various nitro-explosives due to its unique properties. Lan and co-workers reported a novel, stable MOF that was able to distinguish nitroaromatic molecules with different numbers of $-NO_2$ groups through the shift of PL spectra due to the formation of the exciplex.[240] A fluorescent naphthalene dicarboxylic acid with a d_{10} metal Zn ion yielded a highly emissive 3D framework, which demonstrated discriminative power to detect nitro aromatic molecules with different numbers of $-NO_2$ groups based on fluorescence quenching.[241] The quenching efficiency depended on the dipole-dipole and π-stack interactions of the nitro-explosives. NT possessed the higher dipole moment than the other investigated analytes, and had stronger interactions with MOF, thus leading to higher quenching efficiency. For PA, charge transfer mechanism was responsible for the observed fluorescence quenching; while the π-stack complex with strong binding energy with the MOF compound was attributed to the observed fluorescence quenching by TNT.

32 | *Chem. Soc. Rev.*, 2015, **00**, 1-3

This journal is © The Royal Society of Chemistry 20xx

Sensory material with smaller size and higher porosity favours the diffusion of analytes and reduces the response time. MOF nanotube[242], MOF nanofiber[243], surfactant-assisted nanorods[244], magnetic nanospheres[245], microwave-assisted nanoparticles[246] and MOF micrometer size particles[231] have also been reported in order to improve the sensitivity and response time. Parkin's recent work reiterated the key importance of MOF porosity in sensing applications and highlighted the value of uniform microcrystals to sensitivity in explosives detection.[247] They proposed that the flatter and more uniform crystals gave greater access to the material on the sensing substrate, and thus improved response. In addition, Qiu et al. used a self-sacrificing template to synthesize MOF nanotubes.[242] The resultant fluorescent MOF nanotubes showed fast, highly sensitive, selective, and reversible detection for trace-level of nitroaromatic explosives, indicating that the tubular MOF nanostructures was a great material for the detection of explosives. Biradha et al. reported the preparation of metal-organic gels, which possessed one-dimensional nanofibrous polymeric network, and the formation was determined by the intermolecular aromatic π-π interaction and some other weak interactions within and between the networks.[248] The as-synthesized gels demonstrated significant quenching response to nitrobenzene and dinitrophenol.

The development of the novel synthetic methods besides solvothermal reaction for MOF preparation is another popular research topic in recent years. Two novel MOF-74 analogs with –OH groups on their pore surfaces were constructed by functional phenyl-acrylic acid and 4,4'-bipyridyl through multi-component self-assembly at room temperature.[228] The two MOF showed exceptional fluorescence quenching and enhancement behaviour exposure to different types of aromatic molecules. A facile electroplating method was also used to prepare MOF ($Zn_3(BTC)_2$) films using Zinc electrodes in a 1,3,5-benzenetricarboxylic acid electrolyte by Cao's group.[249] Metal-organic gel provided another new and simple form of MOF, and had been used for explosives detection by different research groups.[233, 248]

Besides popular MOFs, Jiang et al. reported on the synthesis of covalent organic frameworks (COFs) and their application in explosive sensing.[250] By virtue of various factors such as the pyrene column ordering as luminescence emitter, the permanent porosity and high surface area by the azine-linked frameworks, the azine edges as docking sites for hydrogen-bonding interactions, and the extended π conjugation network as a media for exciton migration, the COF demonstrated as a great candidate for high sensitivity and selectivity in chemosensing, for example, the selective detection of picric acid. In addition, Pu and coworkers reported a one-step approach to synthesize COF based polymeric nanoparticles through poly-condensation between melamine and terephthalaldehyde.[251] The nanoparticles demonstrated significant improvement in selectivity and sensitivity in TNT detection, with a LOD of 1.8 nM.

6. Bio-inspired fluorescent materials for explosives detection

In recent years, bio-based materials such as peptide, protein and DNA have been employed for fluorescence-based explosive detection. The bio-materials can be functionalized in two different roles. In the first role, the biomaterial is only used as support or functional layer. Kool and co-workers designed and added multiple fluorophores onto a DNA backbone and tried to address the current limitations of fluorescent materials such as limited sensor diversity and flexibility.[252] DNA-like oligomers can be synthesized rapidly in widely varied sequences and lengths as well as straightforwardly in large combinatorial libraries. In the study, oligomeric fluorophores behaved as vapor sensors with varied responses beyond simple quenching, and demonstrated sequence-based responses for multiple classes of analytes. In addition, the library-based synthesis and screening approach enabled facile evaluation of various sensors for many analytes. Strano et al. found that a class of peptides from the bombolitin family endowed near-infrared fluorescent single-walled nanotube (SWNT) to transduce specific changes in their conformation.[253] Resolution of an entire class of molecules at the single-molecule level can be achieved by the nanotube via reporting the optical transduction of the secondary structure and conformational structure changes to a polypeptide in solution. The wavelength shifting of peptide functionalized SWNT exhibited explosives concentration dependent properties.

Since bovine serum albumin (BSA) has electron rich amino groups on the surface, it has been widely used in functionalization of fluorophores due to formation of a Meisenheimer complex by the chemical interactions between TNT and the free amino groups on BSA, such as BSA protected quantum clusters[164, 165] and quantum dots[161]. Besides BSA, some other biomaterials were also exploited, including peptides for preparing nanotubes[254] and cellulose for building the cavities and pathways for explosive molecule diffusion[255]. Very recently, Suri and co-workers reported on using TNT specific aptamer and antibodies tagged with respective FRET pair for explosives detection.[256] The as-developed sensor showed excellent sensitivity with LOD of 0.4 nM.

Secondly, researchers are harnessing fluorescent properties of biomaterials such as fluorescent proteins to serve as explosives sensors. Generally, the fluorescence of protein is caused by three intrinsic fluorophores present in the protein, such as tryptophan, tyrosine, and phenyl alanine residues.[23] The intrinsic fluorescence of many proteins is mainly contributed by tryptophan alone. In Hick's study, the fluorescent properties of proteins were applied for explosive quenching, taking advantage of the fact that tryptophan excitation can be quenched by numerous agents.[257] This seminal work provides the foundation for production of an array of genetically-modified fluorescent proteins for in vitro biosensors capable of rapid, simultaneous, sensitive and selective detection of a wide range of explosive agents. When excited with UV light, it was the tryptophan that absorbed the

excitation light. The energy can be emitted directly from the tryptophan with a maximum emission wavelength of ~ 340 nm, or it can be transferred to the chromophore by FRET and lead to visible emission. Tryptophans were in the hydrophobic interior of a protein. For all of the fluorescent proteins, the tryptophan residues were located near the chromophore on the interior of β-barrel structure, which also accounted for poor sensitivity to explosives detection in their study. Inspired by Ghosh's work[34] and taking advantage of unique properties of fluorescent proteins, our group recently reported highly-sensitive (LOD as low as 17.2 nM), ultra-selective (about two orders of K_{SV} values larger than that of other nitro-explosives) and rapid detection of picric acid in aqueous phase through quenching of BSA fluorescence (Fig. 27).[36] In addition, we observed two linearities in the SV plot, which bended downward at higher concentrations. The phenomenon was attributed to the presence two fluorophores, and could work in explosives detection over a broad range of concentrations, different from commonly bending upward of SV plot. The extraordinary sensing performance was ascribed to electron transfer and fluorescence resonance energy transfer mechanisms as well as acid-base pairing interactions between amino groups of BSA and picrate anions of PA in aqueous
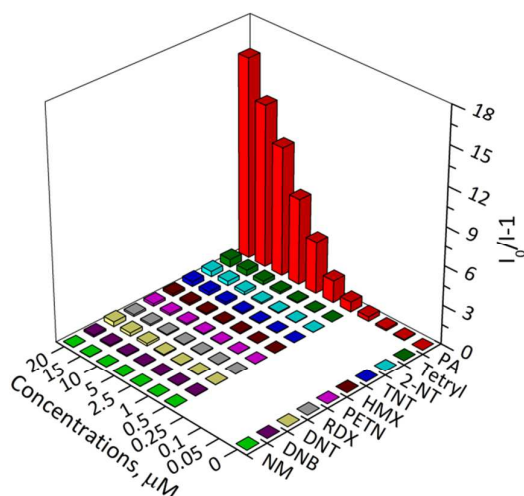

Fig. 27 Stern-Volmer plots of BSA fluorescent sensors with different nitro-based explosives. Adapted with permission from Ref. 36. Copyright 2014 the Royal Society of Chemistry.

solution. The present study provides a new route to the design of a cheap and simple explosive fluorescence sensor which is completely biodegradable and environmentally-friendly.

Based on the green fluorescent protein and bioluminescent genes, Belkin et al. reported on the construction of genetically engineered *Escherichia coli* strains with bioreceptor for the detection of explosives.[258] It was demonstrated that both TNT and DNT were metabolized by *E. coli* and that the induction of fluorescence was caused by unidentified degradation products. The work presented the first study of an engineered *E. coli* whole cell sensor strained for DNT and TNT detection. Besides engineered bacteria, the plants were also applied as

chemosensors in explosive detection.[259] As contaminant concentration increased, significant declines in photosynthesis and leaf fluorescence occurred for all the investigated explosives such as RDX and TNT, which suggested that plant physiology may serve as a novel method for explosive contamination stress detection.

The research on fluorescent protein for explosives detection is still in its infancy, it is anticipated that through the engineering of protein related to its emission spectra and size, a variety of fluorescent proteins could serve as the next generation of explosive sensors. As we have discussed before, the environmental issues of current fluorescent sensory materials may necessitate the development of environmental-friendly bio-based fluorescent materials.

7. Aggregation induced emission (AIE) - active materials for explosives detection

Beyond the fluorescent materials discussed above, aggregation induced emission (AIE)-active fluorescent materials in explosive detection have become a popular research topic recently. Tang's group have discovered and pioneered a new phenomenon of AIE effect that is exactly opposite to the aggregation-caused quenching discussed above. In AIE
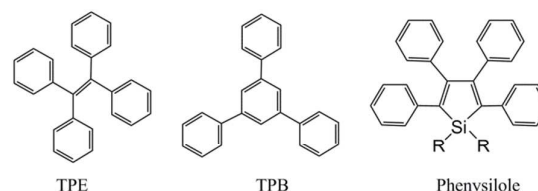

Fig. 28 Small molecules for AIE materials such as tetraphenylethene (TPE), triphenylbenzene (TPB) and siloles.

materials, a series of small molecules, such as tetraphenylethene (TPE), triphenylbenzene (TPB) and siloles, are induced to emit efficiently by aggregation (Fig. 28).

The Tang group reported a series of polymers containing AIE-active moieties.[260-268] These AIE-active polymers are virtually non-luminescent when molecularly dissolved in their good solvents, but emit intensely when aggregated in their poor solvents or fabricated into thin solid films and work effectively as nitro-explosives sensors. For example, a TPE-containing poly(aroyltriazole) (PI, Fig. 29A) showed AIE phenomenon with increasing solvent water content.[260] At a water content of 90%, the polymer exhibited a fluorescence quantum yield 61-fold higher than in pure THF solvent (Fig. 29B), and was able to detect picric acid down to 1 ppm with a Stern-Volmer constant of 2.1×10^4 M^{-1} (Fig. 29C). The quenching effect for picric acid detection was observed with super-quenching, and the Stern-Volmer plot bended upward with the increase of explosives concentrations. The sensitivities for picric acid were further enhanced when those AIE-active units were incorporated into 3D hyper-branched polymer structures.[261, 262] Recently, the same group introduced AIE units, such as silole and TPE, into the linear and/or hyper-
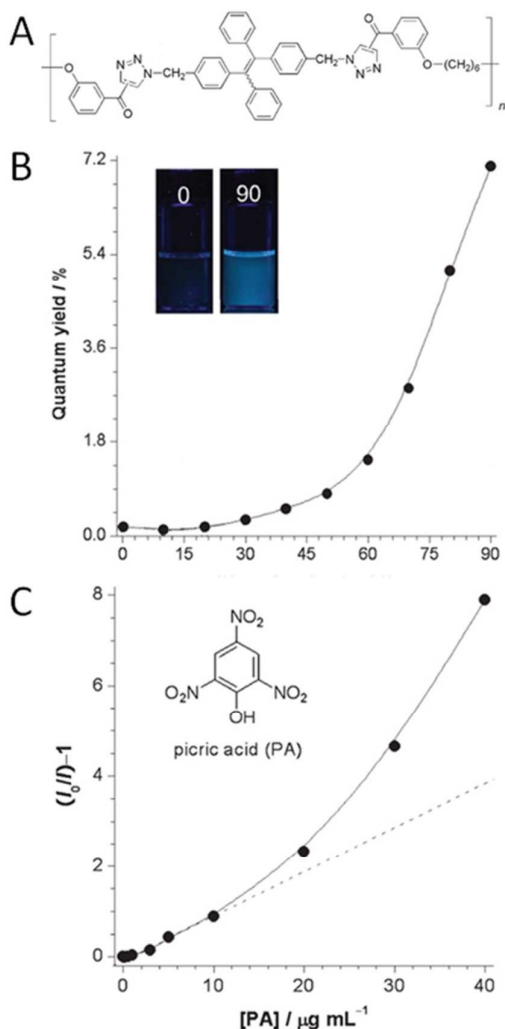
34 | *Chem. Soc. Rev.*, 2015, **00**, 1-3

This journal is © The Royal Society of Chemistry 20xx

Fig. 29 (A) Structures of a TPE-containing poly(aroyltriazole) polymer (PI); (B) Variation of the quantum yields of PI in THF/H$_2$O mixtures with different H$_2$O fractions. Inset shows the photographs of PI solutions in pure THF and THF/H$_2$O mixtures with 90% H$_2$O under illumination of a handheld UV lamp; and (C) Stern-Volmer Plots of PI with different concentrations of PA. Reproduced with permission from Ref. 260. Copyright 2009 Wiley-VCH.

branched polymers by various methods in order to further improve their sensing performance. Most of their early studies were performed for explosives detection in solution and using solid-state materials, while for explosives vapor detection using AIE-active materials was very rare. The same group reported on the electrospun AIE based polymer films, which exhibited remarkable and enhanced sensing performance to explosives vapors compared to dense films.[269] Very recently, Scherf et al. synthesized two polytriphenylamines with TPE side groups, which also exhibited AIE-active properties and demonstrated the ability to detect nitro-explosives (TNB) vapors.[270]

A series of propeller-shaped molecules are non-emissive when molecularly dissolved but emit intensely when aggregated or fabricated in solid films, and the restriction of intramolecular rotation (RIR) has been rationalized as the AIE mechanism. hb-PIa and hb-PIb containing similar chains to TPE were synthesized to investigate AIE features and mechanisms.[264] The AIE features of hb-PIa and hb-PIb could be attributed to their intrinsic architectures. According to the RIR mechanism, even after the TPE units have been incorporated into the polymer branches, their peripheral phenyl rings can still rotate freely in the solution state, making the polymers non-emissive. In the aggregated state, however, the intramolecular rotation was restricted, which effectively blocked the non-radiative energy dissipation channels of the polymers and thus turned on their light emission. In order to further probe the mechanism of AIE, Bhalla et al. designed a series of AIE-active molecules based on pentacenequinone derivatives.[271] Through viscosity, temperature and time resolved fluorescence studies, the work confirmed that AIE phenomenon was at the cost of aggregation driven growth and restriction of intramolecular rotation.

Recently, Tong's group developed a series of TPE-based
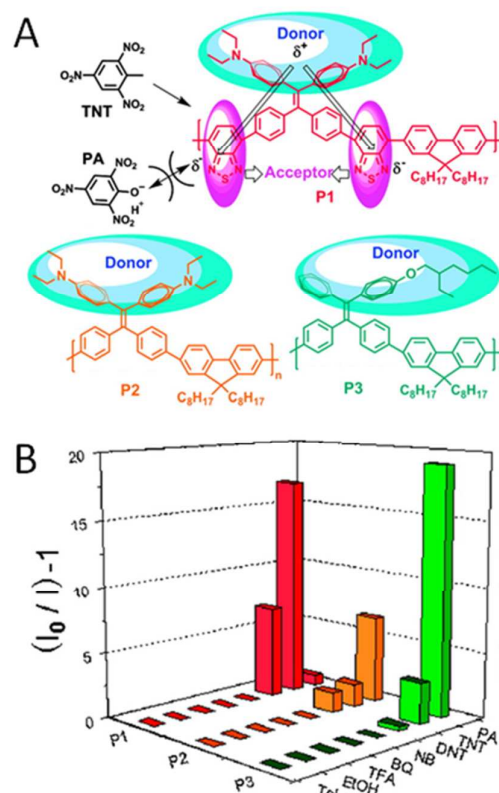

Fig. 30 (A) Structures of P1-P3 and their interactions with TNT and PA; and (B) Effects of different analytes (0.2 mM) on the emission of the polymer films in aqueous solutions (I$_0$ and I are the PL intensities of the film in the absence and presence of the analyte, respectively). Reprinted with permission from Ref. 272. Copyright 2011 the American Chemical Society.

polymers (Fig. 30) for discrimination of TNT and picric acid in aqueous solution based on the intrachain donor-acceptor architectures.[272] Those AIE-active polymers exhibited bright emission in spin-coated films with TPE as electron-donating groups. Polymer P1 contained an acceptor group, 2,1,3-benzothiadiazole, in its backbone and formed a donor-acceptor conjugated polymer, while P3 was donor-only polymer. The acceptor group in P1 was negative charged and had an electrostatic repulsion to negatively charged picric acid anions in aqueous solution, which blocked the PET process from P1 to picric acid. This phenomenon did not occur in the presence of TNT with P1, so P1 was selective to TNT with a K_{SV} of 1.2×10^5 M^{-1} and a detection limit of 23 ppb and, which was almost 2 orders lower than for picric acid. On the other hand, P3 was selective to picric acid with the detection limit of 2 ppb and the K_{SV} constant of 2.8×10^4 M^{-1}, due to the lower LUMO value of picric acid than for TNT. The normalized fluorescence intensity (I_0/I) with different analytes of the polymer films were shown in Fig. 30B, which clearly demonstrated the selective detection and differentiation of TNT and picric acid.

Besides the popular small molecule units for developing of AIE-active materials (Fig. 28), Bhalla and co-workers designed two Hexa-peri-hexabenzocoronene (HBC) based derivatives incorporated with two rotors which can induce AIE enhancement by restricting the ratio of water in solution of aggregates.[273] The aggregates of both derivatives formed spherical aggregation and behaved as highly sensitive and selective chemosensors for picric acid. The sensors showed K_{SV} constants as high as 3.2×10^6 M^{-1} and 2.0×10^6 M^{-1}, respectively. These values, to the best of our knowledge, were the two largest values reported for PA fluorescent sensors. The high sensitivity and selectivity to PA detection can be attributed to its tendency to protonate the NH_2 groups in derivative and its high polarizability compared to other derivatives. Furthermore, the current sensors showed the potentials to detect PA vapors as low as attogram level. The same group further synthesized pentacenequinone derivatives by Suzuki-Miyaura coupling reaction for explosive detection.[271]

Making use of nanotechnologies, Yu's group designed AIE-luminogen functionalized materials such as mesoporous materials.[274, 275] Such materials combined the benefits of the unique properties of mesoporous materials and AIE luminogen of TPE, which improved mass transport and strengthened interactions with adsorbed molecules.

To our surprise, almost all the AIE fluorescent materials have been focused on the sensitive and selective detection of picric acid. This is possibly due to PA's lower LUMO value, unique absorption spectrum, or the protonation which contributed to acid-base interactions between PA and amino group on AIE materials. The detection of TNT is of more significance and should be investigated in future using this new kind of fluorescent materials. Although there is one report relating to AIE active phosphorescent material for TNT detection, low sensitivity makes it unattractive in real applications.[276] Therefore, AIE-based sensors with better sensitivity for TNT detection needs more research efforts and could be achieved by shaping the morphology of AIE material films and tuning

the LUMO levels of AIE active materials appropriately matching the LUMO level of TNT for effective electron transfer.

8.   Conclusions and future outlook

The needs for homeland security and demining activities result in an intense interest of the explosives detection. The fluorescence based methods hold much promise to satisfy most of the criteria required for an effective sensing platform, such as high sensitivity and selectivity, fast speed, simplicity, portability, and low-cost. The fluorescent materials integrating with other technologies such as electronics, imaging, and sensor design could play more important roles in real explosives detection such as buried landmines, environmental contamination in soil, groundwater and seawater.

NAC explosives, such as TNT, DNT and picric acid, have been intensely investigated with established detection methods, however, direct detection of RDX, PETN and the continually increasing variety of explosives compounds encountered by police and security agencies worldwide are still remaining a huge challenge. It has been reported that using currently effective sensing tools such as FidoXT, IMS, mass spectrometry, are not able to directly detect RDX and PETN, or only able to detect the modified RDX or its degradation product.[277] Considering their vast use in plastic bonded explosives, RDX and PETN are important explosive targets for sensing and devote more efforts. It is highly desirable to develop a fluorescent detection system that not only detects a broad range of nitrated explosives, including NACs, nitroalkanes, nitroamines, and nitrate esters, but also differentiates them. Through designing selective reactions between fluorescent materials and different explosives, it is possible to generate some novel fluorescent materials that can selectively detect and differentiate different explosives.

Moreover, researchers should have more practical view on designing novel explosive sensing systems. Currently, most of explosives fluorescent probes are developed and tested in the laboratory environment. Although the detection sensitivities of fluorescent probes for NACs has reached satisfactory levels, their applicability for directly detecting TNT or DNT vapors from packed bombs or landmines under real circumstances is not addressed and unknown. Current technologies accomplish indirect explosive detection by sensing more volatile taggant, such as DMNB. Beyond laboratory tests, further development should be more focusing on real situations such as explosive detection in fields and transportation hubs. The demand to detect explosives from a safe standoff distance presents another interesting direction for explosives detection in real applications. Recently our group has reported the naked-eye based detection of buried explosives, which is attractive.[183, 184] Due to the benefits such as simplicity and without the use of advanced equipment, visual-based explosives detection could benefit a lot in real applications. In addition, for ease of visual detection, a change in the luminescence color in the presence of an analyte is a more desirable indicator than the disappearance of luminescence.

ARTICLE

For any real application, sensory materials also need to meet several requirements such as low cost, environmental-friendly, and long term stability. PPE conjugated polymers are one kind of materials which have been used in commercialized devices. However, these polymers require complicated and time-consuming synthetic routes from monomer design to polymerization, which is a clear drawback for mass production. Photo-stability issues of conjugated polymers have also aroused much attention recently.[278] As well known, other popular fluorescent materials such as PAHs, quantum dots and MOFs also have problems such as toxicity, which may contaminate the environment and be toxic to the plants, animals or human beings. These potential issues require researchers to develop novel, low-cost, environmental-friendly and stable fluorescent materials. In this regard, it seems to be a promising choice to use high-performance small molecule fluorophores as the model units to modify the side chains of commercially available conjugated polymers, as the modification on the side polymer chains could be accomplished in a much simpler one-step reaction. By carefully designing the modification sites, the functionalized polymer may obtain higher sensitivities with extended exciton migration and better processability. Moreover, supramolecular systems were recently reported with excellent sensing performance, and could hold great promise in explosive detection if they would solve the issues such as high cost and low-scalability. Recently we used fluorescent proteins to develop an environmental-friendly explosive sensor with high sensitivity and ultra-selectivity.[36] Such environmental-friendly fluorescent proteins can be mass-produced with low cost. Therefore, genetically engineered fluorescent protein with appropriate functions might be one of the attractive research directions in explosive detection.

Regarding the sensing mechanism, PET mechanism plays a role in most quenching response in explosive detection, but this process is considered as trivial and non-selective in general, since the quenching of fluorescence may result from electron-deficient compounds other than nitrated explosives. Therefore, the sensing mechanisms relying on more selective and efficient interactions are predicted to further develop in next few years such as FRET, electron exchange, ICT, etc., which can be realized through rational design of the fluorescent sensing materials. For example, the introduction of primary amines has been applied to selectively sense nitroaromatics, such TNT and Tetryl, through FRET quenching.[41-43] The other perspective of FRET utilization is selective detection of picric acid through tuning the emission spectra of fluorophores to efficiently overlap with absorption spectrum of picric acid.

Fluorescence quenching method still dominates in fluorescence-based explosives detection, however, it is necessary to exploit other fluorescence phenomena for explosives sensing. Theoretically, any phenomenon that results in a change of fluorescence intensity (quenching or enhancement), wavelength, anisotropy, or lifetime can be used for sensing. It is anticipated that fluorescence enhancement is a more sensitive technique due to its little influence by fluorescence background. Generally, explosives lead to fluorescence quenching due to PET process from excited fluorophore to electron deficient explosives. Through optimization of molecular orbitals of fluorophores, it is anticipated that electron transfer direction is reversed for some explosives, thus leading to reversed sensing phenomena for different explosives. Furthermore, it is highly attractive to design a sensing system in which nitro-explosives can interrupt the already existed quenching process, thus leading to fluorescence enhancement. Phenomena of spectra shift and lifetime changes are also expected to be applied for explosives sensing in the near future. Through harnessing the advantages of these phenomena, the future will witness that fluorescence methods play more important roles in sensing explosives.

It is also very attractive to develop bi-modual sensors for explosive detection as they can greatly enrich the information output. Bi-modular sensor can be realized by integrating fluorescence technology with other sensing technologies.[279] For example, conjugated polymers are one of the most popular fluorescent materials for the detection of nitro explosives. Besides fluorescence response, some polymers also show resistivity/conductivity changes upon exposure to explosives. Sensing reliability, sensitivity or selectivity could be improved through integration of different sensing technologies into one sensor. As reported, through the integration of fluorescence quenching and photoconductivity experiments, TNT and DNT were detected and differentiated.[90] In addition, integration of fluorescence and surface enhanced Raman scattering (SERS) was another achieved solution in bi-modual explosive detection through metal enhanced fluorescence. For example, Pradeep's group designed Au core/silica shell structures for enhanced fluorescence and Raman scattering, thus realizing selective visual detection of TNT at the sub-zeptomolar level.[167] By combining the high sensitivity and selectivity offered by SERS with the fluorescence method, the accuracy and reliability of the detection technique was greatly enhanced.

The use of sensor arrays is another popular solution to address the issues of poor selectivity that perplexed explosives detection. In conjunction with artificial neural network, the data from sensor array can be used to detect and differentiate a broad range of explosives. Very recently, a sensor array was achieved through utilization of 3 novel fluorescent polymeric sensory membranes.[280] Upon exposure to explosive vapors, the fluorescence variation, both turn-on and turn-off were recorded and simultaneous treated using multivariate techniques, thus permitting the differentiation of the explosives from explosive mimics or interferents, the discrimination between explosives, the ability to assess the probability of false non-detection of an explosive and probability of false detection. The fluorescent spectra in terms of intensity vs. wavelength at various times for each of the 3 membranes had a highly defined internal structure, and only 3 principal components (PCs) were needed for the description of each membrane using principle component analysis (PCA). PCA allows for both discrimination between explosive and their mimics and for distinction between the 3 explosives.

Another future trend in fluorescence-based explosive detection is to better understand the involved sensing mechanisms and the relation between sensing material and sensing performance. Up to date, most of the fluorescent sensory materials used in explosive detection have been developed empirically and/or by a method of trial and error. Therefore, it is desirable to use theory prediction (such as molecular orbitals) to rationally design the sensing materials. To accomplish this goal, simulation and theory studies are necessary to be integrated with material synthesis and rational design in order to achieve materials with better electronic structures and predictable sensing performance. For example, density functional theory computation is a powerful tool to study the electronic properties of luminescent materials and analyte interactions from a theoretical perspective. By deliberately tuning the crystal structures, composition and porosity, optimal electronic structures, optical emission and redox properties of sensing materials, the sensing performance would be significantly improved, which could establish guidelines for the material design and develop reliable criteria for predicting and identifying the most suitable materials for sensitive and selective detection of explosives. Besides the materials development, understanding how the analyte molecules diffuse into the sensing films and interact with the chromophore is another direction for mechanism studies. Shaw and co-workers applied Quartz crystal microbalance (QCM) and neutron reflectance (NR) to analyze the diffusion of nitroaromatics to dendrimer films, and they found that the sorption process was spontaneous and independent of the film thickness.[281] Combination of QCM, NR, and ab initio quantum chemistry calculations provided insights into ascertaining the sorption process in sensing materials for nitro-explosives.

In this review, we mainly focused on the fluorescence method for explosive detection. However, several new techniques such as surface enhanced Raman scattering have emerged as powerful tools and competed with fluorescence method vigorously for explosives detection in recent years, which cannot be overlooked. Since its discovery in 1970s, SERS has led to a new sensing research field, because it provides benefits such as high selectivity (molecular fingerprint) and ultra-sensitivity (enhanced signals).[282, 283] Different researchers reported on the selective and sensitive detection of TNT using Raman technique, and LOD was achieved at 100 femtomolar level[284, 285] or even 15 attomolar level[286], which was much lower than those of fluorescence based methods for explosives detection. Although SERS demonstrates outstanding performance in sensing explosives, it encounters several issues such as poor reproducibility and high-cost of equipment. We anticipate that the fluorescence-based explosives detection and SERS-based explosives detection can play complementary roles in future.

Although fluorescence-based explosive detection encounters many challenges in terms of sensitivity, selectivity, stability and cost, we believe, with current advances in rational design of sensory materials and progress in simulation and

computation modelling, fluorescent-based explosive sensors will have a promising and bright future.

Acknowledgements

Notes and references

‡ Footnotes relating to the main text should appear here. These might include comments relevant to but not central to the matter under discussion, limited experimental and spectral data, and crystallographic data.

1   M. E. Germain and M. J. Knapp, *Chem. Soc. Rev.*, 2009, **38**, 2543-2555.
2   Y. Salinas, R. Martinez-Manez, M. D. Marcos, F. Sancenon, A. M. Costero, M. Parra and S. Gil, *Chem. Soc. Rev.*, 2012, **41**, 1261-1296.
3   N. P. Saravanan, S. Venugopalan, N. Senthilkumar, P. Santhosh, B. Kavita and H. G. Prabu, *Talanta*, 2006, **69**, 656-662.
4   U. S. E. P. Agency, U.S. Environmental Protection Agency, Washington, DC, 2011.
5   ATF, *Federal Register*, 2010, **75**, 70291-70293.
6   T. F. Jenkins, D. C. Leggett and T. A. Ranney, US Army Cold Regions Research and Engineering Laboratory, Special Report 99-21, Hanover, 1999.
7   H. Östmark, S. Wallin and H. G. Ang, *Propellants, Explos., Pyrotech.*, 2012, **37**, 12-23.
8   P. Kolla, *Anal. Chem.*, 1995, **67**, A184-A189.
9   S. J. Toal, D. Magde and W. C. Trogler, *Chem. Commun.*, 2005, 5465-5467.
10 X. Wang, Y. Guo, D. Li, H. Chen and R.-C. Sun, *Chem. Commun.*, 2012, **48**, 5569-5571.
11 H. H. Hill and G. Simpson, *Field Anal. Chem. Technol.*, 1997, **1**, 119-134.
12 D. S. Moore, *Rev. Sci. Instrum.*, 2004, **75**, 2499-2512.
13 M. E. Walsh, *Talanta*, 2001, **54**, 427-438.
14 H. X. Zhang, J. S. Hu, C. J. Yan, L. Jiang and L. J. Wan, *Phys. Chem. Chem. Phys.*, 2006, **8**, 3567-3572.
15 E. R. Goldman, G. P. Anderson, N. Lebedev, B. M. Lingerfelt, P. T. Winter, C. H. Patterson and J. M. Mauro, *Anal. Bioanal. Chem.*, 2003, **375**, 471-475.
16 S. J. Toal and W. C. Trogler, *J. Mater. Chem.*, 2006, **16**, 2871-2883.
17 I. A. Buryakov, T. I. Buryakov and V. T. Matsaev, *J. Anal. Chem.*, 2014, **69**, 616-631.
18 S. W. Thomas, G. D. Joly and T. M. Swager, *Chem. Rev.*, 2007, **107**, 1339-1386.
19 A. Alvarez, J. M. Costa-Fernández, R. Pereiro, A. Sanz-Medel and A. Salinas-Castillo, *Trends Anal. Chem.*, 2011, **30**, 1513-1525.
20 S. Rochat and T. M. Swager, *ACS Appl. Mater. Interfaces*, 2013, **5**, 4488-4502.
21 Z. Hu, B. J. Deibert and J. Li, *Chem. Soc. Rev.*, 2014, **43**, 5815-5840.
22 Y. Ma, S. Wang and L. Wang, *Trends Anal. Chem.*, 2015, **65**, 13-21.
23 J. R. Lakowicz, *Principles of Fluorescence Spectroscopy*, Springer, Singapore, 2006.
24 M. S. Meaney and V. L. McGuffin, *Anal. Chim. Acta*, 2008, **610**, 57-67.

25 B. Valeur, *Molecular Fluorescence: Principles and Applications* Wiley-vch, 2002.

26 G. He, N. Yan, J. Yang, H. Wang, L. Ding, S. Yin and Y. Fang, *Macromolecules*, 2011, **44**, 4759-4766.

27 H. Nie, H. Lv, L. Yao, Y. Pan, Y. Zhao, P. Li, G. Sun, Y. Ma and M. Zhang, *J. Hazard. Mater.*, 2014, **264**, 474-480.

28 S. Madhu, A. Bandela and M. Ravikanth, *R. Soc. Chem. Adv.*, 2014, **4**, 7120-7123.

29 X. Liu, Y. Xu and D. Jiang, *J. Am. Chem. Soc.*, 2012, **134**, 8738-8741.

30 S. Pramanik, C. Zheng, X. Zhang, T. J. Emge and J. Li, *J. Am. Chem. Soc.*, 2011, **133**, 4153-4155.

31 Z. Hu, S. Pramanik, K. Tan, C. Zheng, W. Liu, X. Zhang, Y. J. Chabal and J. Li, *Cryst. Growth Des.*, 2013, **13**, 4204-4207.

32 Y.-Z. Zhang, X. Xiang, P. Mei, J. Dai, L.-L. Zhang and Y. Liu, *Spectrochim. Acta, Part A*, 2009, **72**, 907-914.

33 C. R. Cantor, *Biophysical chemistry: Part II: Techniques for the study of biological structure and function*, Macmillan, 1980.

34 S. S. Nagarkar, B. Joarder, A. K. Chaudhari, S. Mukherjee and S. K. Ghosh, *Angew. Chem. Int. Ed.*, 2013, **52**, 2881-2885.

35 D. Dinda, A. Gupta, B. K. Shaw, S. Sadhu and S. K. Saha, *ACS Appl. Mater. Interfaces*, 2014, **6**, 10722-10728.

36 X. Sun, X. Ma, C. V. Kumar and Y. Lei, *Anal. Methods*, 2014, **6**, 8464-8468.

37 Y. Wang, A. La, C. Brückner and Y. Lei, *Chem. Commun.*, 2012, **48**, 9903-9905.

38 L. Feng, H. Li, Y. Qu and C. Lu, *Chem. Commun.*, 2012, **48**, 4633-4635.

39 E. R. Goldman, I. L. Medintz, J. L. Whitley, A. Hayhurst, A. R. Clapp, H. T. Uyeda, J. R. Deschamps, M. E. Lassman and H. Mattoussi, *J. Am. Chem. Soc.*, 2005, **127**, 6744-6751.

40 N. R. Walker, M. J. Linman, M. M. Timmers, S. L. Dean, C. M. Burkett, J. A. Lloyd, J. D. Keelor, B. M. Baughman and P. L. Edmiston, *Anal. Chim. Acta*, 2007, **593**, 82-91.

41 J. L. Geng, P. Liu, B. H. Liu, G. J. Guan, Z. P. Zhang and M. Y. Han, *Chem.-Eur. J.*, 2010, **16**, 3720-3727.

42 Q. L. Fang, J. L. Geng, B. H. Liu, D. M. Gao, F. Li, Z. Y. Wang, G. J. Guan and Z. P. Zhang, *Chem.-Eur. J.*, 2009, **15**, 11507-11514.

43 D. M. Gao, Z. Y. Wang, B. H. Liu, L. Ni, M. H. Wu and Z. P. Zhang, *Anal. Chem.*, 2008, **80**, 8545-8553.

44 Y. Xia, L. Song and C. Zhu, *Anal. Chem.*, 2011, **83**, 1401-1407.

45 J. R. Cox, P. Müller and T. M. Swager, *J. Am. Chem. Soc.*, 2011, **133**, 12910-12913.

46 H. Tong, L. Wang, X. Jing and F. Wang, *Macromolecules*, 2003, **36**, 2584-2586.

47 Y. Xu, B. Li, W. Li, J. Zhao, S. Sun and Y. Pang, *Chem. Commun.*, 2013, **49**, 4764-4766.

48 D. A. Olley, E. J. Wren, G. Vamvounis, M. J. Fernee, X. Wang, P. L. Burn, P. Meredith and P. E. Shaw, *Chem. Mater.*, 2011, **23**, 789-794.

49 X. Sun, Y. Liu, G. Shaw, A. Carrier, S. Dey, J. Zhao and Y. Lei, *ACS Appl. Mater. Interfaces*, 2015.

50 T. M. Swager, *Acc. Chem. Res.*, 1998, **31**, 201-207.

51 J. S. Yang and T. M. Swager, *J. Am. Chem. Soc.*, 1998, **120**, 5321-5322.

52 P. M. Cotts, T. M. Swager and Q. Zhou, *Macromolecules*, 1996, **29**, 7323-7328.

53 J.-S. Yang and T. M. Swager, *J. Am. Chem. Soc.*, 1998, **120**, 11864-11873.

54 G. V. Zyryanov, M. A. Palacios and P. Anzenbacher, *Org. Lett.*, 2008, **10**, 3681-3684.

55 S. Yamaguchi and T. M. Swager, *J. Am. Chem. Soc.*, 2001, **123**, 12087-12088.

56 S. Zahn and T. M. Swager, *Angew. Chem.-Int. Edit.*, 2002, **41**, 4225-4230.

57 D. Zhao and T. M. Swager, *Macromolecules*, 2005, **38**, 9377-9384.

58 G. He, N. Yan, J. Y. Yang, H. Y. Wang, L. P. Ding, S. W. Yin and Y. Fang, *Macromolecules*, 2011, **44**, 4759-4766.

59 Z. Wang, Z. Y. Wang, J. Ma, W. J. Bock and D. Ma, *Polymer*, 2010, **51**, 842-847.

60 S. Chen, Q. Zhang, Q. Liu, J. Gu, L. Zhang, J. Zhou, X. Fan and L. Fang, *React. Funct. Polym.*, 2011, **71**, 1008-1015.

61 D. F. Zhu, Q. G. He, H. M. Cao, J. G. Cheng, S. L. Feng, Y. S. Xu and T. Lin, *Appl. Phys. Lett.*, 2008, **93**.

62 C. M. Deng, Q. G. He, J. G. Cheng, D. F. Zhu, C. He and T. Lin, *Synt. Met.*, 2009, **159**, 320-324.

63 J. Feng, Y. Li and M. Yang, *Sens. Actuator B-Chem.*, 2010, **145**, 438-443.

64 C. P. Chang, C. Y. Chao, J. H. Huang, A. K. Li, C. S. Hsu, M. S. Lin, B. R. Hsieh and A. C. Su, *Synt. Met.*, 2004, **144**, 297-301.

65 K. Saxena, P. Kumar and V. K. Jain, *J. of Lumin.*, 2010, **130**, 2260-2264.

66 L. H. Chen, D. McBranch, R. Wang and D. Whitten, *Chem. Phys. Lett.*, 2000, **330**, 27-33.

67 T. L. Duniho, B. J. Laughlin, A. A. Buelt, W. F. Baker, C. A. Conrad and R. C. Smith, *J. Polym. Sci., Part A: Polym. Chem.*, 2014, **52**, 1487-1492.

68 A. Rose, Z. G. Zhu, C. F. Madigan, T. M. Swager and V. Bulovic, *Nature*, 2005, **434**, 876-879.

69 C. M. Deng, Q. G. He, C. He, L. Q. Shi, J. G. Cheng and T. Lin, *J. Phys. Chem. B*, 2010, **114**, 4725-4730.

70 D. Gopalakrishnan and W. R. Dichtel, *J. Am. Chem. Soc.*, 2013, **135**, 8357-8362.

71 H. Li, J. Wang, Z. Pan, L. Cui, L. Xu, R. Wang, Y. Song and L. Jiang, *J. Mater. Chem.*, 2011, **21**, 1730-1735.

72 H. Zhang, L. Feng, B. Liu, C. Tong and C. Lü, *Dyes Pigm.*, 2014, **101**, 122-129.

73 Y. Y. Long, H. B. Chen, Y. Yang, H. M. Wang, Y. F. Yang, N. Li, K. A. Li, J. Pei and F. Liu, *Macromolecules*, 2009, **42**, 6501-6509.

74 H. H. Nguyen, X. Li, N. Wang, Z. Y. Wang, J. Ma, W. J. Bock and D. Ma, *Macromolecules*, 2009, **42**, 921-926.

75 S. W. Thomas, J. P. Amara, R. E. Bjork and T. M. Swager, *Chem. Commun.*, 2005, 4572-4574.

76 N. Venkatramaiah, S. Kumar and S. Patil, *Chem. Commun.*, 2012, **48**, 5007-5009.

77 H. Leng and W. Wu, *React. Funct. Polym.*, 2012, **72**, 206-211.

78 P. Marks, S. Cohen and M. Levine, *J. Polym. Sci., Part A: Polym. Chem.*, 2013, **51**, 4150-4155.

79 B. Xu, Y. Xu, X. Wang, H. Li, X. Wu, H. Tong and L. Wang, *Polym. Chem.*, 2012, **4**, 5056-5059.

80 H. Ma, L. Yao, P. Li, O. Ablikim, Y. Cheng and M. Zhang, *Chem. Eur. J.*, 2014, **20**, 11655-11658.

81 Y. J. Hu, S. Z. Tan, G. L. Shen and R. Q. Yu, *Anal. Chim. Acta*, 2006, **570**, 170-175.

82 H. Nie, Y. Zhao, M. Zhang, Y. Ma, M. Baumgarten and K. Muellen, *Chem. Commun.*, 2011, **47**, 1234-1236.

83 H. Nie, G. Sun, M. Zhang, M. Baumgarten and K. Müllen, *J. Mater. Chem.*, 2012, **22**, 2129-2132.

84 E. Sabatani, Y. Kalisky, A. Berman, Y. Golan, N. Gutman, B. Urbach and A. Sa'ar, *Opt. Mater.*, 2008, **30**, 1766-1774.

85 Y. Liu, R. C. Mills, J. M. Boncella and K. S. Schanze, *Langmuir*, 2001, **17**, 7452-7455.

86 W.-E. Lee, C.-J. Oh, I.-K. Kang and G. Kwak, *Macromol. Chem. Phys.*, 2010, **211**, 1900-1908.

87 M. Laurenti, E. Lopez-Cabarcos, F. Garcia-Blanco, B. Frick and J. Rubio-Retama, *Langmuir*, 2009, **25**, 9579-9584.

88 G. Nagarjuna, A. Kumar, A. Kokil, K. G. Jadhav, S. Yurt, J. Kumar and D. Venkataraman, *J. Mater. Chem.*, 2011, **21**, 16597-16602.

89 Y. Long, H. Chen, H. Wang, Z. Peng, Y. Yang, G. Zhang, N. Li, F. Liu and J. Pei, *Anal. Chim. Acta*, 2012, **744**, 82-91.

90 B. Balan, C. Vijayakumar, M. Tsuji, A. Saeki and S. Seki, *J. Phys. Chem. B*, 2012, **116**, 10371-10378.

91 S. Chen, Q. Zhang, J. Zhang, J. Gu and L. Zhang, *Sens. Actuator B-Chem.*, 2010, **149**, 155-160.

92 Y. Li, W. Zhang, Z. Sun, T. Sun, Z. Xie, Y. Huang and X. Jing, *Eur. Polym. J.*, 2015, **63**, 149-155.

93 M. E. Kose, B. A. Harruff, Y. Lin, L. M. Veca, F. Lu and Y.-P. Sun, *J. Phys. Chem. B*, 2006, **110**, 14032-14034.

94 X. Wang, H. Zeng, L. Zhao and J.-M. Lin, *Talanta*, 2006, **70**, 160-168.

95 W. Wei, R. Lu, S. Tang and X. Liu, *J. Mater. Chem. A*, 2015, **3**, 4604-4611.

96 S. Hussain, A. H. Malik, M. A. Afroz and P. K. Iyer, *Chem. Commun.*, 2015, **51**, 7207-7210.

97 A. Saxena, M. Fujiki, R. Rai and G. Kwak, *Chem. Mat.*, 2005, **17**, 2181-2185.

98 H. Sohn, R. M. Calhoun, M. J. Sailor and W. C. Trogler, *Angew. Chem.-Int. Edit.*, 2001, **40**, 2104-2105.

99 H. Sohn, M. J. Sailor, D. Magde and W. C. Trogler, *J. Am. Chem. Soc.*, 2003, **125**, 3821-3830.

100 S. J. Toal, D. Magde and W. C. Trogler, *Chem. Commun.*, 2005, 5465-5467.

101 J. C. Sanchez, A. G. DiPasquale, A. L. Rheingold and W. C. Trogler, *Chem. Mat.*, 2007, **19**, 6459-6470.

102 J. C. Sanchez, S. A. Urbas, S. J. Toal, A. G. DiPasquale, A. L. Rheingold and W. C. Trogler, *Macromolecules*, 2008, **41**, 1237-1245.

103 Z. Zhao, Y. Guo, T. Jiang, Z. Chang, J. W. Y. Lam, L. Xu, H. Qiu and B. Z. Tang, *Macromol. Rapid Commun.*, 2012, **33**, 1074-1079.

104 J. C. Sanchez and W. C. Trogler, *J. Mater. Chem.*, 2008, **18**, 3143-3156.

105 H. P. Martinez, C. D. Grant, J. G. Reynolds and W. C. Trogler, *J. Mater. Chem.*, 2012, **22**, 2908-2914.

106 L. H. Zhang, T. Jiang, L. B. Wu, J. H. Wan, C. H. Chen, Y. B. Pei, H. Lu, Y. Deng, G. F. Bian, H. Y. Qiu and G. Q. Lai, *Chem. Asian J.*, 2012, **7**, 1583-1593.

107 B. Dedeoglu, A. Monari, T. Etienne, V. Aviyente and A. S. Özen, *J. Phys. Chem. C*, 2014, **118**, 23946-23953.

108 J. V. Goodpaster and V. L. McGuffin, *Anal. Chem.*, 2001, **73**, 2004-2011.

109 J. V. Goodpaster, J. F. Harrison and V. L. McGuffin, *J. Phys. Chem. A*, 2002, **106**, 10645-10654.

110 K. S. Focsaneanu and J. C. Scaiano, *Photochem. Photobiol. Sci.*, 2005, **4**, 817-821.

111 Y. H. Lee, H. Liu, J. Y. Lee, S. H. Kim, S. K. Kim, J. L. Sessler, Y. Kim and J. S. Kim, *Chem.-Eur. J.*, 2010, **16**, 5895-5901.

112 S.-B. Kim, E.-B. Lee, J.-H. Choi and D.-G. Cho, *Tetrahedron*, 2013, **69**, 4652-4656.

113 P. Singla, P. Kaur and K. Singh, *Tetrahedron Lett.*, 2015, **56**, 2311-2314.

114 K. J. Balkus, T. J. Pisklak, G. Hundt, J. Sibert and Y. F. Zhang, *Microporous Mesoporous Mater.*, 2008, **112**, 1-13.

115 S. Z. Tan, Y. J. Hu, J. W. Chen, G. L. Shen and R. Q. Yu, *Sens. Actuator B-Chem.*, 2007, **124**, 68-73.

116 W. Chen, N. B. Zuckerman, J. P. Konopelski and S. W. Chen, *Anal. Chem.*, 2010, **82**, 461-465.

117 F. Ito, T. Kakiuchi, T. Sakano and T. Nagamura, *Phys. Chem. Chem. Phys.*, 2010, **12**, 10923-10927.

118 N. Venkatramaiah, A. D. G. Firmino, F. A. Almeida Paz and J. P. C. Tome, *Chem. Commun.*, 2014, **50**, 9683-9686.

119 C. Vijayakumar, G. Tobin, W. Schmitt, M. J. Kim and M. Takeuchi, *Chem. Commun.*, 2010, **46**, 874-876.

120 L. P. Ding, J. P. Kang, F. T. Lu, L. N. Gao, X. Yin and Y. Fang, *Thin Solid Films*, 2007, **515**, 3112-3119.

121 J. P. Kang, L. P. Ding, F. T. Lu, S. J. Zhang and Y. Fang, *J. Phys. D-Appl. Phys.*, 2006, **39**, 5097-5102.

122 H. H. Li, J. P. Kang, L. P. Ding, F. T. Lu and Y. Fang, *J. Photochem. Photobiol. A*, 2008, **197**, 226-231.

123 A. Pramanik, M. Bhuyan and G. Das, *J. Photochem. Photobiol. A*, 2008, **197**, 149-155.

124 B. Roy, A. K. Bar, B. Gole and P. S. Mukherjee, *J. Org. Chem.*, 2013, **78**, 1306-1310.

125 N. Niamnont, N. Kimpitak, K. Wongravee, P. Rashatasakhon, K. K. Baldridge, J. S. Siegel and M. Sukwattanasinitt, *Chem. Commun.*, 2013, **49**, 780-782.

126 R. Kumar, S. Sandhu, P. Singh, G. Hundal, M. S. Hundal and S. Kumar, *Asian J. Org. Chem.*, 2014, **3**, 805-813.

127 P. Anzenbacher Jr, L. Mosca, M. A. Palacios, G. V. Zyryanov and P. Koutnik, *Chem. Eur. J.*, 2012, **18**, 12712-12718.

128 P. C. Zhu, L. N. Luo, P. Q. Cen, J. T. Li and C. Zhang, *Tetrahedron Lett.*, 2014, **55**, 6277-6280.

129 H. Wang, X. Xu, L. Li, C. Yang and H. F. Ji, *Micro and Nano Lett.*, 2011, **6**, 763-766.

130 H. Wang, X. Xu, A. Kojtari and H. F. Ji, *J. Phys. Chem. C*, 2011, **115**, 20091-20096.

131 H. Wang, X. Xu, C. Lee, C. Johnson, K. Sohlberg and H. F. Ji, *J. Phys. Chem. C*, 2012, **116**, 4442-4448.

132 A. D. Hughes, I. C. Glenn, A. D. Patrick, A. Ellington and E. V. Anslyn, *Chem.-Eur. J.*, 2008, **14**, 1822-1827.

133 S. Shanmugaraju, S. A. Joshi and P. S. Mukherjee, *J. Mater. Chem.*, 2011, **21**, 9130-9138.

134 M. Rahman and H. J. Harmon, *Spectroc. Acta Pt. A-Molec. Biomolec. Spectr.*, 2006, **65**, 901-906.

135 W. M. Hikal and H. J. Harmon, *J. of Hazard. Mater.*, 2008, **154**, 826-831.

136 S. Tao, J. Yin and G. Li, *J. Mater. Chem.*, 2008, **18**, 4872-4878.

137 S. Y. Tao, Z. Y. Shi, G. T. Li and P. Li, *ChemPhysChem*, 2006, **7**, 1902-1905.

138 S. Y. Tao and G. T. Li, *Colloid Polym. Sci.*, 2007, **285**, 721-728.

139 S. Y. Tao, G. T. Li and H. S. Zhu, *J. Mater. Chem.*, 2006, **16**, 4521-4528.

140 S. Y. Tao, G. T. Li and J. X. Yin, *J. Mater. Chem.*, 2007, **17**, 2730-2736.

141 Y. F. Yang, H. M. Wang, K. Su, Y. Y. Long, Z. Peng, N. Li and F. Liu, *J. Mater. Chem.*, 2011, **21**, 11895-11900.

142 B. Johnson-White, M. Zeinali, K. M. Shaffer, C. H. Patterson, P. T. Charles and M. A. Markowitz, *Biosens. Bioelectron.*, 2007, **22**, 1154-1162.

143 A. Rana and P. K. Panda, *R. Soc. Chem. Adv.*, 2012, **2**, 12164-12168.

144 N. Venkatramaiah, C. F. Pereira, R. F. Mendes, F. A. A. Paz and J. P. C. Tomé, *Anal. Chem.*, 2015, **87**, 4515-4522.

145 C. A. SwamyP and P. Thilagar, *Chem. Eur. J.*, 2015.

146 Y. Ma, H. Li, S. Peng and L. Wang, *Anal. Chem.*, 2012, **84**, 8415-8421.

147 L. Feng, C. Wang, Z. Ma and C. Lü, *Dyes Pigm.*, 2013, **97**, 84-91.

148 W. S. Zou, Y. Q. Wang, F. Wang, Q. Shao, J. Zhang and J. Liu, *Anal. Bioanal. Chem.*, 2013, **405**, 4905-4912.

149 G. Sivaraman, B. Vidya and D. Chellappa, *R. Soc. Chem. Adv.*, 2014, **4**, 30828-30831.

150 G. H. Shi, Z. B. Shang, Y. Wang, W. J. Jin and T. C. Zhang, *Spectroc. Acta Pt. A-Molec. Biomolec. Spectr.*, 2008, **70**, 247-252.

151 Y. Chen, Z. Chen, Y. He, H. Lin, P. Sheng, C. Liu, S. Luo and Q. Cai, *Nanotechnology*, 2010, **21**.

152 R. Freeman and I. Willner, *Nano Lett.*, 2009, **9**, 322-326.

40 | *Chem. Soc. Rev.*, 2015, **00**, 1-3

This journal is © The Royal Society of Chemistry 20xx

153 R. Freeman, T. Finder, L. Bahshi, R. Gill and I. Willner, *Adv. Mater.*, 2012, **24**, 6416-6421.

154 M. Algarra, B. B. Campos, M. S. Miranda and J. C. G. E. Da Silva, *Talanta*, 2011, **83**, 1335-1340.

155 C. Carrillo-Carrión, B. M. Simonet and M. Valcárcel, *Anal. Chim. Acta*, 2013, **792**, 93-100.

156 T. Pazhanivel, D. Nataraj, V. P. Devarajan, V. Mageshwari, K. Senthil and D. Soundararajan, *Anal. Methods*, 2013, **5**, 910-916.

157 S. Xu, H. Lu, J. Li, X. Song, A. Wang, L. Chen and S. Han, *ACS Appl. Mater. Interfaces*, 2013, **5**, 8146-8154.

158 K. Zhang, H. Zhou, Q. Mei, S. Wang, G. Guan, R. Liu, J. Zhang and Z. Zhang, *J. Am. Chem. Soc.*, 2011, **133**, 8424-8427.

159 K. Zhang, L. Yang, H. Zhu, F. Ma, Z. Zhang and S. Wang, *Analyst*, 2014, **139**, 2379-2385.

160 L. Fan, Y. Hu, X. Wang, L. Zhang, F. Li, D. Han, Z. Li, Q. Zhang, Z. Wang and L. Niu, *Talanta*, 2012, **101**, 192-197.

161 S. Liu, F. Shi, L. Chen and X. Su, *Talanta*, 2013, **116**, 870-875.

162 Q. Niu, K. Gao, Z. Lin and W. Wu, *Anal. Methods*, 2013, **5**, 6228-6233.

163 H. Y. Chen, L. W. Ruan, X. Jiang and L. G. Qiu, *Analyst*, 2015, **140**, 637-643.

164 J. Xie, Y. Zheng and J. Y. Ying, *J. Am. Chem. Soc.*, 2009, **131**, 888-889.

165 X. Yang, J. Wang, D. Su, Q. Xia, F. Chai, C. Wang and F. Qu, *Dalton Trans.*, 2014, **43**, 10057-10063.

166 A. Senthamizhan, A. Celebioglu and T. Uyar, *Chem. Commun.*, 2014.

167 A. Mathew, P. R. Sajanlal and T. Pradeep, *Angew. Chem. Int. Ed.*, 2012, **51**, 9596-9600.

168 H. Bai, C. Li and G. Q. Shi, *Sens. Actuator B-Chem.*, 2008, **130**, 777-782.

169 Y. Q. Chen, H. Bai, Q. Chen, C. Li and G. Q. Shi, *Sens. Actuator B-Chem.*, 2009, **138**, 563-571.

170 Y. Z. Liao, V. Strong, Y. Wang, X. G. Li, X. Wang and R. B. Kaner, *Adv. Funct. Mater.*, 2012, **22**, 726-735.

171 X. G. Li, Y. Liao, M. R. Huang, V. Strong and R. B. Kaner, *Chem. Sci.*, 2013, **4**, 1970-1978.

172 K. K. Kartha, S. S. Babu, S. Srinivasan and A. Ajayaghosh, *J. Am. Chem. Soc.*, 2012, **134**, 4834-4841.

173 K. K. Kartha, A. Sandeep, V. C. Nair, M. Takeuchi and A. Ajayaghosh, *Phys. Chem. Chem. Phys.*, 2014, **16**, 18896-18901.

174 G. He, G. Zhang, F. Lue and Y. Fang, *Chem. Mat.*, 2009, **21**, 1494-1499.

175 L. Ding and Y. Fang, *Chem. Soc. Rev.*, 2010, **39**, 4258-4273.

176 H. Wang, Y. Fang, L. P. Ding, L. N. Gao and D. D. Hu, *Thin Solid Films*, 2003, **440**, 255-260.

177 H. Du, G. He, T. Liu, L. Ding and Y. Fang, *J. Photochem. and Photobiol. A*, 2011, **217**, 356-362.

178 J. Liu, Y. Fang and C.-L. Chen, *Langmuir*, 2008, **24**, 1853-1857.

179 T. Liu, L. Ding, G. He, Y. Yang, W. Wang and Y. Fang, *ACS Appl. Mater. Interfaces*, 2011, **3**, 1245-1253.

180 L. Ding, Y. Liu, Y. Cao, L. Wang, Y. Xin and Y. Fang, *J. Mater. Chem.*, 2012, **22**, 11574-11582.

181 C. E. Agudelo-Morales, R. E. Galian and J. Pérez-Prieto, *Anal. Chem.*, 2012, **84**, 8083-8087.

182 K.-Y. Hua, C.-M. Deng, C. He, L.-Q. Shi, D.-F. Zhu, Q.-G. He and J.-G. Cheng, *Chin. Chem. Lett.*, 2013, **24**, 643-646.

183 Y. Wang, A. La, Y. Ding, Y. Liu and Y. Lei, *Adv. Funct. Mater.*, 2012, **22**, 3547-3555.

184 X. Sun, Y. Liu, S. Mopidevi, Y. Meng, F. Huang, J. Parisi, M. P. Nieh, C. Cornelius, S. L. Suib and Y. Lei, *Sens. Actuator B-Chem.*, 2014, **195**, 52-57.

185 G. B. Demirel, B. Daglar and M. Bayindir, *Chem. Commun.*, 2013, **49**, 6140-6142.

186 X. Sun, C. Brückner, M. P. Nieh and Y. Lei, *J. Mater. Chem. A*, 2014, **2**, 14613-14621.

187 L. Guo, B. Zu, Z. Yang, H. Cao, X. Zheng and X. Dou, *Nanoscale*, 2014, **6**, 1467-1473.

188 P. Beyazkilic, A. Yildirim and M. Bayindir, *ACS Appl. Mater. Interfaces*, 2014, **6**, 4997-5004.

189 P. Beyazkilic, A. Yildirim and M. Bayindir, *Nanoscale*, 2014, **6**, 15203-15209.

190 A. Vu, J. Phillips, P. Bühlmann and A. Stein, *Chem. Mater.*, 2013, **25**, 711-722.

191 L. Ding, Y. Bai, Y. Cao, G. Ren, G. J. Blanchard and Y. Fang, *Langmuir*, 2014, **30**, 7645-7653.

192 K. Sarkar, Y. Salinas, I. Campos, R. Martínez-Máñez, M. D. Marcos, F. Sancenõn and P. Amorõs, *ChemPlusChem*, 2013, **78**, 684-694.

193 L. Ma, Y. Wen and N. Yan, *J. Sol-Gel Sci. Technol.*, 2013, **67**, 161-169.

194 S. Burattini, H. M. Colquhoun, B. W. Greenland, W. Hayes and M. Wade, *Macromol. Rapid Commun.*, 2009, **30**, 459-463.

195 X. Y. Wang, C. Drew, S. H. Lee, K. J. Senecal, J. Kumar and L. A. Samuelson, *J. Macromol. Sci.-Pure Appl. Chem.*, 2002, **A39**, 1251-1258.

196 A. Ponnu and E. V. Anslyn, *Supramol. Chem.*, 2010, **22**, 65-71.

197 L. Feng, C. Tong, Y. He, B. Liu, C. Wang, J. Sha and C. Lü, *J. Lumin.*, 2014, **146**, 502-507.

198 A. I. Costa and J. V. Prata, *Sens. Actuator B-Chem.*, 2012, **161**, 251-260.

199 P. D. Barata and J. V. Prata, *Supramol. Chem.*, 2013, **25**, 782-797.

200 P. D. Barata and J. V. Prata, *ChemPlusChem*, 2014, **79**, 83-89.

201 M. Kandpal, A. K. Bandela, V. K. Hinge, V. R. Rao and C. P. Rao, *ACS Appl. Mater. Interfaces*, 2013, **5**, 13448-13456.

202 Y. H. Lee, H. Liu, J. Y. Lee, S. H. Kim, S. K. Kim, J. L. Sessler, Y. Kim and J. S. Kim, *Chem. Eur. J.*, 2010, **16**, 5895-5901.

203 W. Zhu, W. Li, C. Wang, J. Cui, H. Yang, Y. Jiang and G. Li, *Chem. Sci.*, 2013, **4**, 3583-3590.

204 W. Zhu, C. Wang, W. Li, C. A. Tao, J. Cui, H. Yang, Y. Jiang and G. Li, *J. Mater. Chem. A*, 2013, **1**, 11741-11747.

205 T. Naddo, Y. K. Che, W. Zhang, K. Balakrishnan, X. M. Yang, M. Yen, J. C. Zhao, J. S. Moore and L. Zang, *J. Am. Chem. Soc.*, 2007, **129**, 6978-6979.

206 T. Naddo, X. M. Yang, J. S. Moore and L. Zang, *Sens. Actuator B-Chem.*, 2008, **134**, 287-291.

207 C. Y. Zhang, Y. K. Che, X. M. Yang, B. R. Bunes and L. Zang, *Chem. Commun.*, 2010, **46**, 5560-5562.

208 Y. Che, D. E. Gross, H. Huang, D. Yang, X. Yang, E. Discekici, Z. Xue, H. Zhao, J. S. Moore and L. Zang, *J. Am. Chem. Soc.*, 2012, **134**, 4978-4982.

209 M. Wang, V. Vajpayee, S. Shanmugaraju, Y.-R. Zheng, Z. Zhao, H. Kim, P. S. Mukherjee, K.-W. Chi and P. J. Stang, *Inorg. Chem.*, 2011, **50**, 1506-1512.

210 S. Shanmugaraju, S. A. Joshi and P. S. Mukherjee, *Inorg. Chem.*, 2011, **50**, 11736-11745.

211 D. Samanta and P. S. Mukherjee, *Dalton Trans.*, 2013, **42**, 16784-16795.

212 K. Acharyya and P. S. Mukherjee, *Chem. Commun.*, 2014, **50**, 15788-15791.

213 V. Balzani, P. Ceroni, A. Juris, M. Venturi, S. Campagna, F. Puntoriero and S. Serroni, *Coord. Chem. Rev.*, 2001, **219–221**, 545-572.

214 S. Glazier, J. A. Barron, N. Morales, A. M. Ruschak, P. L. Houston and H. D. Abruna, *Macromolecules*, 2003, **36**, 1272-1278.

215 A. Narayanan, O. Varnavski, O. Mongin, J. P. Majoral, M. Blanchard-Desce and T. Goodson, *Nanotechnology*, 2008, **19**.

216 M. Guo, O. Varnavski, A. Narayanan, O. Mongin, J. P. Majoral, M. Blanchard-Desce and T. Goodson, *J. Phys. Chem. A*, 2009, **113**, 4763-4771.

217 A. J. Clulow, P. L. Burn, P. Meredith and P. E. Shaw, *J. Mater. Chem.*, 2012, **22**, 12507-12516.

218 G. Tang, S. S. Y. Chen, P. E. Shaw, K. Hegedus, X. Wang, P. L. Burn and P. Meredith, *Polym. Chem.*, 2011, **2**, 2360-2368.

219 P. E. Shaw, H. Cavaye, S. S. Y. Chen, M. James, I. R. Gentle and P. L. Burn, *Phys. Chem. Chem. Phys.*, 2013, **15**, 9845-9853.

220 P. E. Shaw, S. S. Y. Chen, X. Wang, P. L. Burn and P. Meredith, *J. Phys. Chem. C*, 2013, **117**, 5328-5337.

221 Z. Ding, Q. Zhao, R. Xing, X. Wang, J. Ding, L. Wang and Y. Han, *J. Mater. Chem. C*, 2013, **1**, 786-792.

222 B. Gole, S. Shanmugaraju, A. K. Bar and P. S. Mukherjee, *Chem. Commun.*, 2011, **47**, 10046-10048.

223 S. Shanmugaraju, H. Jadhav, R. Karthik and P. S. Mukherjee, *R. Soc. Chem. Adv.*, 2013, **3**, 4940-4950.

224 B. Gole, W. Song, M. Lackinger and P. S. Mukherjee, *Chem. Eur. J.*, 2014, **20**, 13662-13680.

225 A. Lan, K. Li, H. Wu, D. H. Olson, T. J. Emge, W. Ki, M. Hong and J. Li, *Angew. Chem. Int. Ed.*, 2009, **48**, 2334-2338.

226 S. Pramanik, Z. Hu, X. Zhang, C. Zheng, S. Kelly and J. Li, *Chem. Eur. J.*, 2013, **19**, 15964-15971.

227 D. Banerjee, Z. Hu, S. Pramanik, X. Zhang, H. Wang and J. Li, *CrystEngComm*, 2013, **15**, 9745-9750.

228 G.-l. Liu, Y.-j. Qin, L. Jing, G.-y. Wei and H. Li, *Chem. Commun.*, 2013, **49**, 1699-1701.

229 B. Gole, A. K. Bar and P. S. Mukherjee, *Chem. Eur. J.*, 2014, **20**, 13321-13336.

230 S. S. Nagarkar, A. V. Desai and S. K. Ghosh, *Chem. Commun.*, 2014, **50**, 8915-8918.

231 B. Gole, A. K. Bar and P. S. Mukherjee, *Chem. Commun.*, 2011, **47**, 12137-12139.

232 Y.-N. Gong, L. Jiang and T.-B. Lu, *Chem. Commun.*, 2013, **49**, 11113-11115.

233 S. Barman, J. Anand Garg, O. Blacque, K. Venkatesan and H. Berke, *Chem. Commun.*, 2012, **48**, 11127-11129.

234 D. Tian, Y. Li, R. Y. Chen, Z. Chang, G. Y. Wang and X. H. Bu, *J. Mater. Chem. A*, 2014, **2**, 1465-1470.

235 D. Tian, R.-Y. Chen, J. Xu, Y.-W. Li and X.-H. Bu, *APL Mat.*, 2014, **2**, -.

236 Z.-F. Wu, B. Tan, M.-L. Feng, A.-J. Lan and X.-Y. Huang, *J. Mater. Chem. A*, 2014, **2**, 6426-6431.

237 S. Xie, H. Wang, Z. Liu, R. Dai and L. Huang, *R. Soc. Chem. Adv.*, 2015, **5**, 7121-7124.

238 A. K. Chaudhari, S. S. Nagarkar, B. Joarder and S. K. Ghosh, *Cryst. Growth Des.*, 2013, **13**, 3716-3721.

239 J. H. Lee, J. Jaworski and J. H. Jung, *Nanoscale*, 2013, **5**, 8533-8540.

240 S. R. Zhang, D. Y. Du, J. S. Qin, S. J. Bao, S. L. Li, W. W. He, Y. Q. Lan, P. Shen and Z. M. Su, *Chem. Eur. J.*, 2014, **20**, 3589-3594.

241 K. S. Asha, K. Bhattacharyya and S. Mandal, *J. Mater. Chem. C*, 2014, **2**, 10073-10081.

242 R. Li, Y. P. Yuan, L. G. Qiu, W. Zhang and J. F. Zhu, *Small*, 2012, **8**, 225-230.

243 Y. Xu, Y. Wen, W. Zhu, Y. N. Wu, C. Lin and G. Li, *Mater. Lett.*, 2012, **87**, 20-23.

244 S. B. Ding, W. Wang, L. G. Qiu, Y. P. Yuan, F. M. Peng, X. Jiang, A. J. Xie, Y. H. Shen and J. F. Zhu, *Mater. Lett.*, 2011, **65**, 1385-1387.

245 J. J. Qian, L. G. Qiu, Y. M. Wang, Y. P. Yuan, A. J. Xie and Y. H. Shen, *Dalton Trans.*, 2014, **43**, 3978-3983.

246 W. Zhang, L. G. Qiu, Y. P. Yuan, A. J. Xie, Y. H. Shen and J. F. Zhu, *J. Hazard. Mater.*, 2012, **221-222**, 147-154.

247 M. Jurcic, W. J. Peveler, C. N. Savory, D. O. Scanlon, A. J. Kenyon and I. P. Parkin, *J. Mater. Chem. A*, 2015, **3**, 6351-6359.

248 S. Roy, A. K. Katiyar, S. P. Mondal, S. K. Ray and K. Biradha, *ACS Appl. Mater. Interfaces*, 2014, **6**, 11493-11501.

249 W. J. Li, J. Lü, S. Y. Gao, Q. H. Li and R. Cao, *J. Mater. Chem. A*, 2014, **2**, 19473-19478.

250 S. Dalapati, S. Jin, J. Gao, Y. Xu, A. Nagai and D. Jiang, *J. Am. Chem. Soc.*, 2013, **135**, 17310-17313.

251 J. Liu, S. Yang, F. Li, L. Dong, X. Wang and Q. Pu, *J. Mater. Chem. A*, 2015, **3**, 10069-10076.

252 F. Samain, S. Ghosh, Y. N. Teo and E. T. Kool, *Angew. Chem. Int. Ed.*, 2010, **49**, 7025-7029.

253 D. A. Heller, G. W. Pratt, J. Zhang, N. Nair, A. J. Hansborough, A. A. Boghossian, N. F. Reuel, P. W. Barone and M. S. Strano, *Proc. Natl. Acad. Sci. U. S. A.*, 2011, **108**, 8544-8549.

254 A. Yildirim, H. Acar, T. S. Erkal, M. Bayindir and M. O. Guler, *ACS Appl. Mater. Interfaces*, 2011, **3**, 4159-4164.

255 Q. Niu, K. Gao and W. Wu, *Carbohydr. Polym.*, 2014, **110**, 47-52.

256 P. Sabherwal, M. Shorie, P. Pathania, S. Chaudhary, K. K. Bhasin, V. Bhalla and C. R. Suri, *Anal. Chem.*, 2014, **86**, 7200-7204.

257 A. Gingras, J. Sarette, E. Shawler, T. Lee, S. Freund, E. Holwitt and B. W. Hicks, *Biosens. and Bioelectron.*, 2013, **48**, 251-257.

258 S. Yagur-Kroll, C. Lalush, R. Rosen, N. Bachar, Y. Moskovitz and S. Belkin, *Appl. Microbiol. Biotechnol.*, 2014, **98**, 885-895.

259 S. M. Via, J. C. Zinnert, A. D. Butler and D. R. Young, *Environ. Exp. Bot.*, 2014, **99**, 67-74.

260 A. J. Qin, L. Tang, J. W. Y. Lam, C. K. W. Jim, Y. Yu, H. Zhao, J. Z. Sun and B. Z. Tang, *Adv. Funct. Mater.*, 2009, **19**, 1891-1900.

261 P. Lu, J. W. Y. Lam, J. Z. Liu, C. K. W. Jim, W. Z. Yuan, N. Xie, Y. C. Zhong, Q. Hu, K. S. Wong, K. K. L. Cheuk and B. Z. Tang, *Macromol. Rapid Commun.*, 2010, **31**, 834-839.

262 J. Z. Liu, Y. C. Zhong, P. Lu, Y. N. Hong, J. W. Y. Lam, M. Faisal, Y. Yu, K. S. Wong and B. Z. Tang, *Polym. Chem.*, 2010, **1**, 426-429.

263 R. Hu, J. W. Y. Lam, J. Liu, H. H. Y. Sung, I. D. Williams, Z. Yue, K. S. Wong, M. M. F. Yuen and B. Z. Tang, *Polym. Chem.*, 2012, **3**, 1481-1489.

264 H. Li, H. Wu, E. Zhao, J. Li, J. Z. Sun, A. Qin and B. Z. Tang, *Macromolecules*, 2013, **46**, 3907-3914.

265 R. Hu, J. L. Maldonado, M. Rodriguez, C. Deng, C. K. W. Jim, J. W. Y. Lam, M. M. F. Yuen, G. Ramos-Ortiz and B. Z. Tang, *J. Mater. Chem.*, 2012, **22**, 232-240.

266 H. Zhou, J. Li, M. H. Chua, H. Yan, B. Z. Tang and J. Xu, *Polym. Chem.*, 2014, **5**, 5628-5637.

267 J. Li, J. Liu, J. W. Y. Lam and B. Z. Tang, *R. Soc. Chem. Adv.*, 2013, **3**, 8193-8196.

268 Z. Zhao, T. Jiang, Y. Guo, L. Ding, B. He, Z. Chang, J. W. Y. Lam, J. Liu, C. Y. K. Chan, P. Lu, L. Xu, H. Qiu and B. Z. Tang, *J. Polym. Sci., Part A: Polym. Chem.*, 2012, **50**, 2265-2274.

269 H. Zhou, Q. Ye, W. T. Neo, J. Song, H. Yan, Y. Zong, B. Z. Tang, T. S. A. Hor and J. Xu, *Chem. Commun.*, 2014, **50**, 13785-13788.

270 W. Dong, Y. Pan, M. Fritsch and U. Scherf, *J. Polym. Sci., Part A: Polym. Chem.*, 2015.

42 | *Chem. Soc. Rev.*, 2015, **00**, 1-3

This journal is © The Royal Society of Chemistry 20xx

271   S. Kaur, A. Gupta, V. Bhalla and M. Kumar, *J. Mater. Chem. C*, 2014, **2**, 7356-7363.

272   B. Xu, X. Wu, H. Li, H. Tong and L. Wang, *Macromolecules*, 2011, **44**, 5089-5092.

273   V. Vij, V. Bhalla and M. Kumar, *ACS Appl. Mater. Interfaces*, 2013, **5**, 5373-5380.

274   D. Li, J. Liu, R. T. K. Kwok, Z. Liang, B. Z. Tang and J. Yu, *Chem. Commun.*, 2012, **48**, 7167-7169.

275   C. Miao, D. Li, Y. Zhang, J. Yu and R. Xu, *Microporous Mesoporous Mater.*, 2014, **196**, 46-50.

276   K. S. Bejoymohandas, T. M. George, S. Bhattacharya, S. Natarajan and M. L. P. Reddy, *J. Mater. Chem. C*, 2014, **2**, 515-523.

277   C. J. McHugh, W. E. Smith, R. Lacey and D. Graham, *Chem. Commun.*, 2002, 2514-2515.

278   A. Tournebize, P. Wong-Wah-Chung, S. Thérias, P. O. Bussière, A. Rivaton, T. Caron, F. Serein-Spirau, J. P. Lère-Porte, P. Montméat and J. L. Gardette, *Polym. Degrad. Stab.*, 2012, **97**, 1355-1365.

279   L. Zhang, Y. Han, J. Zhu, Y. Zhai and S. Dong, *Anal. Chem.*, 2015, **87**, 2033-2036.

280   J. L. Pablos, L. A. Sarabia, M. C. Ortiz, A. Mendía, A. Muñoz, F. Serna, F. C. García and J. M. García, *Sens. Actuator B-Chem.*, 2015, **212**, 18-27.

281   M. A. Ali, S. S. Y. Chen, H. Cavaye, A. G. R. Smith, P. L. Burn, I. R. Gentle, P. Meredith and P. E. Shaw, *Sens. Actuator B-Chem.*, 2015, **210**, 550-557.

282   M. D. Porter, R. J. Lipert, L. M. Siperko, G. Wang and R. Narayanan, Chem. Soc. Rev., 2008, **37**, 1001-1011.

283   X. Sun, S. Stagon, H. Huang, J. Chen and Y. Lei, R. Soc. Chem. Adv., 2014, **4**, 23382-23388.

284   S. S. R. Dasary, A. K. Singh, D. Senapati, H. Yu and P. C. Ray, J. Am. Chem. Soc., 2009, **131**, 13806-13812.

285   T. Demeritte, R. Kanchanapally, Z. Fan, A. K. Singh, D. Senapati, M. Dubey, E. Zakar and P. C. Ray, Analyst, 2012, **137**, 5041-5045.

286   H. Zhou, Z. Zhang, C. Jiang, G. Guan, K. Zhang, Q. Mei, R. Liu and S. Wang, Anal. Chem., 2011, **83**, 6913-6917.